NASA TM X-53170

RADIO FREQUENCY EVALUATION OF SA-6 VEHICLE

by OLEN ELY, R. W. HOCKENBERGER, PARLEY HOWELL, AND GEDDES BOONE
Astrionics Laboratory

NASA

George C. Marshall
Space Flight Center,
Huntsville, Alabama

TECHNICAL MEMORANDUM X-53170

RADIO FREQUENCY EVALUATION OF SA-6 VEHICLE

By

Olen Ely, R. W. Hockenberger,
Parley Howell, and Geddes Boone

George C. Marshall Space Flight Center

Huntsville, Alabama

ABSTRACT

123/0

All RF systems performed satisfactorily with the exception of C-band radar, which was approximately 10 to 20 db below the theoretical values of signal strength. This system suffered an additional 10 db drop in signal at 480 seconds; however, it recovered at 560 seconds. This was almost identical to the phenomenon that occurred on SA-5 at 472.8 seconds. This malfunction has been attributed to arcing either in the cabling connecting the radar beacon to the antenna or in one of the connectors.

Signal strength degradation caused by main engine flame was very similar to that of SA-5. However, unlike SA-5, some of the signal strength data contained noise caused by main engine exhaust until inboard engine cutoff at 143 seconds.

Retrorocket ignition caused the signal level of all RF systems to drop below threshold. The C-band radar system recovered within 2.4 seconds, prior to any other system.

The ullage rocket exhaust did not noticeably affect the signal propagation. It is possible that the severe attenuation of the RF signals is caused by combining the ullage rocket and retrorocket exhausts.

NASA – GEORGE C. MARSHALL SPACE FLIGHT CENTER

NASA - GEORGE C. MARSHALL SPACE FLIGHT CENTER

TECHNICAL MEMORANDUM X-53170

RADIO FREQUENCY EVALUATION OF SA-6 VEHICLE

By

Olen Ely, R. W. Hockenberger
Parley Howell, and Geddes Boone

INSTRUMENTATION AND COMMUNICATION DIVISION
ASTRIONICS LABORATORY
RESEARCH AND DEVELOPMENT OPERATIONS

TABLE OF CONTENTS

LIST OF ILLUSTRATIONS

LIST OF ILLUSTRATIONS (Cont'd)

LIST OF ILLUSTRATIONS (Concluded)

RADIO FREQUENCY EVALUATION OF SA-6 VEHICLE

SUMMARY

All RF systems performed satisfactorily with the exception of C-band radar, which was approximately 10 to 20 db below the theoretical values of signal strength. This system suffered an additional 10 db drop in signal at 480 seconds; however, it recovered at 560 seconds. This was almost identical to the phenomenon that occurred on SA-5 at 472.8 seconds. This malfunction has been attributed to arcing either in the cabling connecting the radar beacon to the antenna or in one of the connectors.

Signal strength degradation caused by main engine flame was very similar to that of SA-5. However, unlike SA-5, some of the signal strength data contained noise caused by main engine exhaust until inboard engine cutoff at 143 seconds.

Retrorocket ignition caused the signal level of all RF systems to drop below threshold. The C-band radar system recovered within 2.4 seconds, prior to any other system.

The ullage rocket exhaust did not noticeably affect the signal propagation. It is possible that the severe attenuation of the RF signals is caused by combining the ullage rocket and retrorocket exhausts.

SECTION I. INTRODUCTION

The SA-6 vehicle was launched from pad 37B, Cape Kennedy, Florida, on May 28, 1964, at 17:07:00 Zulu time and inserted into an elliptical orbit at 17:17:35. The flight dramatically demonstrated the capability of the ST-124 guidance system (a closed-loop path guidance) when an inboard engine was prematurely lost at 17:08:57. The first pass orbital parameters varied very little from the expected values (Table 1). SA-6 demonstrated the compatibility of the launch vehicle and the Apollo spacecraft. The spacecraft's environmental parameters during flight were verified and the launch escape system tower jettison scheme was demonstrated.

TABLE 1. ORBITAL PARAMETERS

	Predicted	Actual
Perigee	183 km	176. 96 km
Apogee	230 km	230. 89 km
Inclination	31. 8 deg	31. 78 deg
Period	88. 5 min	88. 62 min

The telemetry system on this vehicle consisted of 16 links transmitted over five groups of two antennas each. The onboard tracking systems included C-band radar, Minitrack, Mistram, Azusa/Glotrac, ODOP, and the radar altimeter.

Table 2 lists the sequence of events that could have affected the signal strength measurements during powered flight. The altitude history of SA-6 is shown in Figure 1. All times given in this report are referenced to range zero.

TABLE 2.   SEQUENCE OF EVENTS

Event	Range Time (seconds)
Range Zero	0.00
First Motion	0.17
EBW Ventport Firing	141.21
Open Lox/Sox Disposal System Valves Nos. 2, 3, 5, and 6	142.32
Cut Off S-I Inboard Engines	143.23
Open Lox/Sox Disposal System Valve No. 4	144.62
Open Lox/Sox Disposal System Valves Nos. 1 and 7	146.02
Cut Off Outboard Engines	149.23
Fire Ullage Rockets	149.50
Fire Separation Nuts S-I/S-IV	149.62
Retrorocket Ignition	149.65
Turn on S-IV Engines Igniters	151.32
Jettison LES Tower	161.62
Jettison S-IV Ullage Rockets	161.62
Jettison Cameras from S-I Stage	174.62
Cut Off All Engines	624.80
Insertion	634.80

SECTION II. VHF TELEMETRY

The VHF telemetry links used on SA-6 are described in Table 3.
Telemetry data were received at the following stations:

Cape Telemetry 2

Cape Telemetry 3

Hangar D

* New Smyrna Beach

Eglin Air Force Base

* Vero Beach

Bermuda

Wallops Island

Grand Bahama Island

San Salvador

Antigua

Ascension Island

Pretoria, South Africa

Carnarvon, Australia

Hawaii

California

White Sands

Green Mountain (MSFC)

---

* Recorded signal strength levels only.

4

TABLE 3. VEHICLE TELEMETRY SYSTEM DESCRIPTION

Link	Frequency (MHz)	Modulation	Power (watts)	Location
F1	241.5	PAM-FM-FM	25	
F2	248.6	PAM-FM-FM	25	
F3	246.3	PAM-FM-FM	25	S-I Stage
F4	243.8	PAM-FM-FM	25	Antenna System 1: F1, F3, S1
S1	252.4	SS-FM	25	Antenna System 2: F2, F4, S2
S2	256.2	SS-FM	25	
F5	249.9	FM-FM/FM	25	
F6	240.2	FM-FM/FM	25	
S3	259.7	SS-FM	25	Instrument Unit
P1	253.8	PCM-FM	12	
D1	251.5	PDM-FM-FM	10	
D2	255.1	PDM-FM-FM	10	S-IV Stage
D3	258.5	PDM-FM-FM	10	
A	237.8	PAM/FM	10	
B	247.3	FM	10	Apollo Boiler Plate BP 13
C	257.3	FM	10	

Links F1, F3, and S1 were transmitted over antenna system 1 and links F2, F4, and S2 over antenna system 2 of the S-I stage. Links F5, F6, S3, and P1 were transmitted over the IU antennas; links D1, D2, and D3 were transmitted from the S-IV stage antennas; and links A, B, and C were transmitted over the Apollo antenna system. The overall performance of the telemetry system is shown in Figure 2. Some typical curves of theoretical and measured signal strength are shown in Figures 3 to 14.

Theoretical values of signal strength are derived from the range equation

$$P_r = P_t \cdot G_r \cdot G_t \left(\frac{\lambda}{4\pi R}\right)^2$$

where P_r – power received

P_t – power transmitted

G_r – gain of the receiving antenna

G_t – gain of transmitting antenna

λ – wavelength

R – line of sight distance

The range is known from the trajectory of the flight, and the gain of the onboard transmitting antenna can be found by comparing the antenna gain contour plots with the signal line-of-sight angles. The theoretical value of signal strength can then be calculated by substitution of these values into the equation. Unfortunately, the antenna gains are taken only every five seconds. Thus some of the nulls that occur within this period may not show up in the theoretical curves. Indeed, periodic fluctuations caused by the antenna pattern nulls have been missed and only upon careful examination of all antenna contours has the null region been discovered. This situation will be alleviated soon. The antenna gains will be taken every two degrees and placed on magnetic tape. These tapes will then be used as an input to a digital computer to increase the accuracy of the theoretical curves.

Because of the various preamplifier gains available and a calibration procedure that excludes the preamplifier, the exact theoretical value may vary by several db. Therefore, when the theoretical value follows the measured but is a constant value above or below it, the theoretical value is shifted to compensate for this discrepancy. This situation could be alleviated by either calibrating in front of the preamplifier or by recording the preamplifier gain.

6

Except for the polarization effects reflected in the antenna gain contour plots, the theoretical values do not indicate any variations caused by such effects as multipath attenuation, rocket engine exhaust, or wave ellipticity. Multipath and rocket exhaust effects on the measured signal level have definite characteristics that are easily identified. However, wave ellipticity is not as easily recognizable. The ellipticity of a wave affects the value of the signal strength as measured by a left or right circularly polarized antenna. If the transmitted wave is linearly polarized, the magnitudes of the right circular and left circular measurements will be equal and one half the power of the linear wave. When the wave ellipticity changes, the gains in one type of polarization will be accompanied by losses in the other polarization since $\vec{E}_t = \vec{E}_R + \vec{E}_L$ where

$\vec{E}_t$ – total electric field strength

$\vec{E}_R$ – right circular electric field strength

$\vec{E}_L$ – left circular electric field strength

By direct comparison of both right and left circular measurements, occurrences that affect both polarizations in the same manner may be attributed to something other than polarization. When the signal level of only one type of polarization changes, it may be concluded that this is caused by a change in power density resulting from an offset in the antenna pattern. Therefore, the gain at this aspect angle, as derived from the antenna gain contour, is changed so that the power radiated in one polarization remains essentially constant while the power in the other changes.

All telemetry links performed satisfactorily on SA-6. The PCM link was lost prematurely because of a wiring error external to the system. The relay, through which the PCM link power was supplied, was connected to the short-lifetime battery. Data dropouts occurred during retrorocket burning at all stations and early in the flight at the Cape stations because of multipath reflections. Signal strength fluctuations caused by main engine flame attenuation were experienced at Cape Telemetry 2, Cape Telemetry 3, Hanger D, Eglin AFB, and New Smyrna Beach from 100 to 143 seconds. Data dropouts were also experienced at these stations during this time period. The other stations have a favorable aspect angle during this time and are not subjected to flame attenuation.

The attenuation caused by main engine flame was approximately the same on SA-6 as on SA-5. The S-I links experienced greater attenuation than any of the other links. This ranged from 18 db to 31 db at Hanger D and Cape Telemetry 2. The IU, S-IV stage, and spacecraft links experienced from 6 db of attenuation

at the Eglin station to 24 db at Hangar D. As on SA-5, the left circularly polarized signal strengths were affected an average of 2 to 3 db less by main engine flame than the right circular. Also similar to SA-5, the single sideband and PCM links were attenuated slightly less than the FM/FM links.

The stations experiencing flame attenuation were subjected to this interference at different times, depending on the individual aspect angle histories (Fig. 15). The main engine flame does not seem to interfere with the signal propagation until the station-to-vehicle aspect angle (Fig. 18) is less than the vehicle-antenna-to-plume-edge angle by more than three degrees. This indicates that the electrical (or interference) size of the plume is less than the optical size. The difference between these two angles is a function of several factors. The amount of engine thrust and the altitude of the vehicle are important parameters in determining the plume envelope size. The aspect angle is dependent upon the altitude, range, and tilt angles of the vehicle. Thus the difference between the two angles combines most of the important flame attenuation parameters into one function.

By comparing the aspect angle histories (Fig. 15) with the curves of flame attenuation (Figs. 16 through 19), it can be seen that there is a close correlation between flame attenuation and the angle found by subtracting the station-to-vehicle aspect angle from the vehicle-antenna-to-plume-edge aspect angle. (When this angle is greater than zero, the propagation path lies within the flame plume.) If this angle, called angle into the plume, is used in conjunction with the altitude history of the vehicle, then the effect of flame attenuation upon the signal strength of future Saturn vehicles may be roughly predicted.

After staging, the signal strength from the IU, S-IV stage, and spacecraft links became quite smooth, while the S-I stage links experienced severe fluctuations. These variations were caused by the antenna pattern as the vehicle rolled and tumbled. From 220 to 300 seconds, the signal strength experienced degradation caused by the low aspect angle of less than three degrees during this period. When the aspect angle approaches the tail of the vehicle (zero degrees), the accuracy of the aspect angles becomes questionable. Hence the theoretical value of signal strength may be off because of the use of an erroneous antenna gain. In this region, the antenna gain fluctuates severely with a small change in angle.

Figure 20 shows that the signal strength dropped to threshold at the precise time the retrorocket exhaust became visible. Since ullage rockets had

fired 0.14 seconds earlier, it can be assumed that the effects of ullage rockets are negligible compared to the effects of retrorocket exhaust.

SECTION III. TRACKING SYSTEMS

A. C-BAND RADAR

The following stations received C-band radar tracking data:

Cape Kennedy

Patrick Air Force Base

Grand Bahama Island

San Salvador

Grand Turk

Antigua

Ascension Island

Pretoria, South Africa

A summary of the C-band radar coverage is shown in Figure 21.

Signal strength data (Figs. 22 to 26) indicate that the system did not perform as well as was expected. The signal strength levels were continually lower than the theoretical values by as much as 20 db. Most stations were about 10 db low during the first portion of flight. The Cape Kennedy record (Fig. 22) shows a 25 to 30 db null accompanied by severe fluctuations from 65 to 82 seconds because of polarization. These severe fluctuations were caused by antenna searching which was brought about by the low signal level. Patrick Air Force Base (Fig. 23) also recorded the first portion of flight, but the recorder at this station was saturated until 90 seconds after liftoff. This station normally measures about 6 db above the theoretical values. On this flight, the measured value was 13 db below the theoretical signal strength, indicating some discrepancy.

At 480 seconds, at an altitude of 196 km, there was an instantaneous 10 db drop in signal level. This caused the Cape Kennedy and the Grand Bahama Island stations to lose data and the Antigua station data to be questionable. Grand Turk was the only station that received an adequate signal level for tracking

despite this drop. This phenomenon also occurred on the SA-5 vehicle at 472.8 seconds at an altitude of 265 km. However, the signal on SA-6 was much more erratic than on the previous flight. A thorough investigation of this problem was performed at MSFC. There was no indication of trouble in the vehicle's electrical networks. Temperature and vibration measurements were normal during flight. During testing, a connector or cable connecting the beacon to the antenna arced, causing a loss of transmitted power. After replacing this cable, the situation cleared and no further breakdowns could be induced. Further testing of the beacon used on SA-6 (DPN-55) revealed that the tolerance of the transponder was such that a slight change of load phasing (as little as 10 degrees) could cause a 9 MHz frequency shift. It was discovered that the antenna VSWR at the operating frequency placed the transponder at a critical operating point. In an attempt to alleviate this problem, the DPN-55 transponder is being replaced with a DPN-66 on SA-7. Future flights will carry an SST-131 transponder, which provides much greater isolation between antenna and magnetron than the DPN-55 and approximately the same isolation as the DPN-66.

Retrorocket ignition caused a drop to threshold. This was about 25 to 30 db instead of the 45 db experienced on previous flights because of the low signal levels prior to ignition. Except for the Cape Kennedy station, this system was the first to recover from retrorockets. It recovered approximately 2.5 seconds after ignition, but the signal was quite noisy for about 2 seconds after recovery.

B. ODOP

The ODOP system performed exceptionally well during the SA-6 flight and provided some of the best metric data ever received at MSFC from this type of system. The Cape stations maintained phase lock past 400 seconds (Mandy tracked to 520 seconds) and the AGC recordings deviate very little from the theoretical values. The Jade station records (Figs. 27 and 28) deviate about 6 db from 130 to 140 seconds, the Pluto station (Fig. 29) about 22 db from 115 to 130 seconds, and the Tango station (Fig. 30) 22 db from 115 to 130 seconds because of main engine flame attenuation. Some very light main engine flame attenuation (4 db) is seen in the Mandy station record (Fig. 31).

The flame attenuation at Mandy begins at 114 seconds and lasts through 140 seconds, while the Tango and Pluto stations experienced 23 db of attenuation starting at 101 and 115 seconds, respectively. The flame attenuation starts at different times at each station because of the difference in aspect angle histories (Fig. 33). The difference in the amounts of attenuation experienced by each station is caused by the differences in the distances the signal must

travel through the main engine exhaust plume. Figures 34 and 35 are plots of flame attenuation versus time and angle into the exhaust plume, respectively. While the angle into the exhaust plume is not a true indication of the distance through the plume, it is a measure of the relative path length in the plume from each station; i.e., the closer to 90 degrees, the longer the path length. Therefore, it can be seen that increasing attenuation would be expected at the Metro, Mandy, Jade, Pluto, and Tango stations, respectively. The measured values of attenuation verify this except for Pluto experiencing the same amount of attenuation as Tango. However, this amount of attenuation (22 db) may be the maximum amount of flame attenuation possible at either station.

The Metro station (Fig. 32) experienced a 22 db decrease from 137 to 147 seconds. Since there was no noise modulation of the signal at this time, the loss is attributed to polarization losses and ventport firings. Further, it can be seen by comparison of the left circular with the right circular record from Jade (Figs. 27 and 28) that a 12 db polarization null occurs from 135 to 138 seconds. This effect, quite similar at both the Jade and Metro stations, is therefore judged to be the same phenomenon.

EBW ventports were fired at 141.2 seconds and the lox/sox purge valves were vented at 142.3 seconds. These two events occurred within such a short time span that the two effects on each station cannot be separated. The decreases in signal level caused by these events varied from 7.5 to 12 db, but it cannot be determined which event caused the more attenuation.

All stations were blanked out from 149.6 to 155 seconds by the retro-rockets. The UDOP system on SA-5 was also out for six seconds during retro-rocket firing. The Metro phase lock receiver, after retrorocket burning, was still 14 db down for 15 seconds after the standard receiver had fully recovered. The onboard transmitter lost lock during staging. While the transmitter was being brought back to frequency, the station detuned in an attempt to acquire lock, causing the long period of phase-lock loss. However, the signal level of the phase-lock receiver during this period was greater than -97 dbm, well above threshold. Therefore, the system would have recovered fully after a six second interval if lock had been acquired at that time. Signal strength curves from all stations smoothed out greatly after staging; this indicated that the S-I booster flame, while not attenuating the signal specifically, did cause degradation of the signal strengths.

C. AZUSA/GLOTRAC

The following Azusa/Glotrac stations were utilized in support of the SA-6 flight:

Azusa Mark II

Atlantic Site

Bermuda

San Salvador

Grand Turk

Antigua

Signal strength curves for these stations, with the exception of the Atlantic site, are plotted in Figures 36 through 40. The Atlantic Glotrac station received no signal strength data during this test.

Although Bermuda and Antigua received the signal, additional tracking data could have been obtained from these sites if the antenna pattern had been more favorable. According to available antenna contours, these sites were never illuminated by the horizontal component of the radiated signal and only slightly illuminated by the vertical component. The antenna contour gain value, less than -30 db, resulted in minimal periods of usable data. The other Glotrac sites experienced similar, though less severe, effects. The ragged appearance of the signal strength curves is caused by the unfavorable antenna pattern visibility. The signal received at the Azusa MK II station was not severely affected by this condition. Despite the antenna problem, simultaneous phase lock by three or more stations was obtained from approximately 220 to 520 seconds.

Switchover from the Azusa transmitter to the San Salvador transmitter occurred at 535 seconds. Following handover, only the San Salvador and Antigua stations were able to maintain phase lock for longer than 20 seconds.

Azusa MK II and San Salvador dropped to threshold at retrorocket ignition. These sites also experienced a 30 to 35 db drop in signal at 162 seconds because of the jettison of the escape tower.

A new antenna has been installed to provide higher gains for the Glotrac stations on future flights.

Azusa MK II signal strength and phase-lock periods are plotted in Figure 36. This station actively tracked from 0 to 535 seconds, maintaining phase lock from 6 to 535 seconds. A six-second dropout caused by retrorockets began at 149.6 seconds. Reductions in signal level at 40, 50, 60, 70, and 100 seconds correspond to drops in the horizontal component of the antenna pattern (Fig. 41). The signal drop at approximately 162 seconds can be attributed to jettison of the escape tower. More metric data were obtained than on previous flights, but the degradation of signal at separation was more severe for this test.

No data were received from the Atlantic station because of the low elevation angles (8 to 9 degrees) and unfavorable antenna pattern gains. The station fell into an undefined portion of the contour plots where the gains were lower than -15 db.

San Salvador signal strength and phase-lock periods are plotted in Figure 37. Phase lock was essentially continuous from 160 to 550 seconds. The phase unlock at 230 seconds was caused by lack of advance warning of the transmission of the Azusa MK II time tone. Signal strength dips at approximately 345, 360, 380, 410, and 445 seconds correspond to drops in the horizontal component of the antenna gain pattern as shown in Figure 41. Prior to 290 seconds, the line of sight is in an undefined portion of the antenna pattern; therefore, predictions could not be made for this period. Switchover to the San Salvador transmitter occurred at 535 seconds.

Grand Turk signal strength and phase-lock periods are plotted in Figure 38. Phase lock was maintained from 210 to 477 seconds, which was the longest period of continuous lock from any of the Glotrac stations. The signal strength curve from this site is smoother and shows less severe signal fluctuations than those from the other sites. Excellent tracking data were received during this interval. Fluctuations in the antenna gain pattern produced corresponding 5 to 10 db fluctuations in received signal strength at 453, 503, and 527 seconds. Prior to 420 seconds, the station was looking at an undefined portion of the antenna pattern.

Bermuda signal strength and phase-lock periods are shown in Figure 39. The Bermuda site provided little usable tracking data. Phase lock was maintained only between 275 and 385 seconds and for intermittent periods thereafter. This was caused by low elevation angles and the long

range of a 105° azimuth trajectory. Also, Bermuda was looking into an unfavorable portion of the antenna pattern.

Antigua signal strength and phase-lock times are plotted in Figure 40. This station suffered degradation of signal and relatively short periods of phase lock caused by unfavorable antenna pattern visibility. Phase lock was maintained from 405 to 520 seconds and for intermittent periods, not exceeding 30 seconds, after handover.

D. MISTRAM

Mistram I ATSS functions and signal strength versus time are shown in Figure 42. Antenna polarization position and polarization error are plotted in Figure 43.

The signal was detected and phase locked by the ATSS ground receiver at six seconds. Phase lock was maintained until loss of signal at 490 seconds except during retro firing and at handover. Automatic track and polarization track began at 21 seconds and were maintained until 298.6 and 296 seconds, respectively, except during retro firing. Poor aspect angles caused loss of signal approximately two seconds prior to active-passive handover at 299 seconds. Automatic track was resumed at 307 seconds and continued until 490 seconds, followed by a short period of intermittent track to 533 seconds.

In general, Mistram I tracking data were excellent. However, one unpredicted event did occur between 178 and 186 seconds. During this period, the RF line of sight to the vehicle traversed through a portion of the antenna pattern having a sudden 11 db drop in the horizontal component (Fig. 44). The corresponding polarization change of the received signal resulted in a polarization error in excess of 12 degrees at the ground receiver and a corresponding 6 to 8 db drop in signal strength. The error signal caused the antenna tracker to rotate through approximately 187 degrees before locking in at 186 seconds. The polarization error was transmitted as present position pointing data to the remote sites, causing similar reductions in signal strength level in the PMSS data receivers. The overall metric data were not affected during this event.

Mistram II ATSS functions and signal strength versus time are shown in Figure 45. Antenna polarization position plots are shown in Figure 46, and polarization errors are plotted in Figure 45.

14

The Mistram II site acquired the signal at 89 seconds, lost phase lock at 98 seconds, reacquired at 102 seconds, and continued until the expected dropout at 149.7 seconds. Automatic track was intermittent until 106 seconds, after which continuous track was maintained until retrorocket dropout.

Persistent difficulty was encountered in obtaining and maintaining automatic polarization track throughout the passive mode. The only period of automatic polarization track was from 204 to 212 seconds. Between 110 and 150 seconds, polarization was manually rotated through 793 degrees in an unsuccessful attempt to locate and track the maximum field component. The polarization error was consistently in excess of 30 degrees; although for automatic polarization track, servo errors must be 15 degrees or less. As the antenna approached the cross polarized condition at approximately 75 degrees, the servo was unable to properly distinguish between azimuth and elevation errors. The resulting antenna mispointing produced severe reductions in the received signal levels and caused complete dropouts on two occasions.

Phase lock was reestablished at 153 seconds and a brief period of automatic track occurred between 154 and 168 seconds. The signal experienced a drop of approximately 25 db when polarization was rotated through 82 degrees between 160 and 165 seconds in a further attempt to obtain automatic polarization track. Automatic track was resumed at 175 seconds, but was interrupted at 212 seconds when the polarization was again manually rotated through 90 degrees. Phase lock was maintained but automatic track was lost for six seconds during this period. Signal strength remained low until 220 seconds when the antenna polarization was returned to 320 degrees. From 240 to 300 seconds, polarization was manually rotated through 920 degrees, which produced several fluctuations in the signal level. The largest of these fluctuations was a 10 db drop at 267 seconds. After handover at 300 seconds, the antenna appeared to be cross polarized, which made automatic track difficult until the polarization was manually rotated through 60 degrees at 318 seconds. Signal level fluctuations of 20 to 25 db occurred during this period. Automatic track was maintained from 318 to 580 seconds. Manual polarization tracking was used throughout the active mode.

Correlation of the Mistram II measured signal strength dropouts with polarization and the vehicle antenna radiation pattern is difficult because of the periods of manual polarization rotation and the complete lack of automatic polarization tracking. The horizontal antenna pattern nulls of 5 to 8 db occurred at approximately 175, 230, and 260 seconds. These correspond fairly closely to the signal dropout periods at 165 to 175, 210 to 220, and 265 to 270 seconds. The antenna radiation pattern variations may have been partly responsible for

difficulty in polarization tracking during the passive mode. Less severe events occurred on SA-5, producing correlated dropouts with the polarization tracking functions at approximately the same time periods.

E. MINITRACK

The Minitrack system successfully tracked SA-6 throughout its flight, but no telemetry measurements were transmitted on this flight.

A graph of theoretical and measured signal strength from the Mandy station is shown in Figure 47. The measured values deviate from the theoretical values in several places. An unexplained 20 db drop occurred at approximately 60 seconds. The decrease began at 40 seconds and recovered by 80 seconds. From 110 seconds through retrorocket firing, main engine flame caused from 6 db to 15 db loss in signal strength. Lox/sox purge valve opening caused a 14 db decrease at 146 seconds, and retrorocket ignition caused the system to drop at least 37 db to below threshold.

An unexplained phenomenon occurred from 220 to 320 seconds. The signal level was 15 db below the theoretical value and appeared to be modulated much the same as the signal during main engine flame. However, the aspect angle was very unfavorable (1 to 2 degrees) during this period. The station was looking into a null in the antenna pattern which could have caused these perturbations.

This system experienced severe phase errors during the time of S-I stage main engine flame attenuation, during retrorocket ignition, and after 200 seconds. The errors resulting from main engine and retrorocket flame were expected. However, no interference was anticipated after retrorocket burning. Careful investigation leads to the theory that the fluctuations are probably caused by a combination of slow AGC response at the ground receiver and lobing in the antenna patterns. During this period, the aspect angle was approximately one degree or less off the tail of the vehicle and the antenna pattern in this vicinity contained numerous fluctuations. The data from SA-7 should help to verify the cause of these phase errors.

SECTION IV. SPECIAL SYSTEMS

A. DIGITAL COMMAND SYSTEM

A special experiment utilizing the onboard digital command system was performed on Ascension Island for the first time. The purpose of this experiment was to test the use of this digital command system with the onboard computer system. Coded signals were transmitted to the command receiver by an AN/FRW-2 transmitter. When received and decoded onboard, they were sent to the onboard computer, which is capable of controlling the vehicle. Two indications were used to determine if the data were received. An FM-FM telemetry link transmitted a relay reset pulse which indicated that the entire 35 bit word had been received. The second indication was given by the PCM-FM telemetry link which sampled the computer message and transmitted it back to the ground to compare with the transmitted message. A total of 273 words was transmitted to the vehicle from Ascension Island, and indications are that all 273 words were received onboard.

At the last minute, the decision was made to try to interrogate the receiver from Green Mountain. The purpose of this test was to determine how this system would work under very unfavorable conditions. The maximum elevation angle reached by the vehicle from this station was three degrees. Along with the rolling and tumbling of the vehicle, this was one of the worst conditions under which the system would ever have to operate. Two groups of messages were transmitted to the vehicle. In the first group, 71 words were transmitted and 70 were definitely received and accepted onboard. In the second group, 67 words were transmitted and 65 were definitely received onboard. The messages that were lost occurred at elevation angles well below one degree. The results of both of these tests exceeded all expectations.

B. COMMAND DESTRUCT SYSTEM

Each live stage carried two command destruct receivers. The AGC voltage was monitored on a 120-sample-per-second channel, recorded, and played back after separation. The playback indicated that this receiver received the carrier through the period of retrorocket ignition without losing capture. Some question has arisen as to the validity of this measurement. If this signal did pass through the flame without being completely blacked out, it was the only one that did. Particular attention will be given to this problem in the future because of the importance of the command system.

C. RADAR ALTIMETER

The increased sensitivity of the altimeter over that of previous flights enabled this system to operate satisfactorily throughout most of the flight. The system provided acceptable data from 160 to 640 seconds with the exception of a 100 second period from 360 to 460 seconds when dropouts occurred. Prior to 360 seconds, there seemed to be a bias in the data of approximately -140 meters. After 460 seconds the error seemed to be reduced to -90 meters. This was probably caused by an error in the preflight calibration procedure which can be corrected for future flights.

D. ONBOARD TELEVISION CAMERAS

SA-6 carried two television cameras. One was placed in the lower area of engine compartment 2 to obtain general information about the operation of the engine components. The other was placed on the exterior of the interstage of the S-I and S-IV stages to view staging. Problems existed in both locations.

The lens of the external camera gradually became coated with some substance, probably thermal lag, which caused the picture to fade out. Staging helped to restore the picture and the system recovered sufficiently to see the S-IV stage as it left the S-I stage. The movie cameras on SA-5 had the same problem, but this was alleviated on SA-6 by a self purging system. However, there was not time to install this system on the television cameras. A similar purge system will be used on the external television cameras for future flights to improve the picture quality and increase the amount of information available.

The internal camera worked well and detected a vapor cloud in the engine compartment during flight. However, this cloud eclipsed the engine components and caused loss of the picture at 19 seconds. This condition improved only slightly later in flight.

The TV signal was attenuated by the S-I booster flame. This attenuation reached a peak of 16 db at 131 seconds, causing the signal level to drop below the threshold of the receiver (Fig. 48). The attenuation was severe enough to cause eight seconds of signal loss from 126 to 134 seconds. To overcome this problem, a television ground station has been requested at Vero Beach where the aspect angle history is such that no main engine flame attenuation is experienced. The signal strength from this system (Fig. 49) was acceptable although it was from 6 to 10 db down from the theoretical during the first 150 seconds of flight. The variations in signal level after 150 seconds are caused by rolling and tumbling of the S-I stage where the cameras were located, but there

18

does not seem to be any explanation for the low signal level during the first 150 seconds. Signal levels from the SA-5 flight (similar to SA-6) compare favorably with both SA-5 and SA-6 theoretical values. The Mandy station calibrated their system in front of the preamplifier, thereby excluding any error in calculated values caused by the inclusion of an erroneous preamplifier gain.

SECTION V. CONCLUSIONS AND RECOMMENDATIONS

As a result of the data from the SA-6 flight, several changes either have been made or are in the process of being made. The DPN-55 radar beacon, flown on SA-6, has been replaced because it was very sensitive to slight changes in VSWR. Power output and VSWR measurements have been added to the C-band system.

A new Azusa/Glotrac antenna has been put on the SA-7 vehicle to improve this system's coverage. This should result in more high quality metric data.

Since Vero Beach provides an advantageous aspect angle history, it has been requested that both a telemetry and a television ground station be installed at this site. This would eliminate any interference from the main engine exhaust plume. Since this represents from 16 to 25 db of attenuation, loss of data would be prevented during this time interval.

If the Mistram transmitter antenna on the instrument unit could be located 10 to 15 degrees closer to Fin I, the system performance could be improved. The gain variations associated with 105 degree launch azimuth at Mistram I and II would be smoothed and the polarization dropouts experienced on SA-5 and SA-6 would be considerably reduced.

Additional information about the effects of rocket engine exhaust has been gathered. It has been definitely shown that the maximum attenuation based on altitude alone cannot be predicted. A more dominant factor is the angle the line-of-sight propagation path makes with the edge of the exhaust plume. This may be caused by either the angle of incidence or the length of path inside the plume, or both. Investigations to date tend to show that maximum attenuation is a function of both altitude and the angle the propagation path makes with the exhaust plume edge.

As on SA-5, ullage rockets alone had no noticeable effect on RF signal propagation. It is recommended that an investigation be conducted to study the feasibility of using ullage rocket fuels for retrorockets and to study the effects of such a substitution on RF signal propagation.

The task of analysis of actual flight signal strength data would be greatly simplified if, wherever possible, calibrations could be made in front of any system preamplifier. If the calibration procedure used was noted in the station log and sent with the data, the need for "engineering judgments" would be greatly reduced. This would increase the accuracy of the calculated values of signal strength and would help to eliminate any deviations caused by system performance.

To increase the accuracy of the theoretical (calculated) values of signal strength and to separate antenna pattern effects from external disturbances, two different types of antenna gain calculations are being considered. One is the possibility of increasing the number of points taken to plot the antenna gain. At present, the gain is measured every ten degrees around the vehicle. The possibility of recording the gain every two degrees is being considered. This would necessitate the use of magnetic tape to store the antenna patterns and the rewriting of several computer programs for compatibility.

A second method of improving the accuracy of the theoretical values is that of using a vehicle scale model with the actual trajectory. The antenna gain at any time would then be measured from the scale model rather than taken from a chart. This method would eliminate the linear interpolations necessary with the antenna gain contour charts, and the resolution would be limited only by the servo system used to position the model.

20
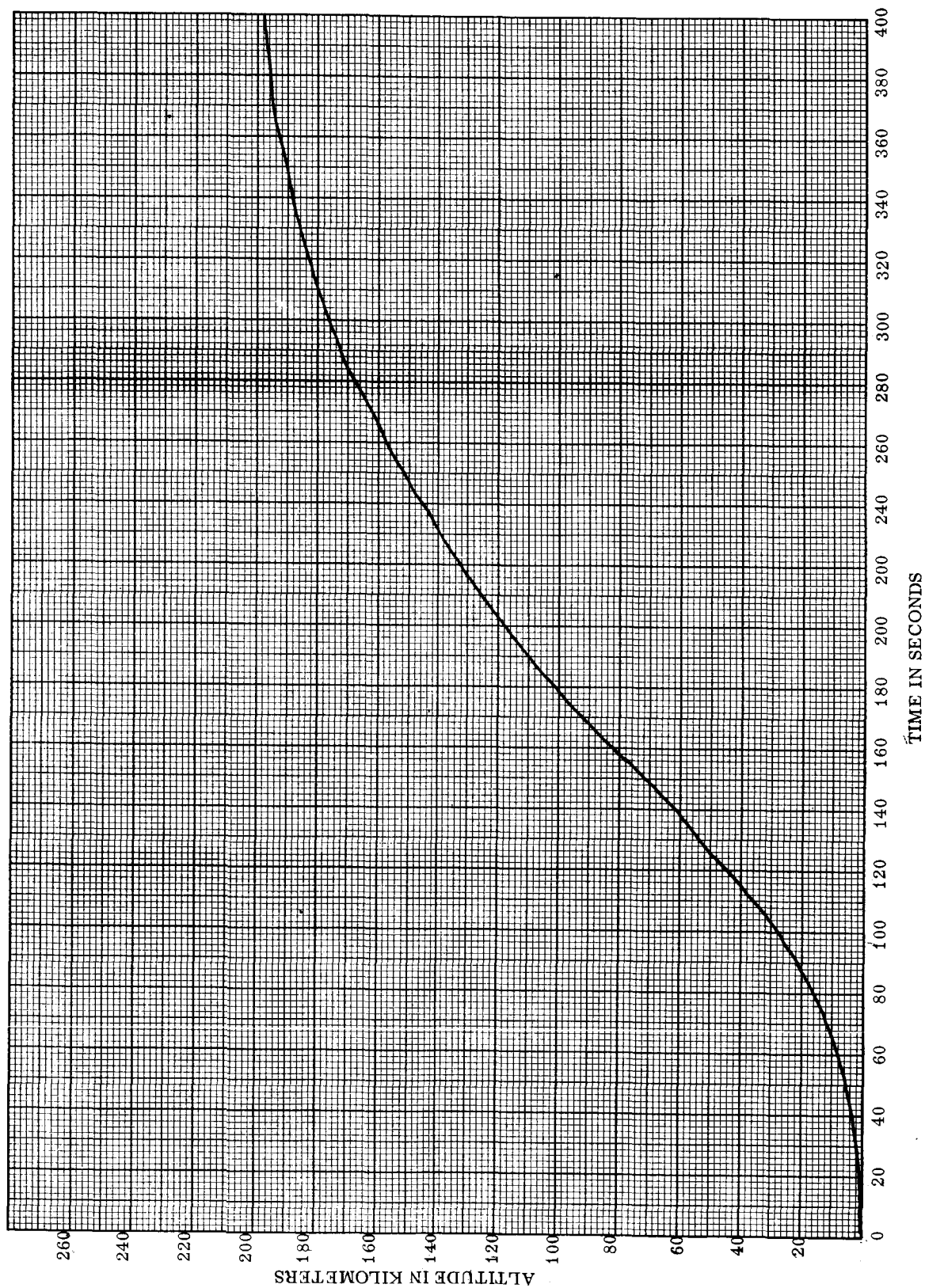
FIGURE 1. ALTITUDE HISTORY

21
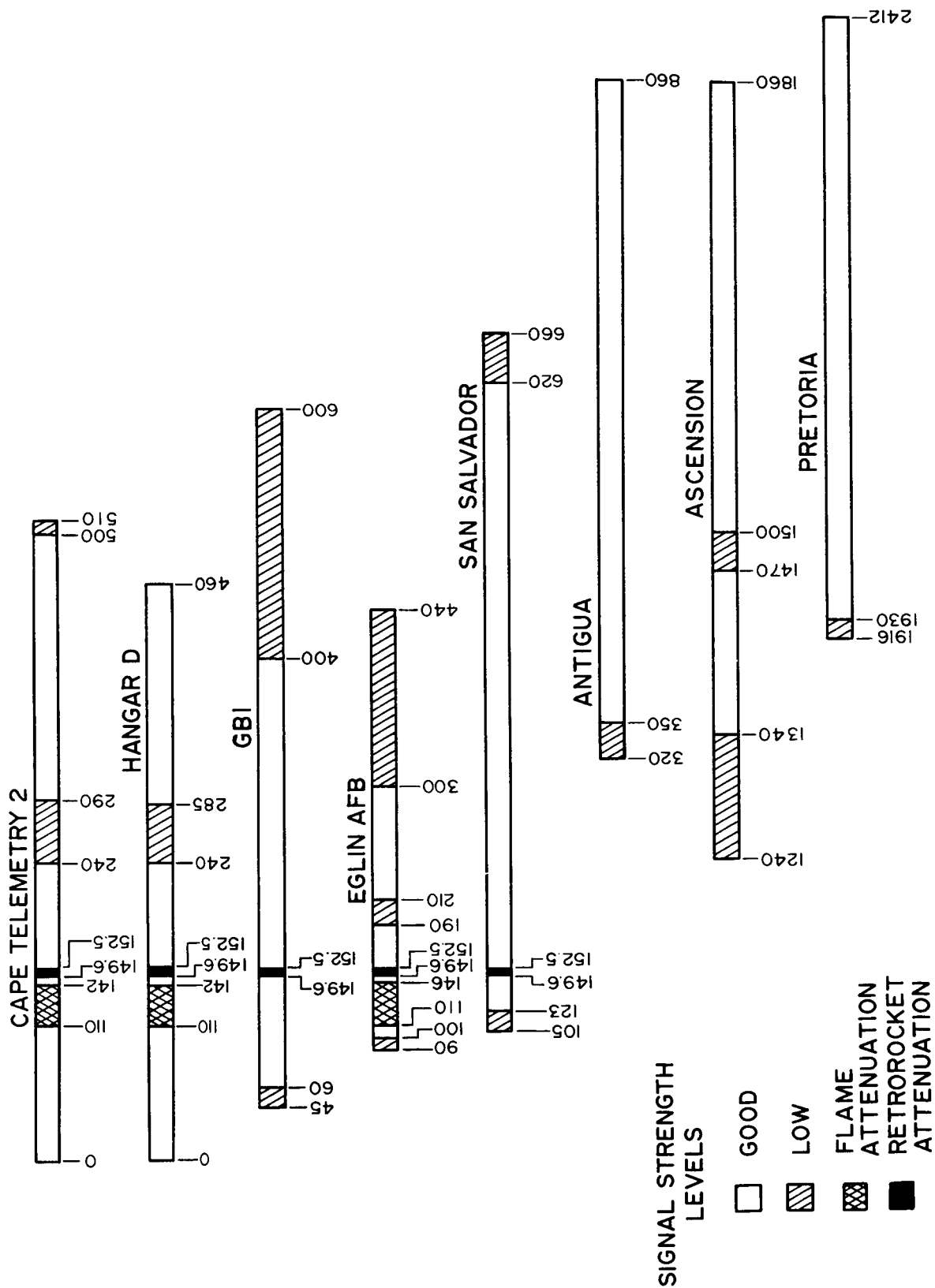
FIGURE 2. TELEMETRY STATION COVERAGE
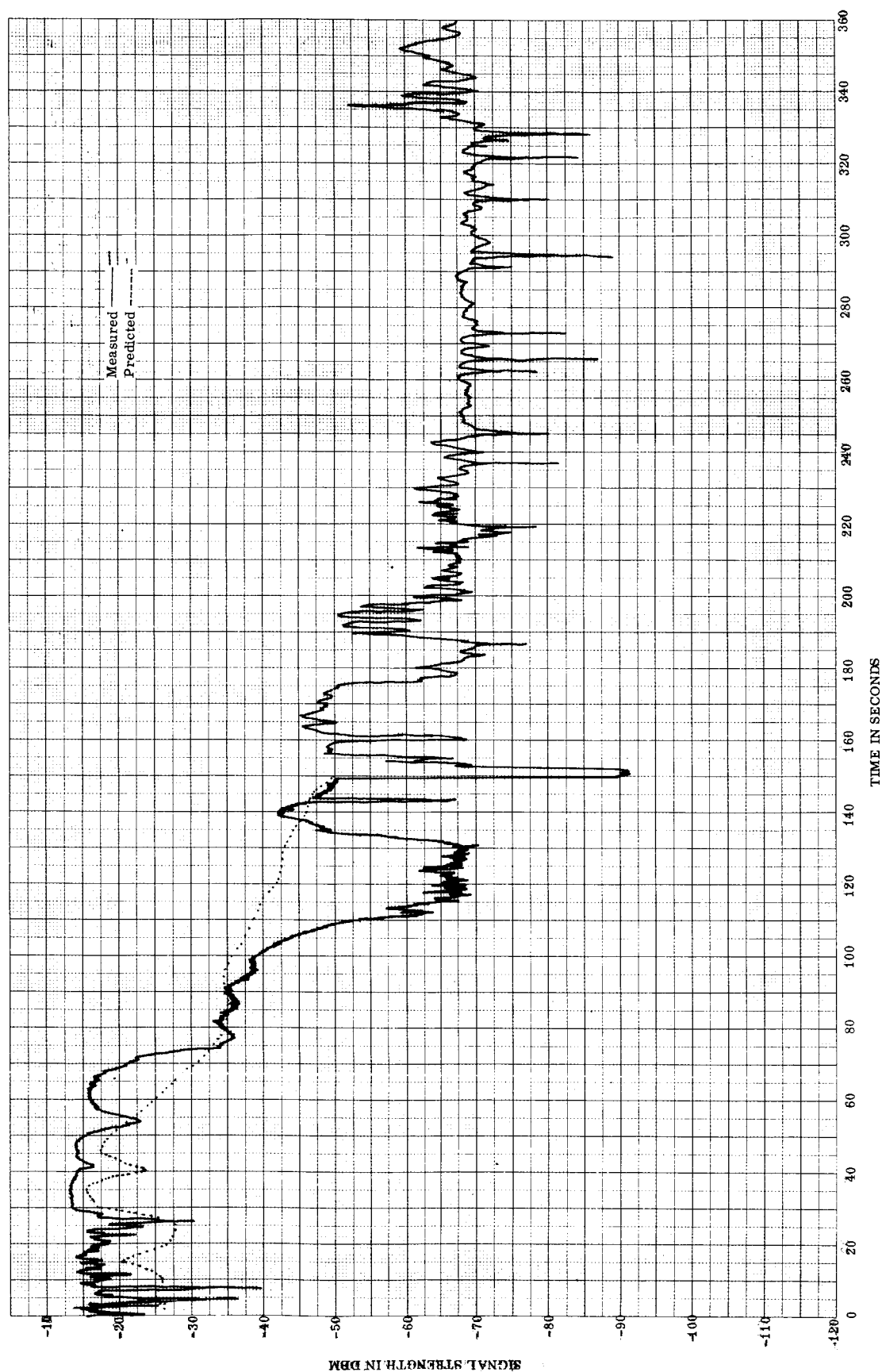
FIGURE 3. CAPE TELEMETRY 2 SIGNAL STRENGTH, LINK F1, LEFT CIRCULAR POLARIZATION

23
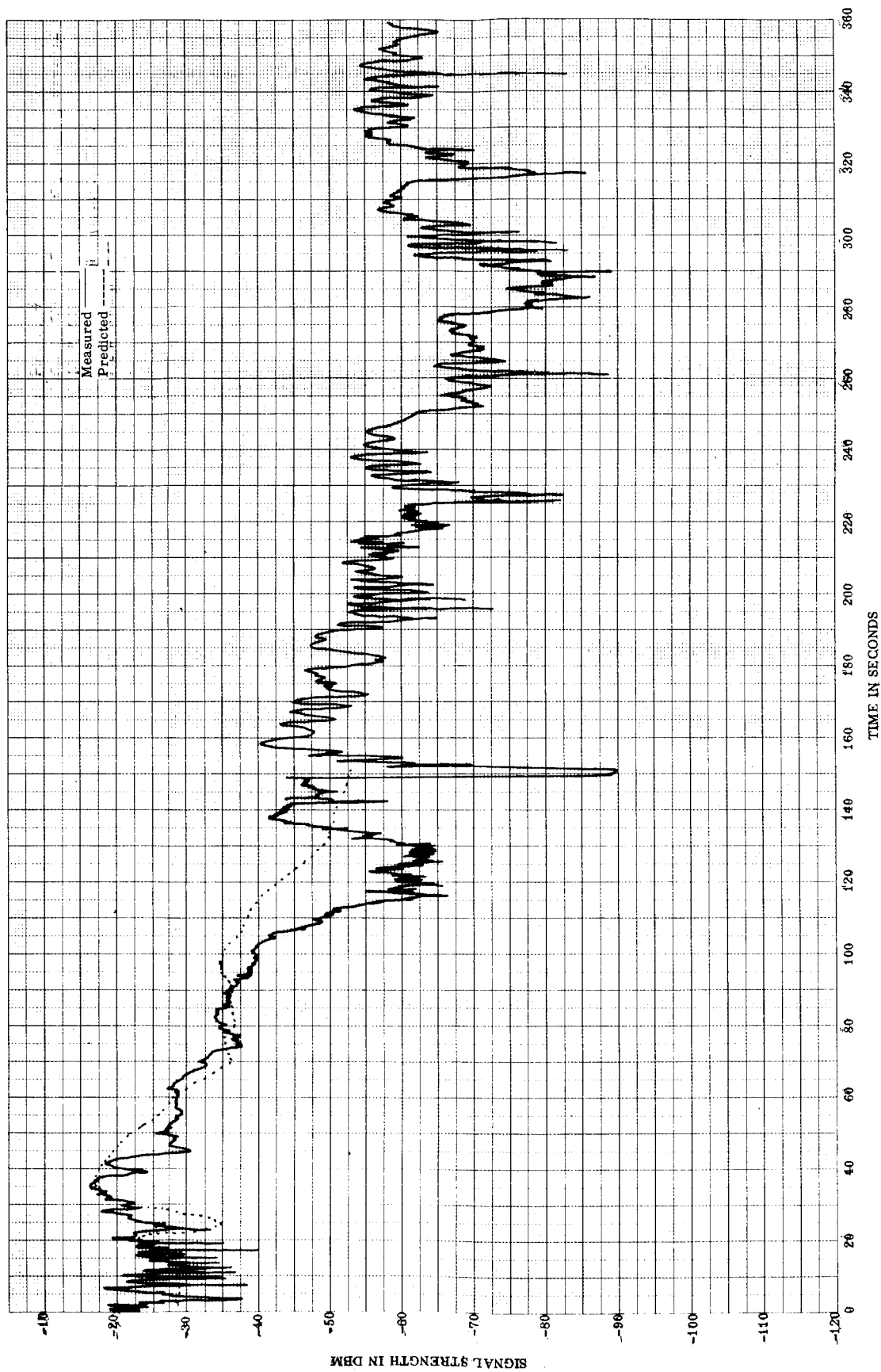
FIGURE 4. CAPE TELEMETRY 2 SIGNAL STRENGTH, LINK S2, LEFT CIRCULAR POLARIZATION
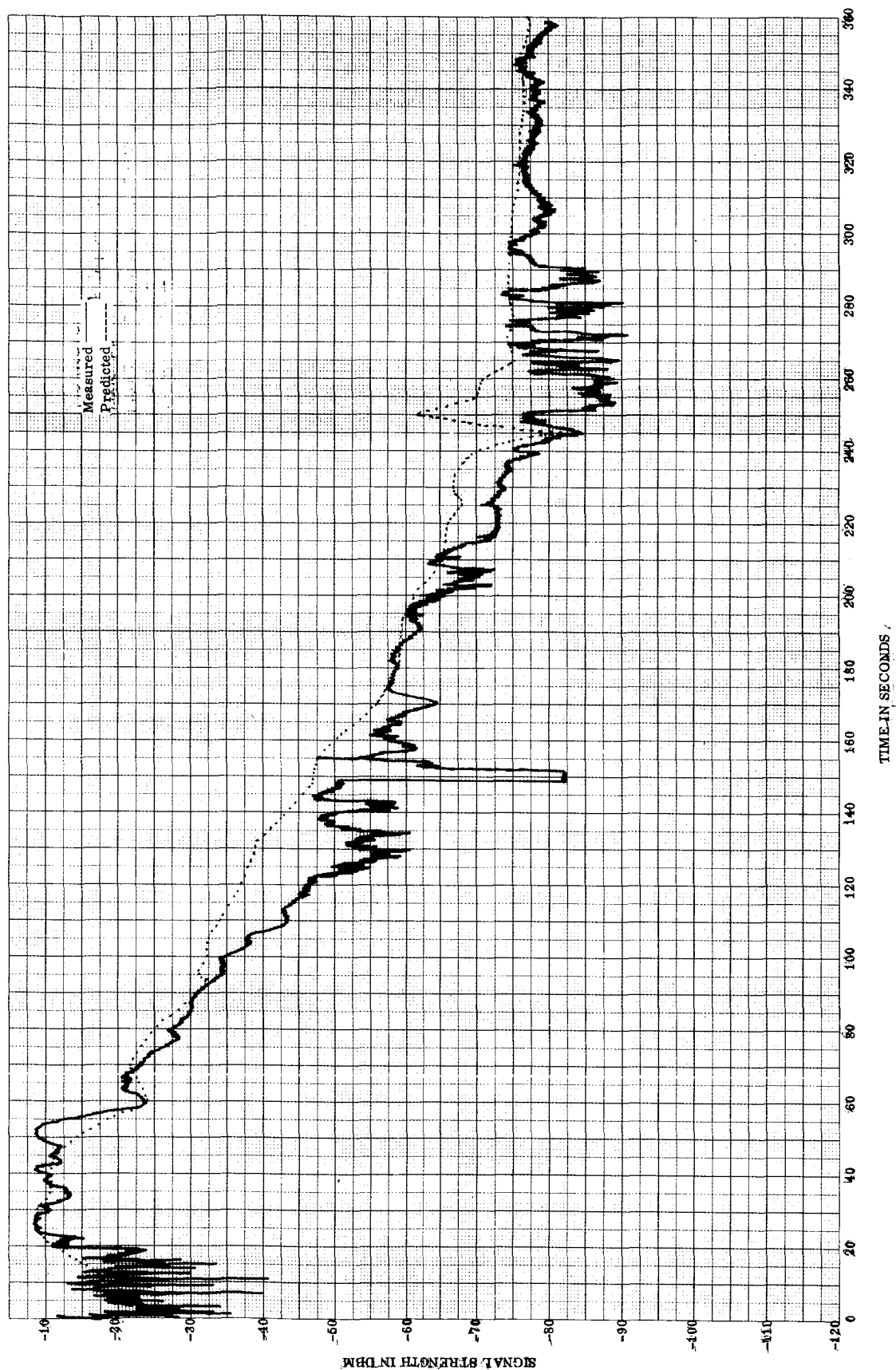
FIGURE 5. CAPE TELEMETRY 2 SIGNAL STRENGTH, LINK F6, RIGHT CIRCULAR POLARIZATION

25
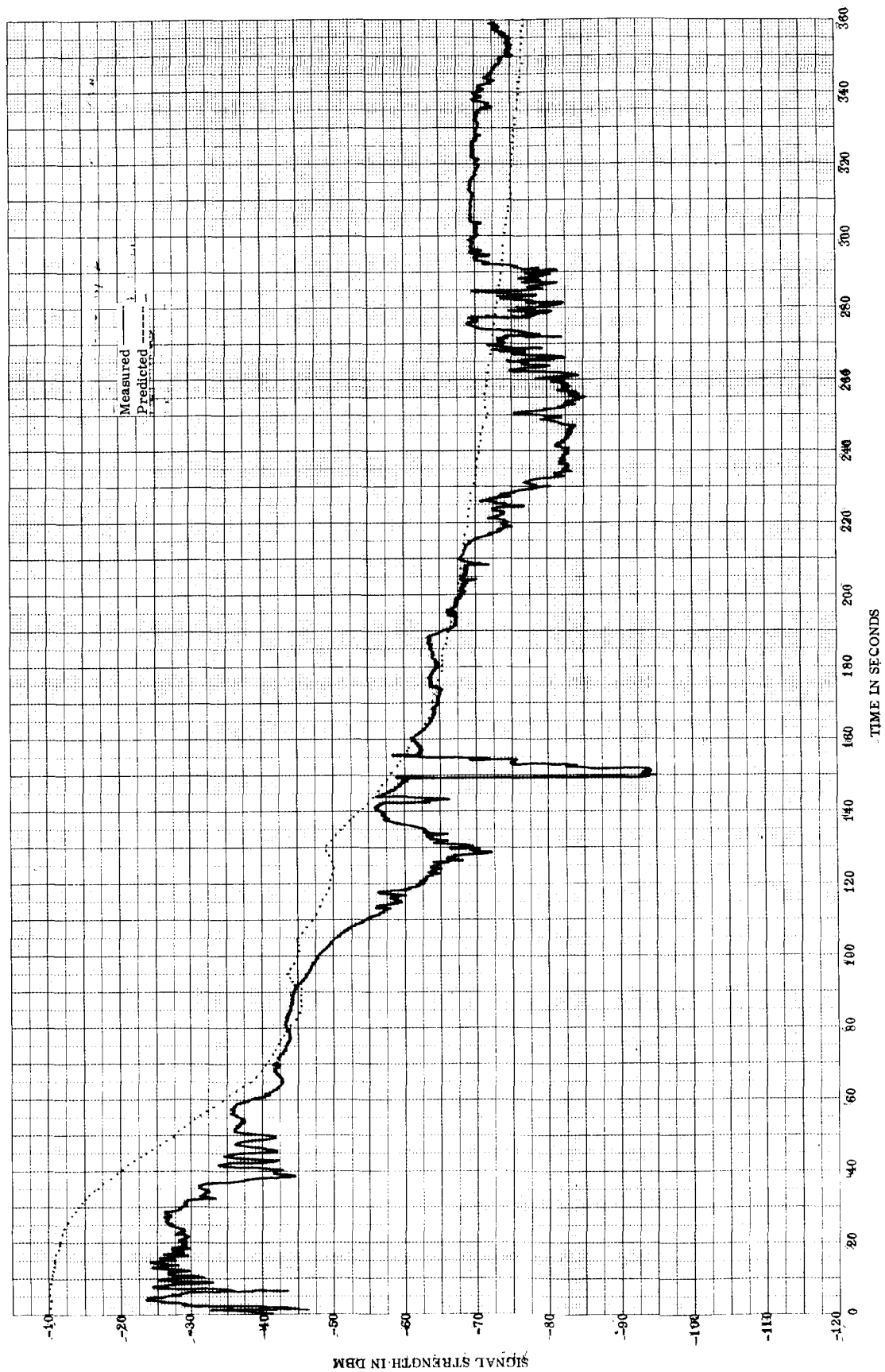
FIGURE 6. CAPE TELEMETRY 2 SIGNAL STRENGTH, LINK C, LEFT CIRCULAR POLARIZATION

26
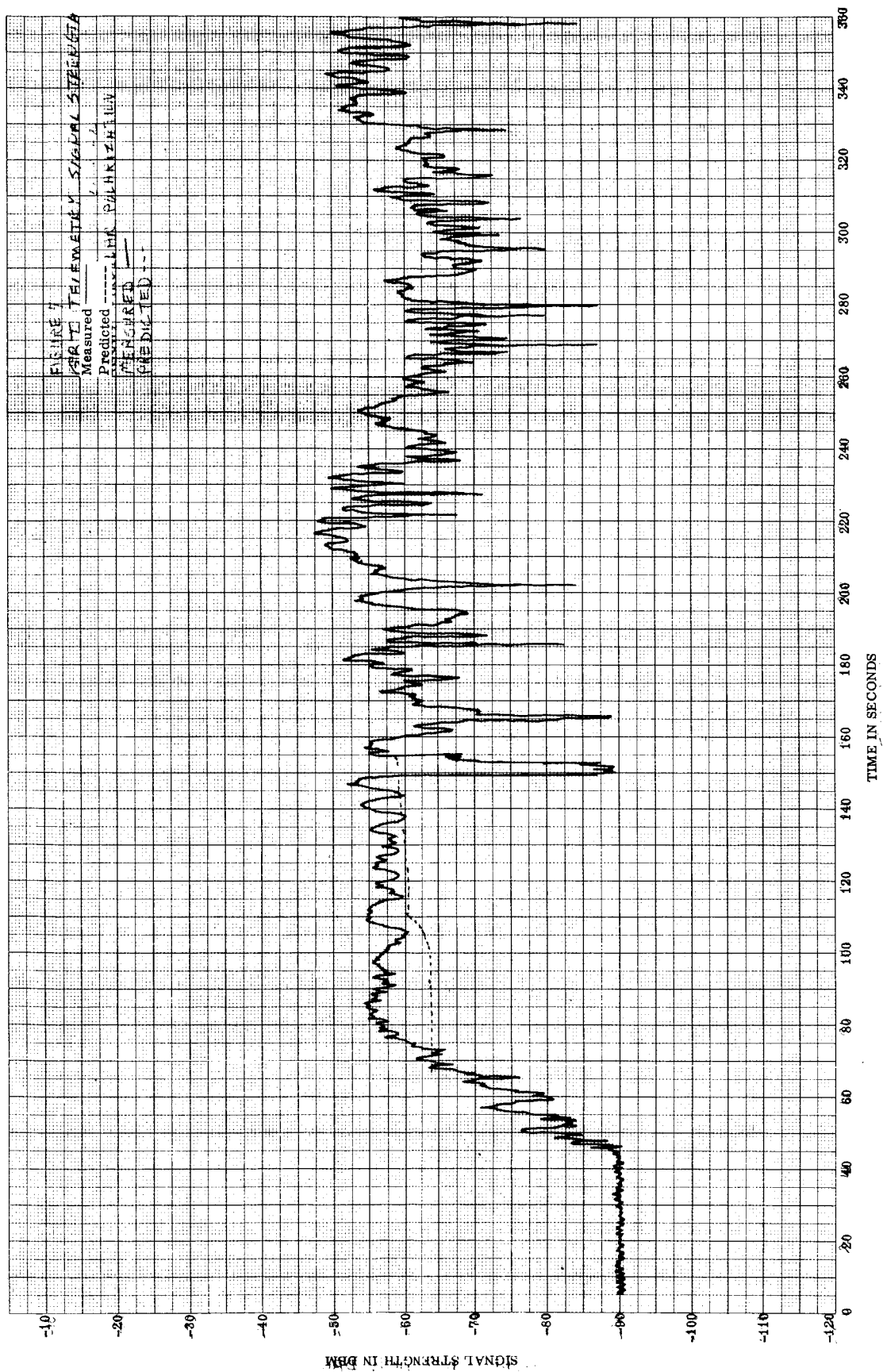
FIGURE 7. GBI TELEMETRY SIGNAL STRENGTH, LINK F2, RIGHT CIRCULAR POLARIZATION

27
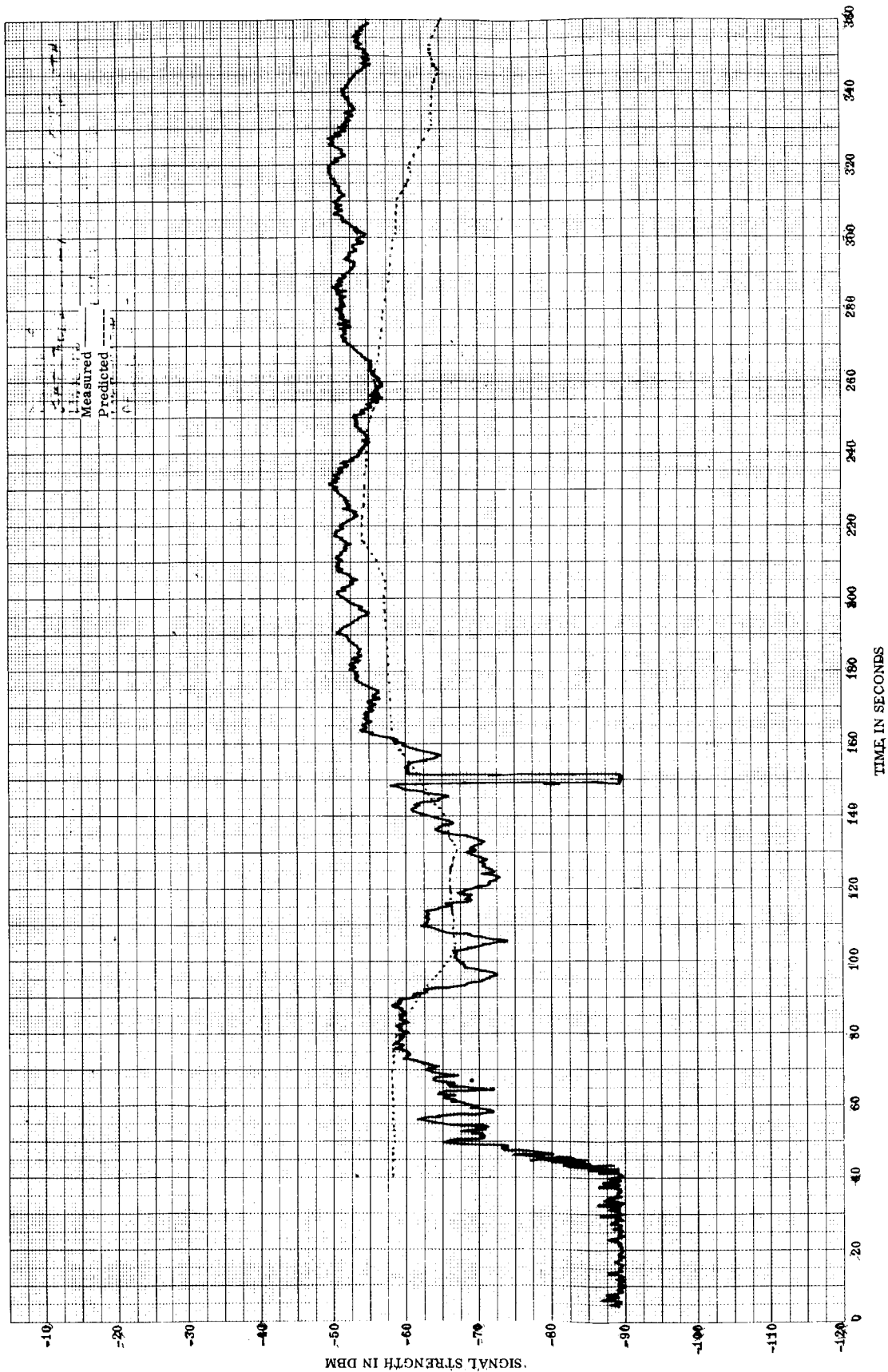
FIGURE 8. GBI TELEMETRY SIGNAL STRENGTH, LINK F6, RIGHT CIRCULAR POLARIZATION

28
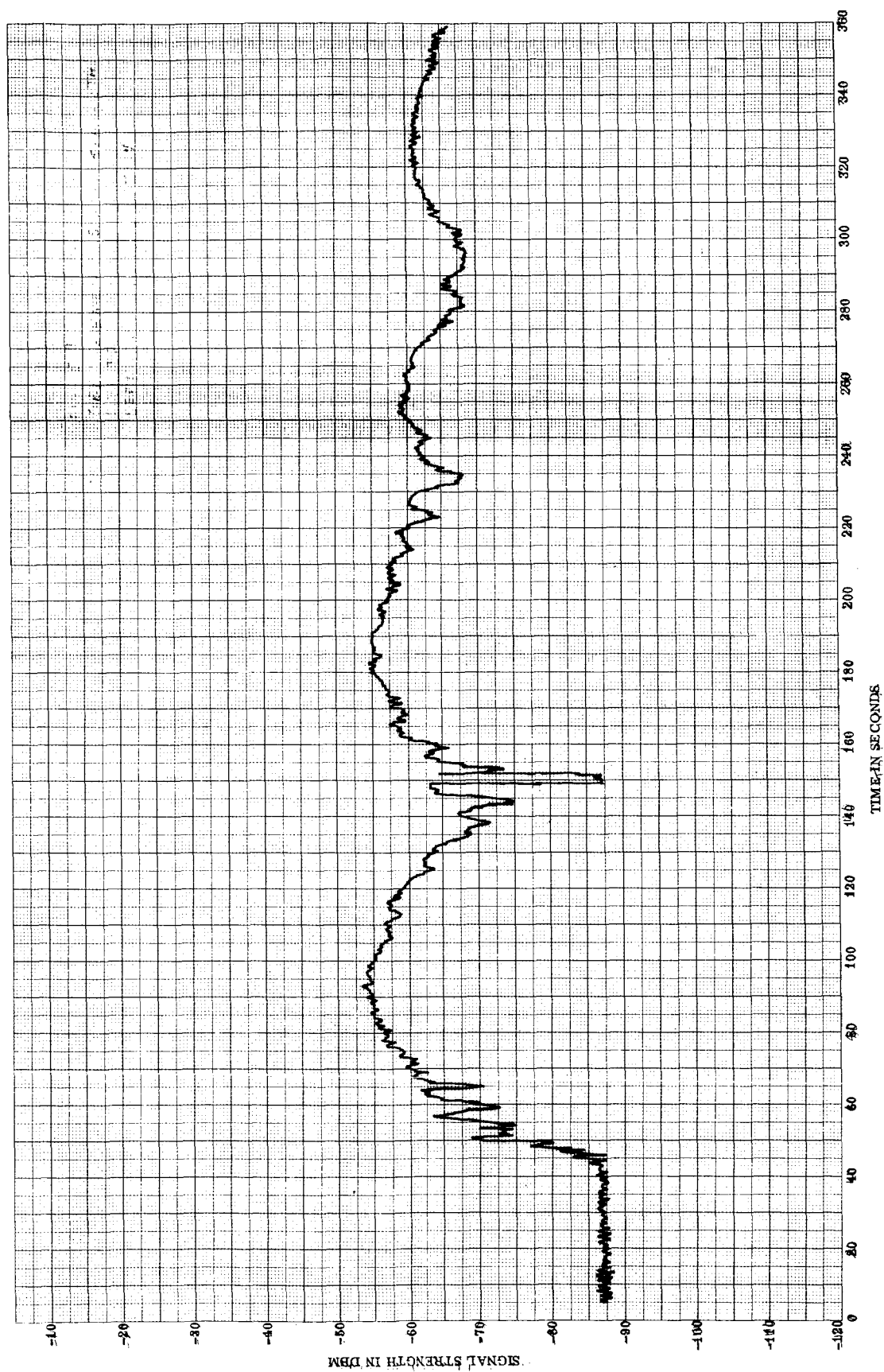
FIGURE 9. GBI TELEMETRY SIGNAL STRENGTH, LINK D2, LEFT CIRCULAR POLARIZATION

29
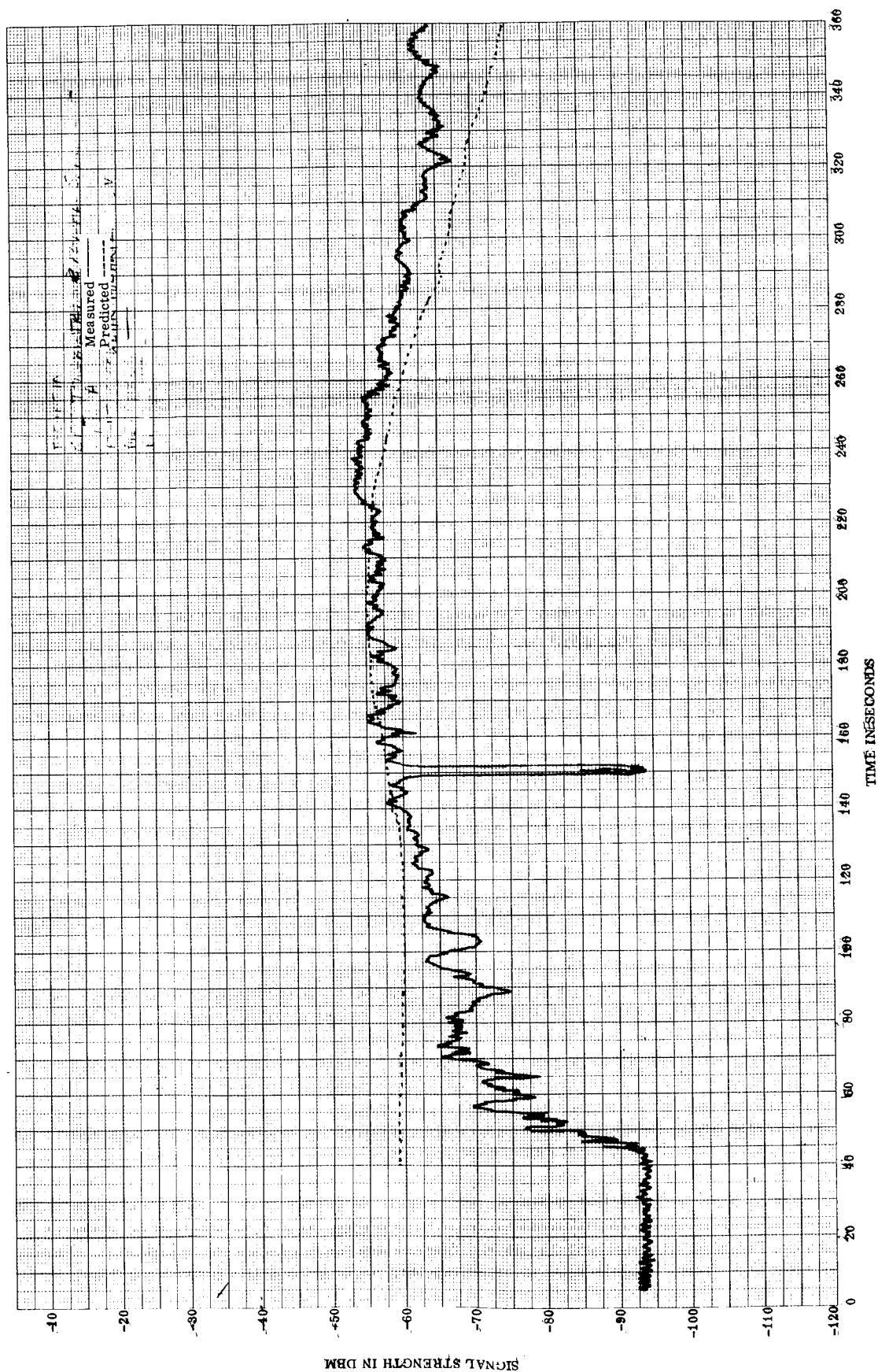
FIGURE 10. GBI TELEMETRY SIGNAL STRENGTH, LINK A, RIGHT CIRCULAR POLARIZATION

30
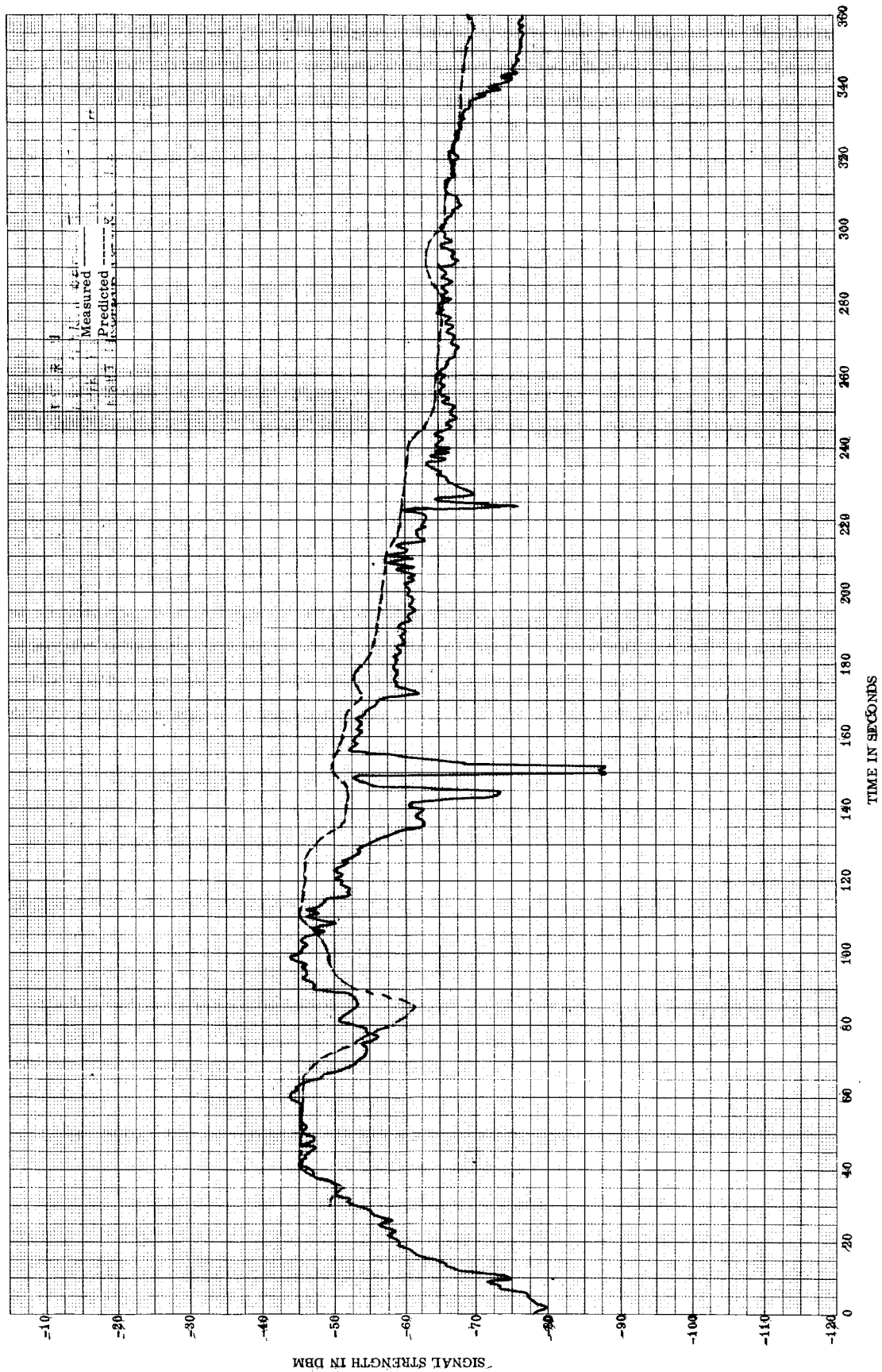
FIGURE 11. NEW SMYRNA BEACH TELEMETRY SIGNAL STRENGTH, LINK F6, RIGHT CIRCULAR
POLARIZATION

31
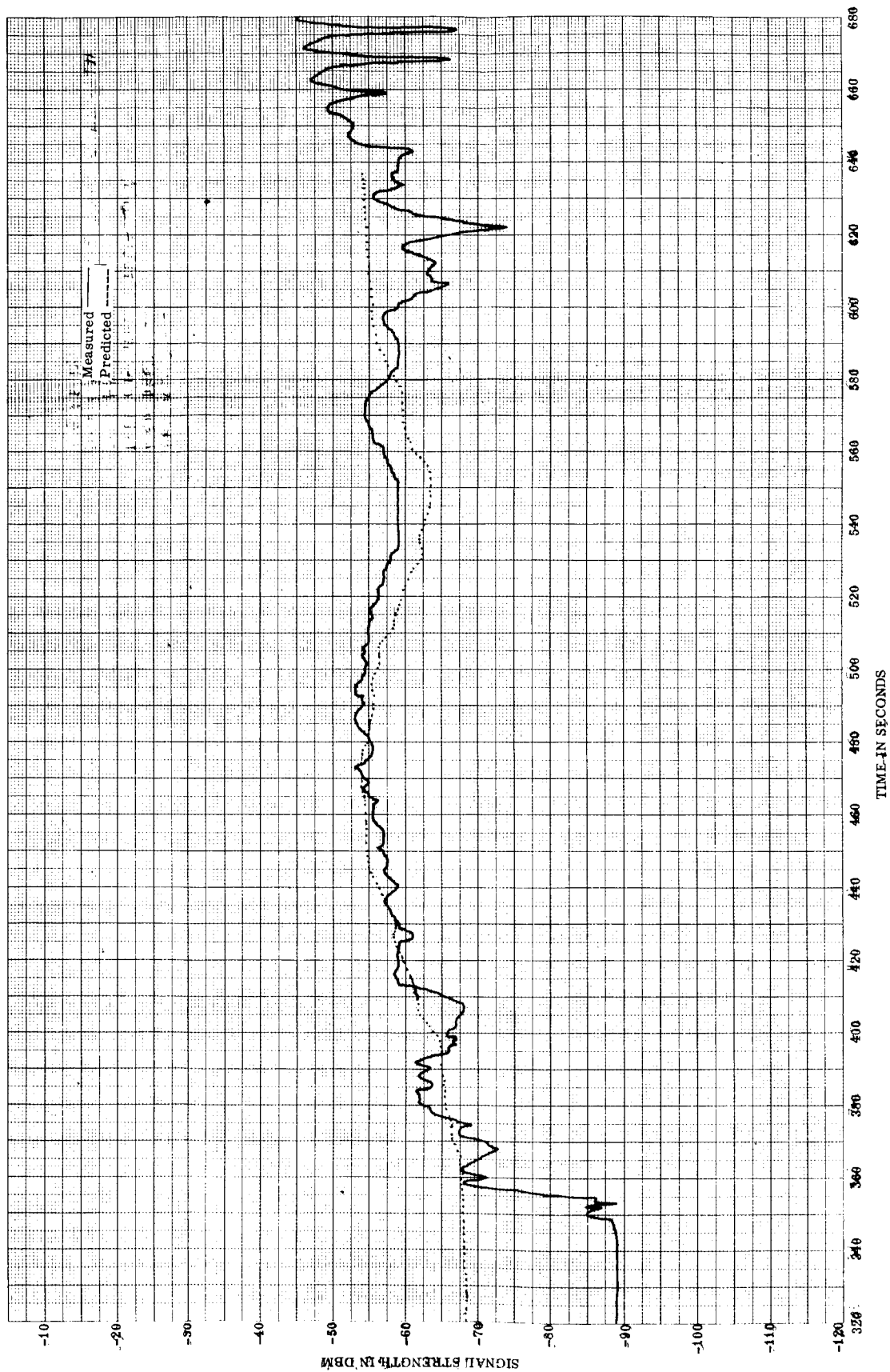
FIGURE 12.   ANTIGUA TELEMETRY SIGNAL STRENGTH, LINK F6, LEFT CIRCULAR POLARIZATION

32
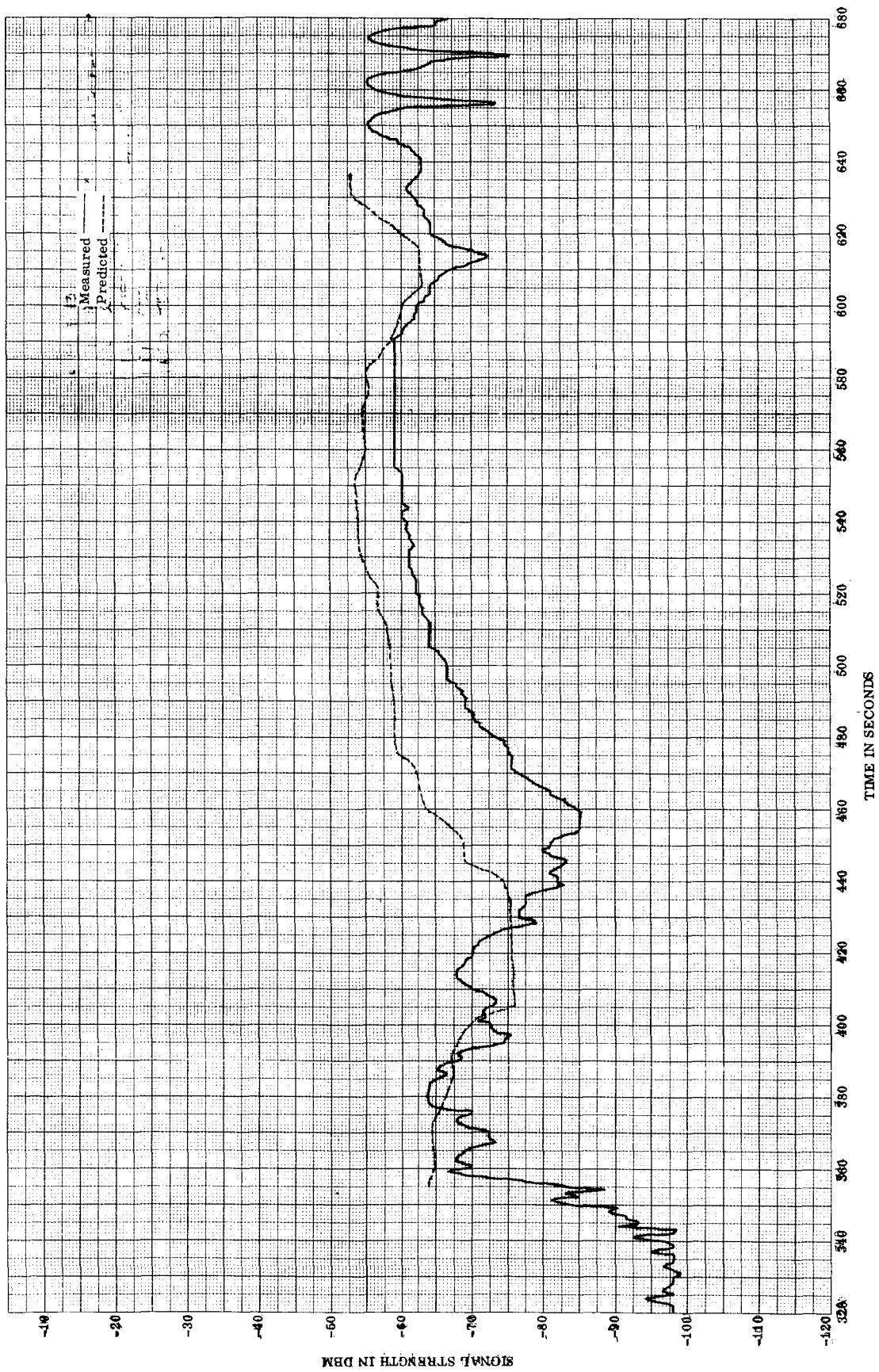
FIGURE 13. ANTIGUA TELEMETRY SIGNAL STRENGTH, LINK D2, RIGHT CIRCULAR POLARIZATION

33
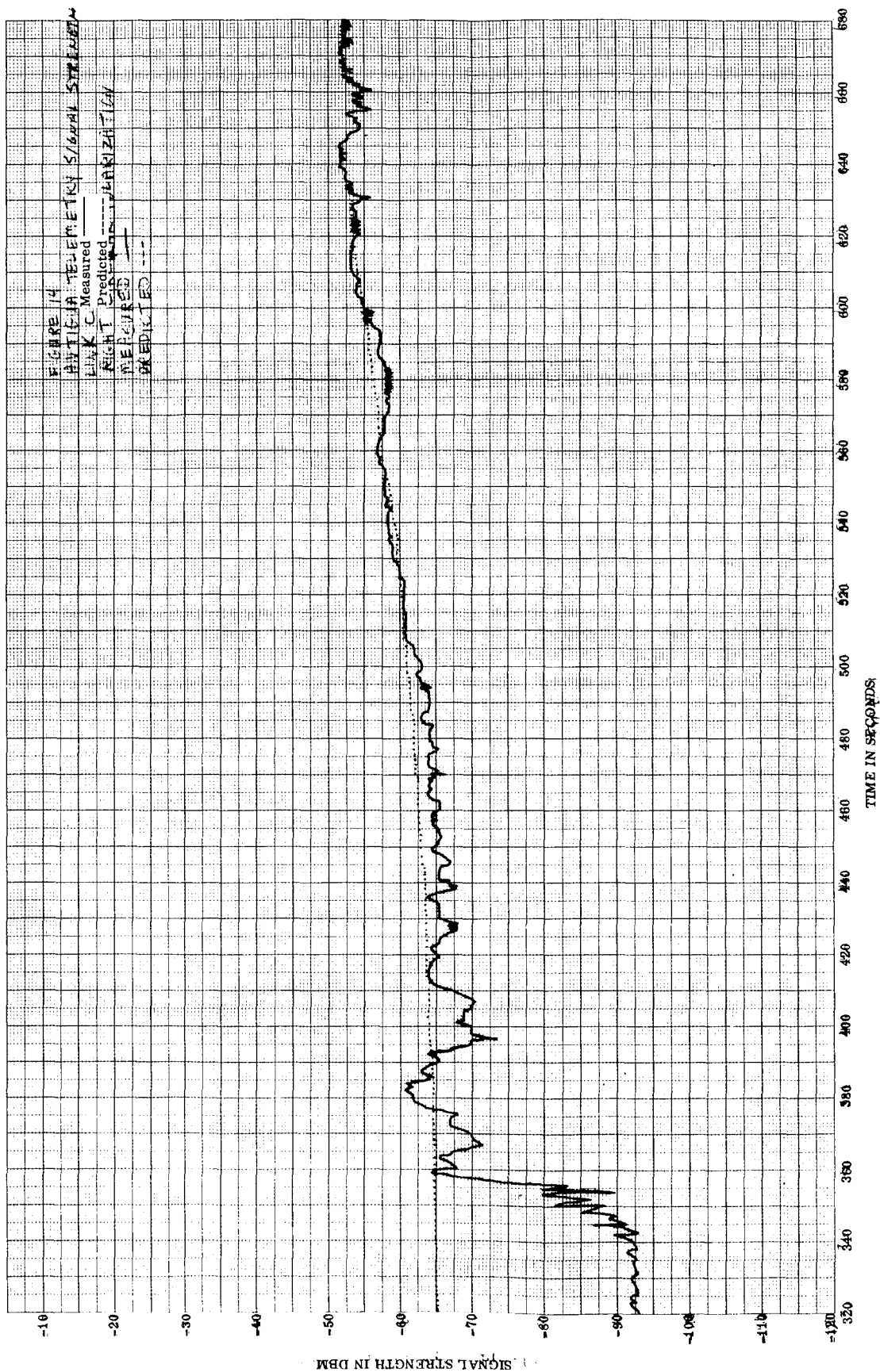
FIGURE 14. ANTIGUA TELEMETRY SIGNAL STRENGTH, LINK C, RIGHT CIRCULAR POLARIZATION

34
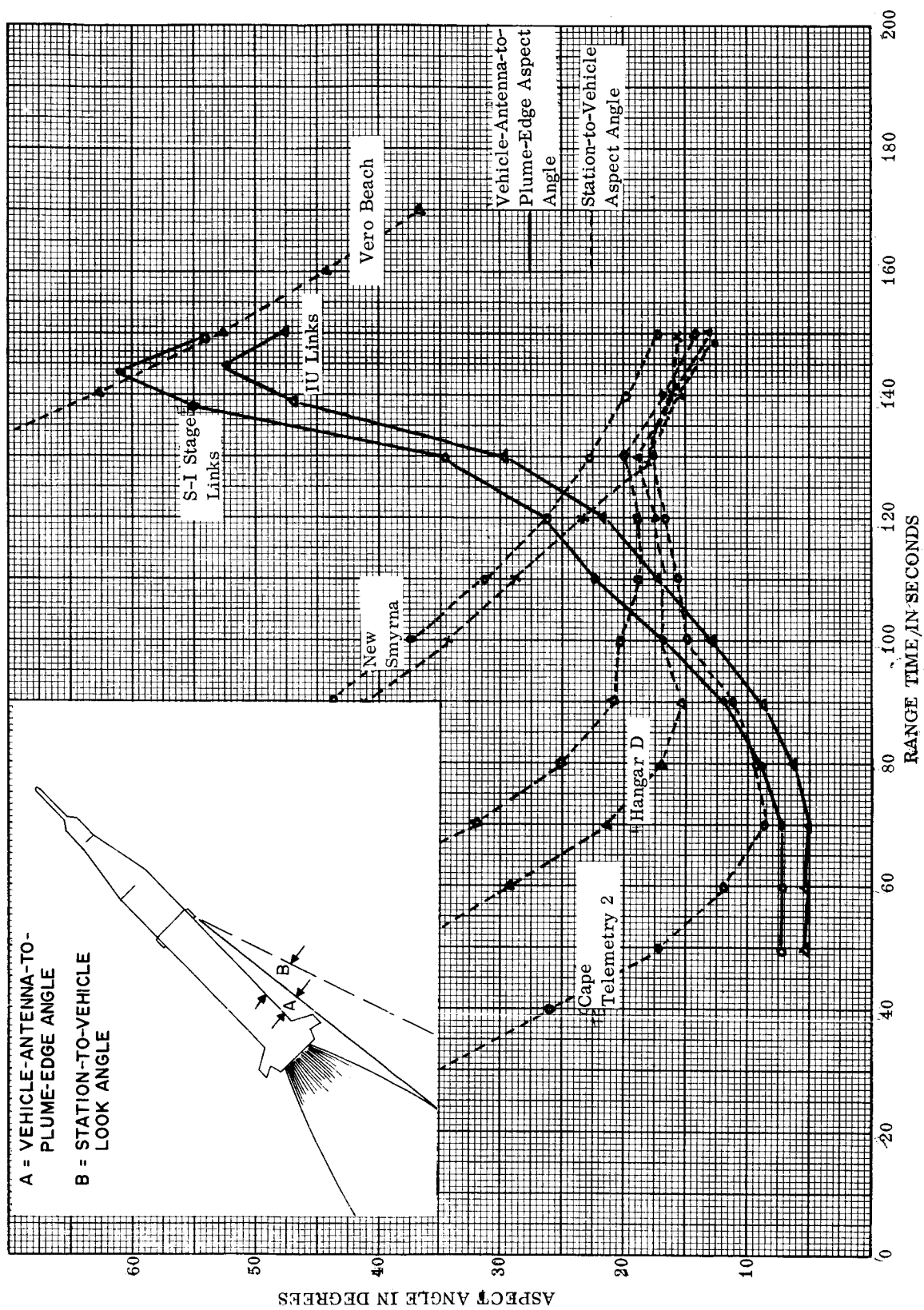
FIGURE 15. TELEMETRY ASPECT ANGLE HISTORIES
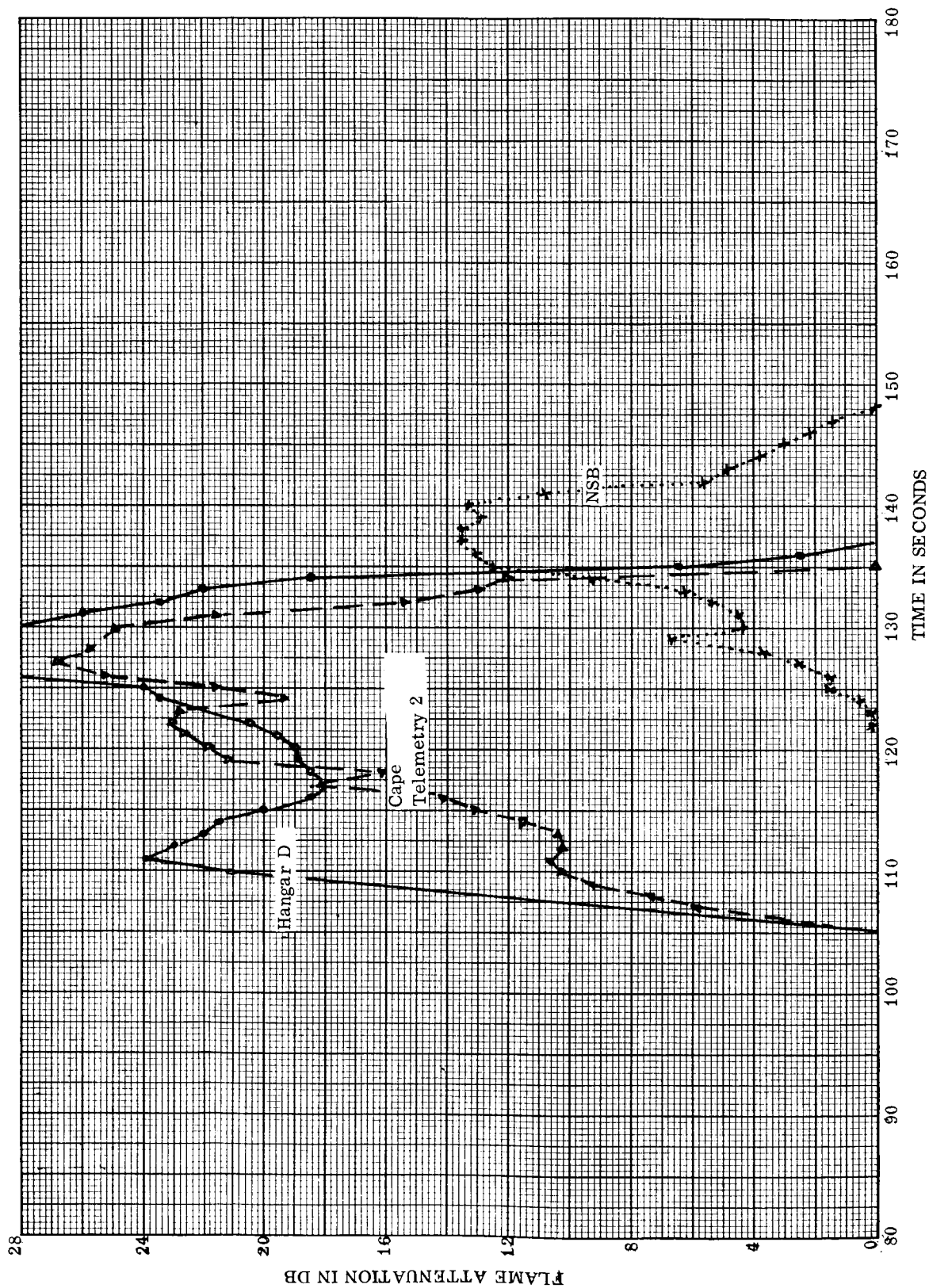
FIGURE 16. FLAME ATTENUATION, S-I STAGE TELEMETRY
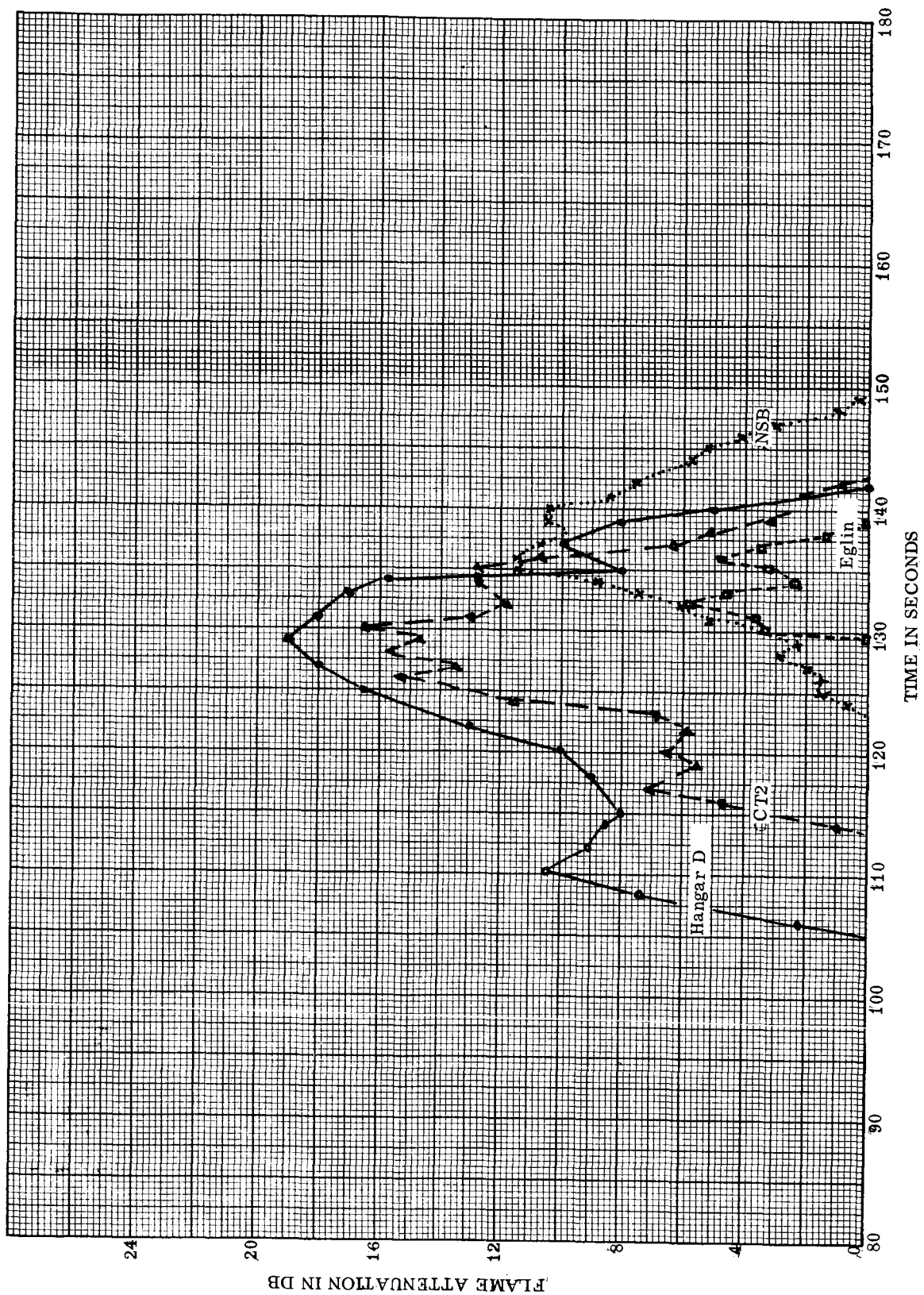
FIGURE 17. FLAME ATTENUATION, IU TELEMETRY
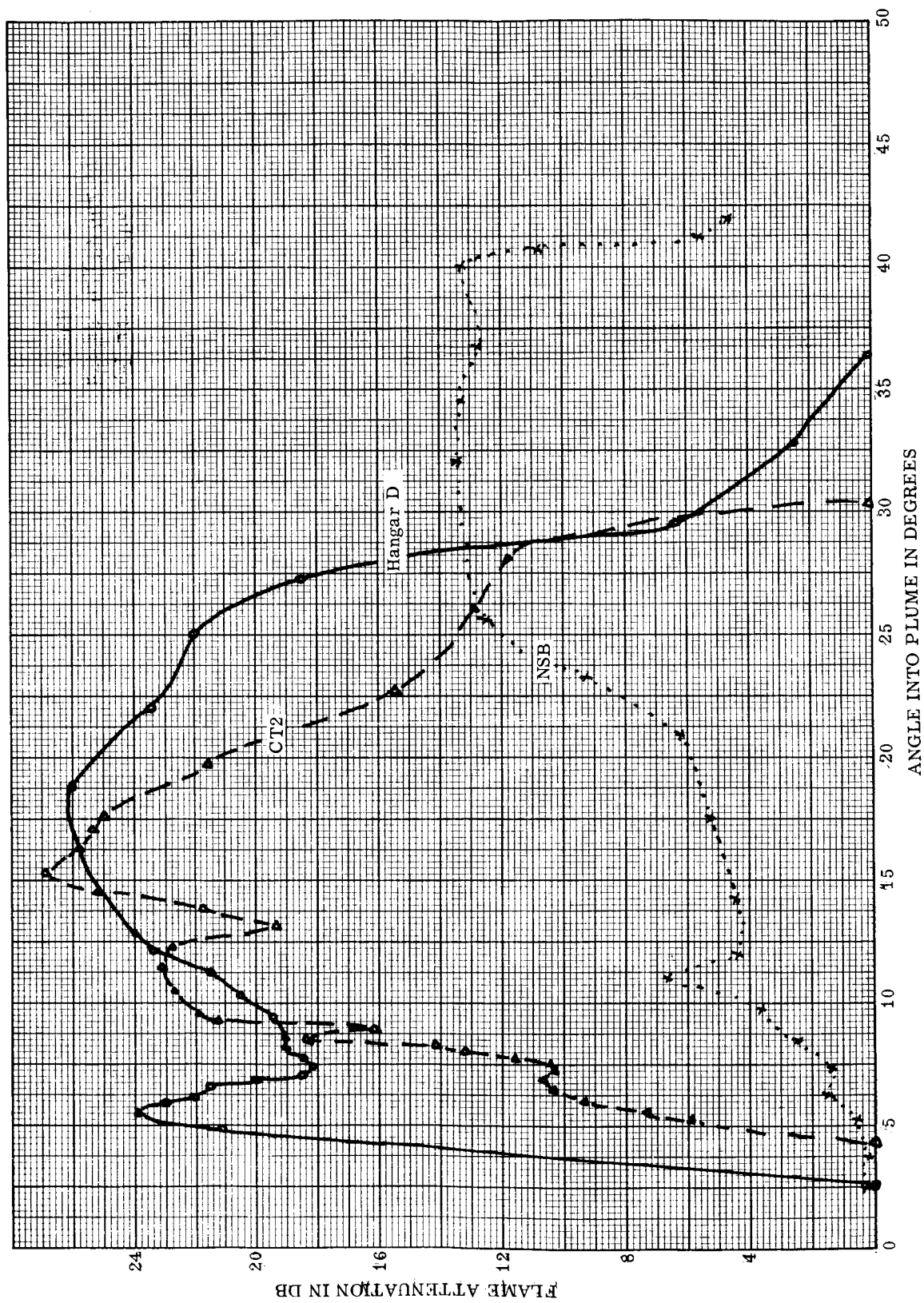
FIGURE 18. FLAME ATTENUATION, S-I STAGE TELEMETRY

38
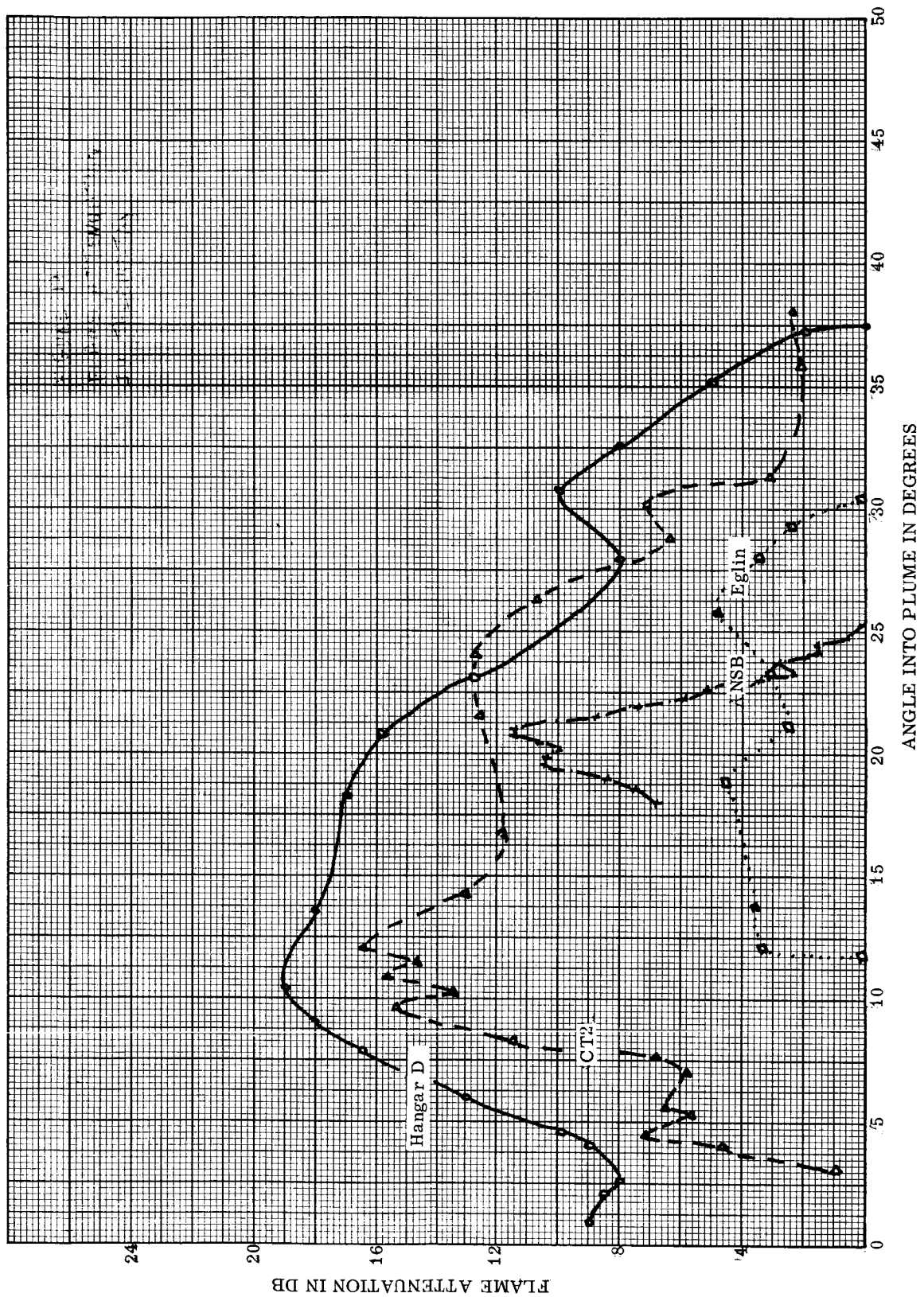
FIGURE 19. FLAME ATTENUATION,IU TELEMETRY
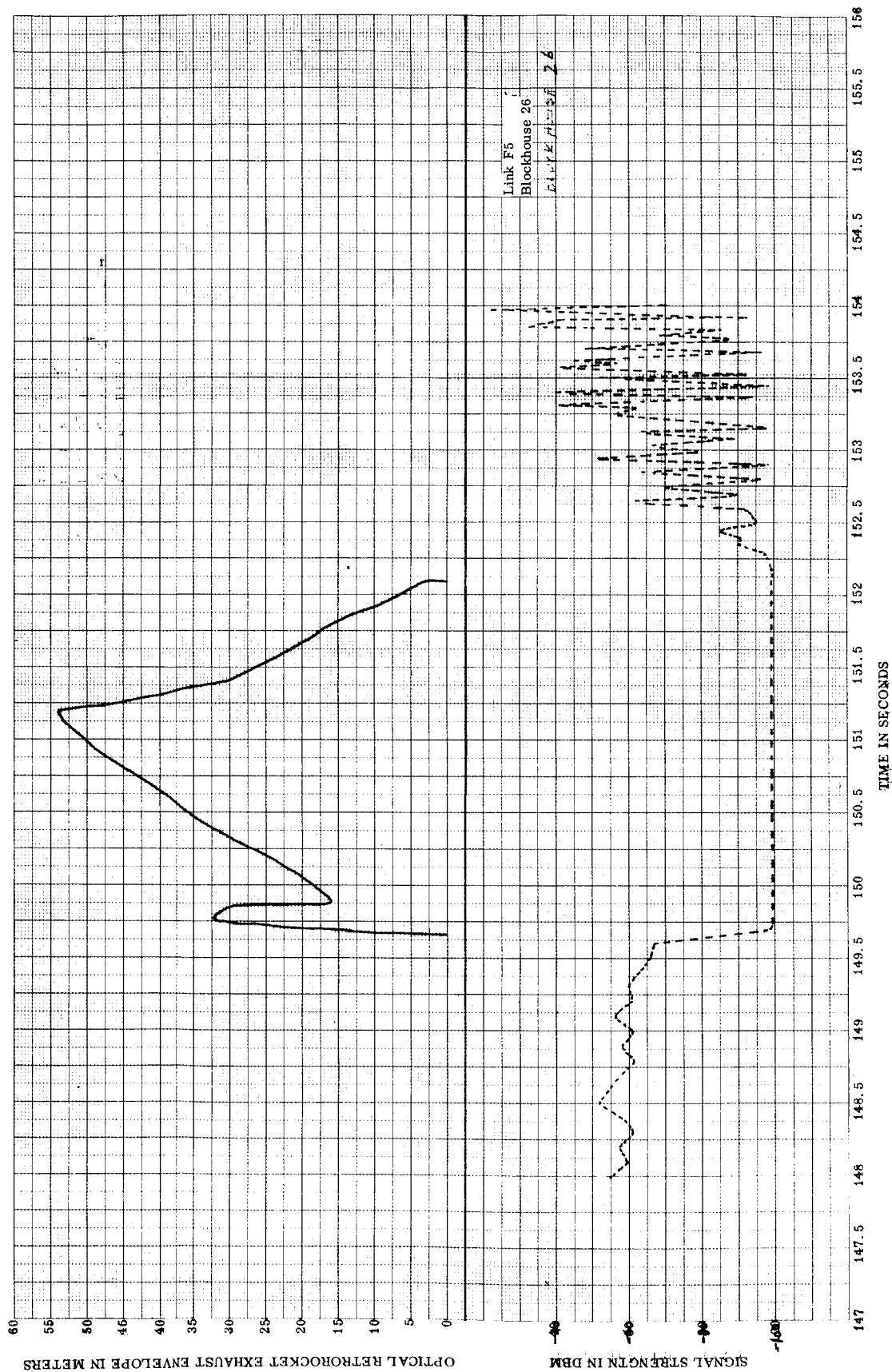
FIGURE 20.   RETROROCKET EXHAUST HISTORY AND SIGNAL STRENGTH CORRELATION

40
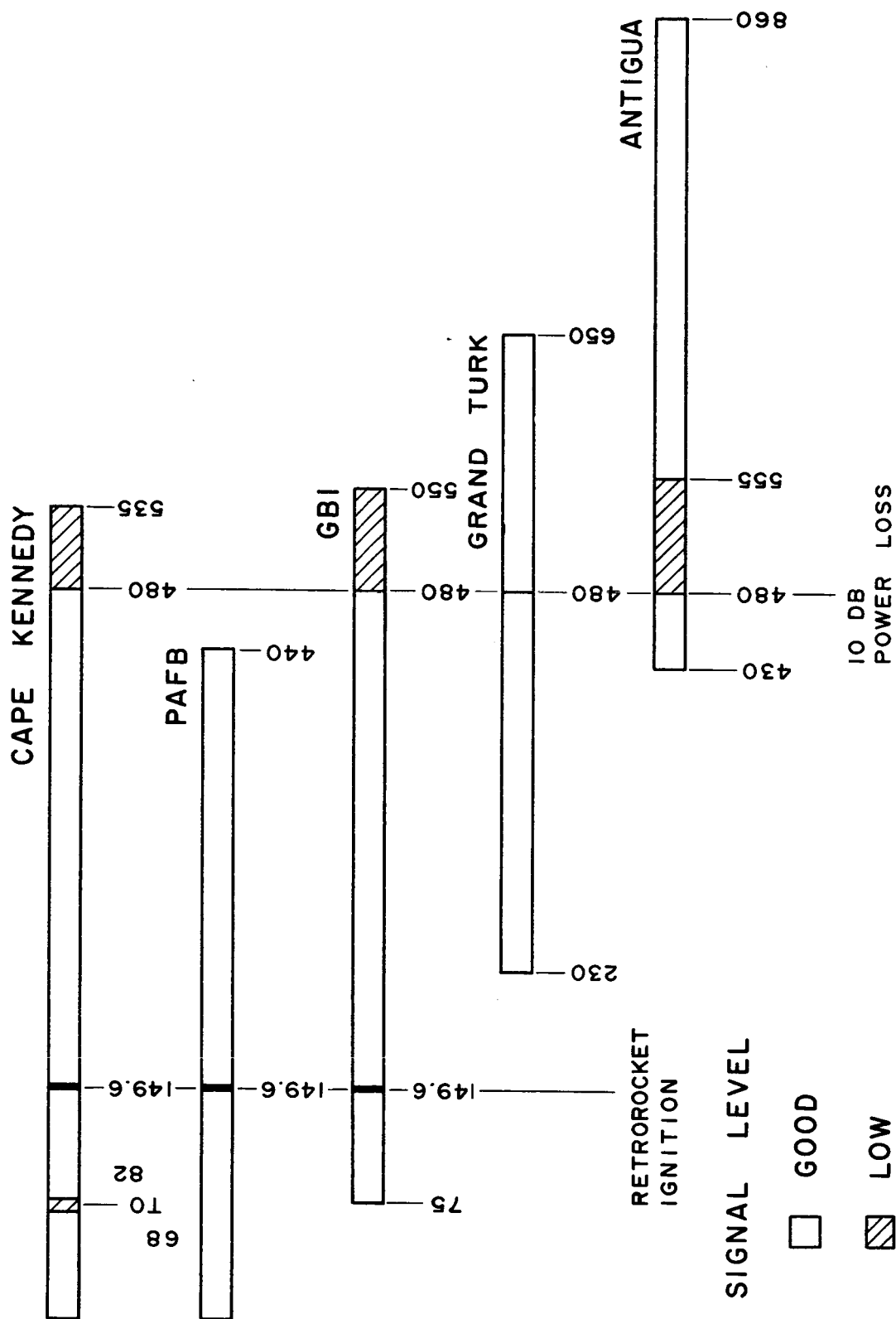
FIGURE 21. C-BAND RADAR PERFORMANCE
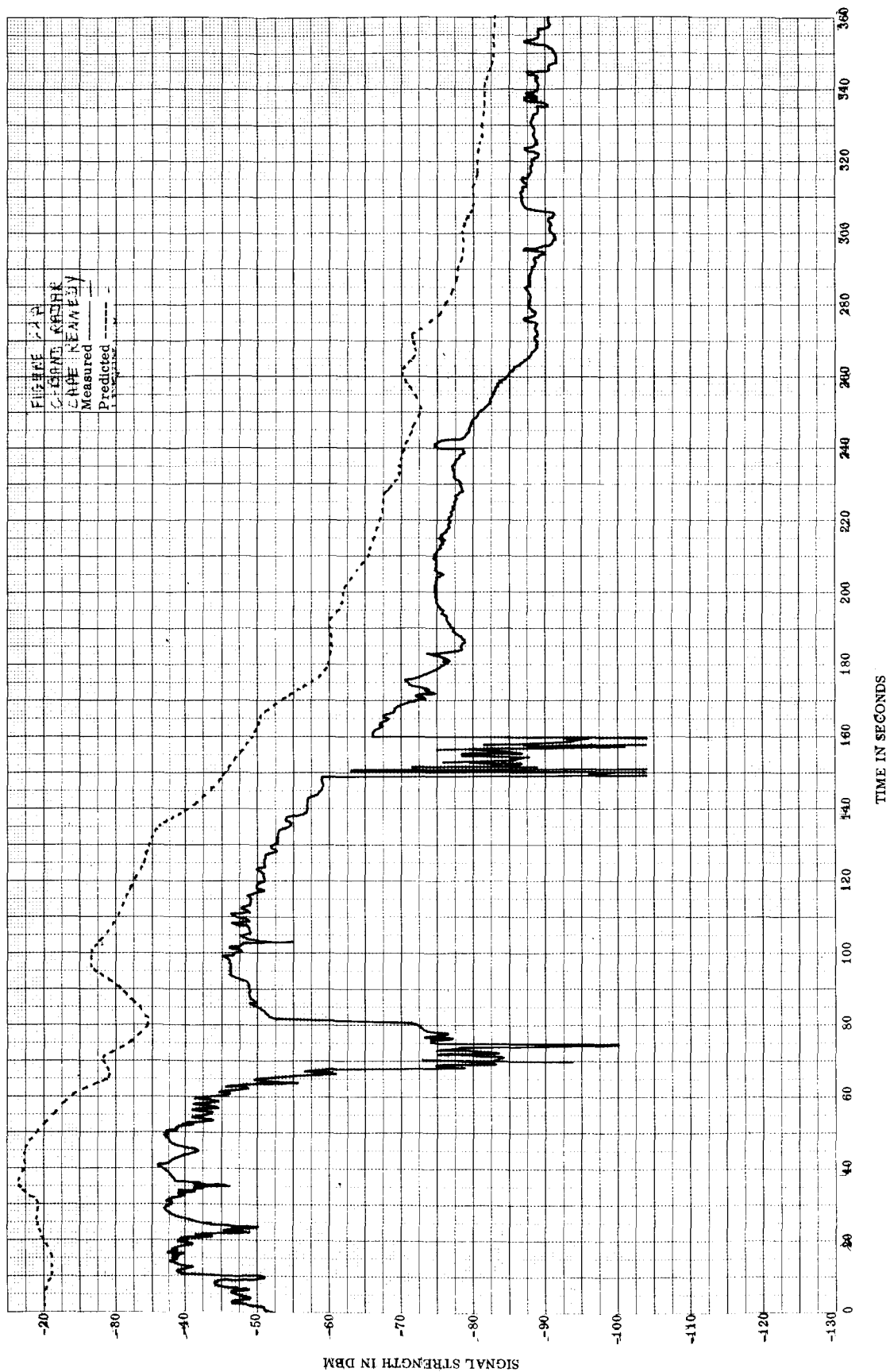
FIGURE 22A.   C–BAND RADAR, CAPE KENNEDY

42
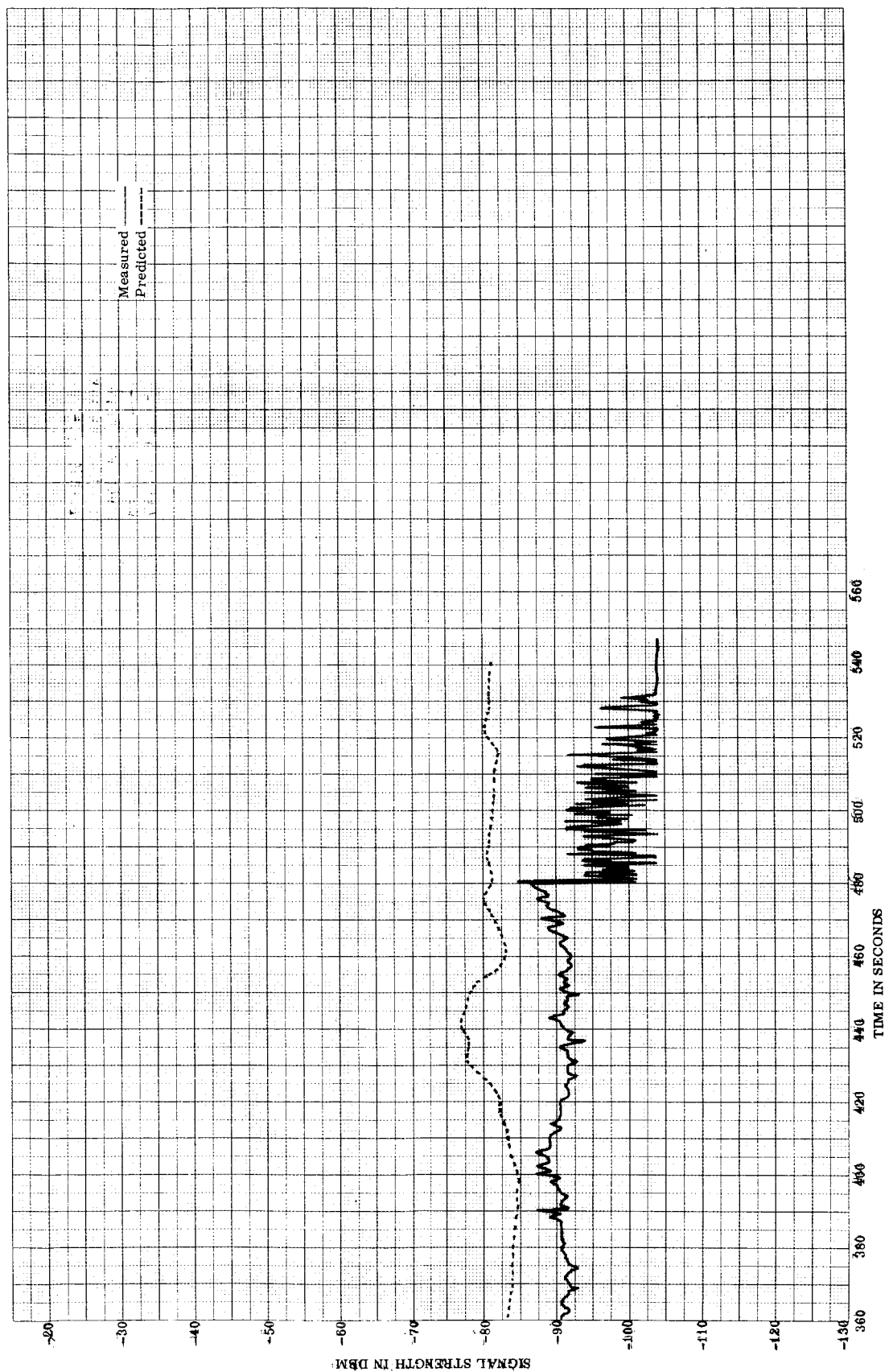
FIGURE 22B. C-BAND RADAR, CAPE KENNEDY
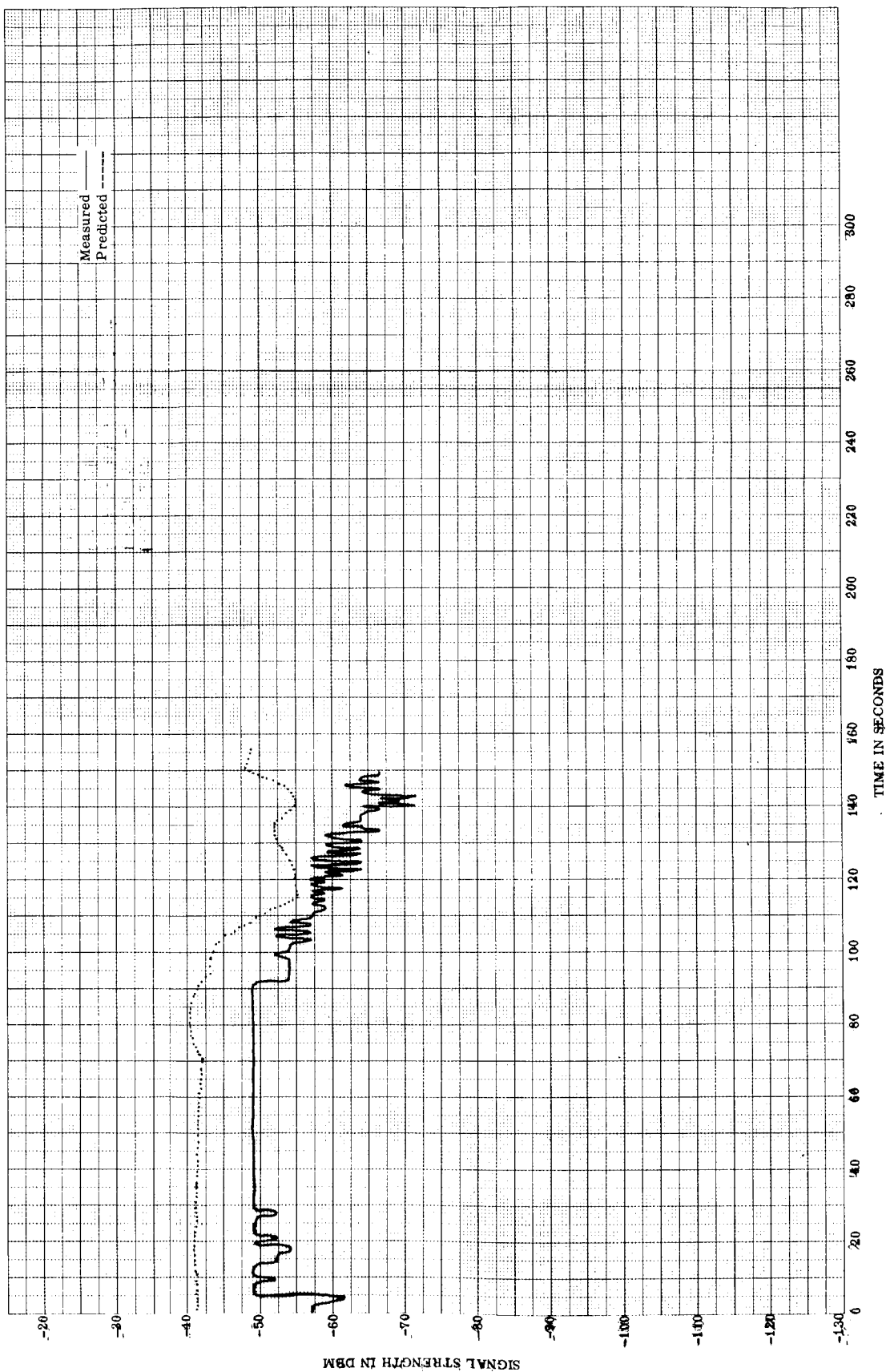
FIGURE 23.   C-BAND RADAR, PATRICK AIR FORCE BASE

44
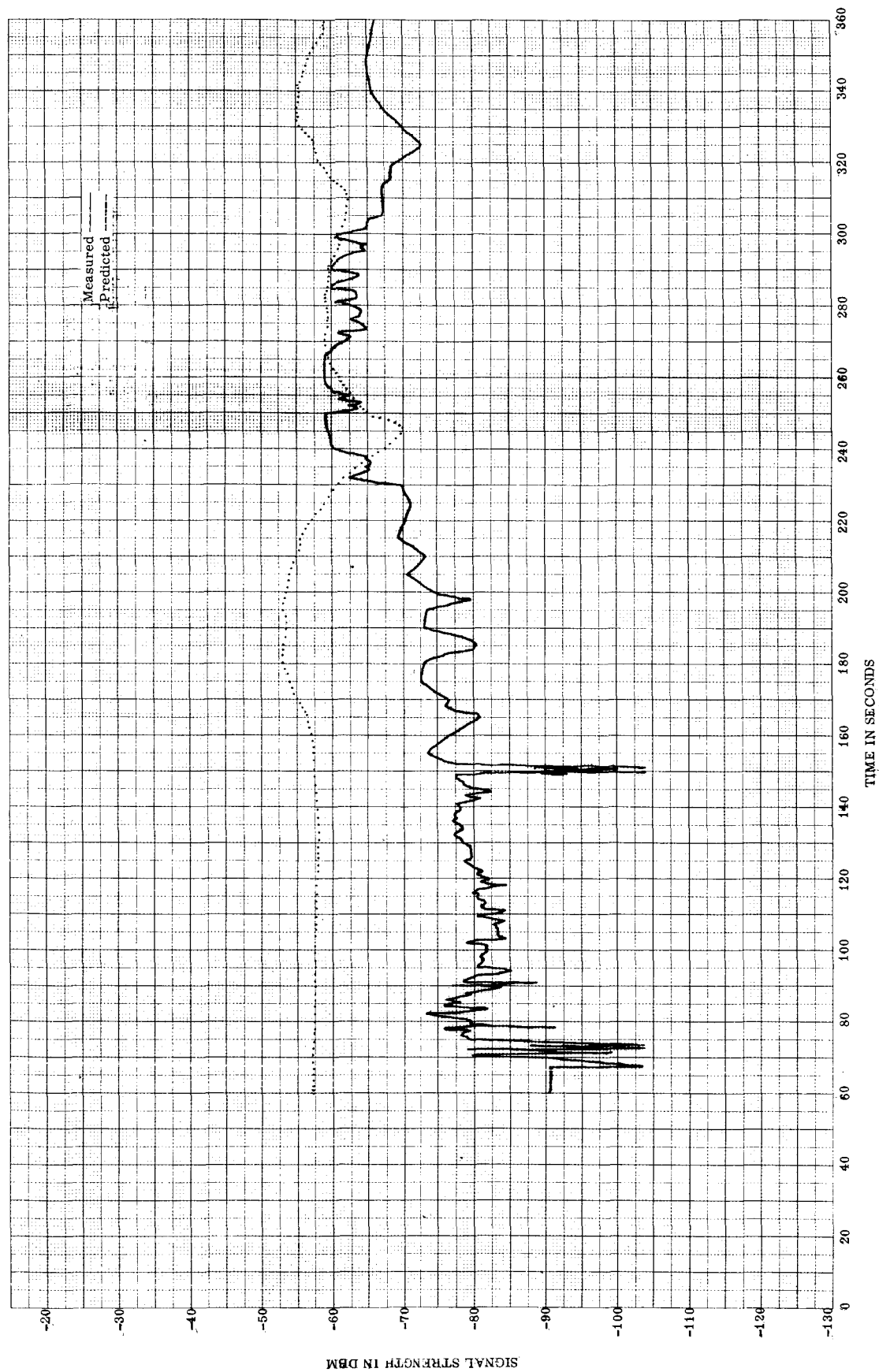
FIGURE 24A.   C-BAND RADAR, GRAND BAHAMA ISLAND
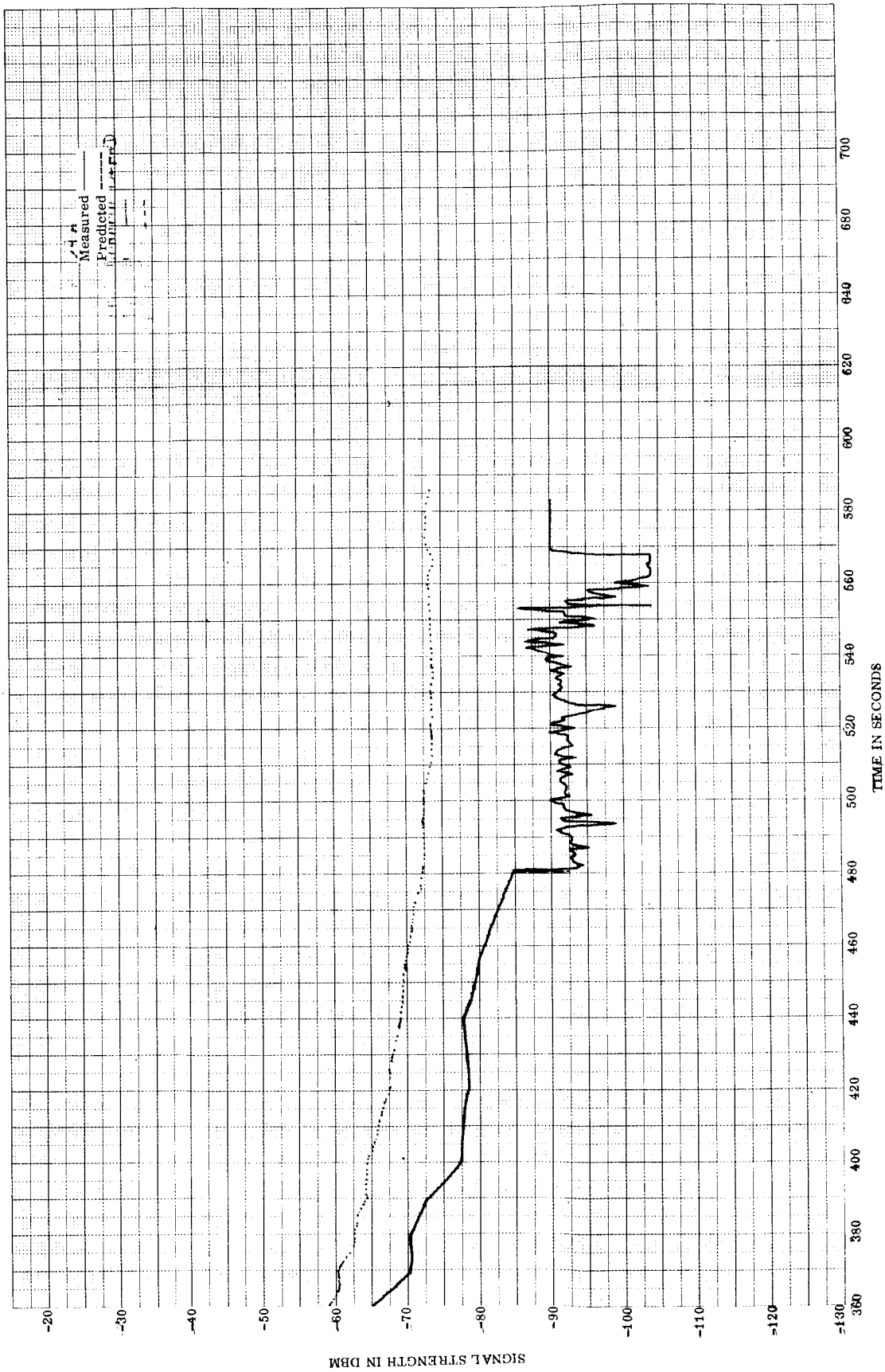
FIGURE 24B. C–BAND RADAR, GRAND BAHAMA ISLAND

46
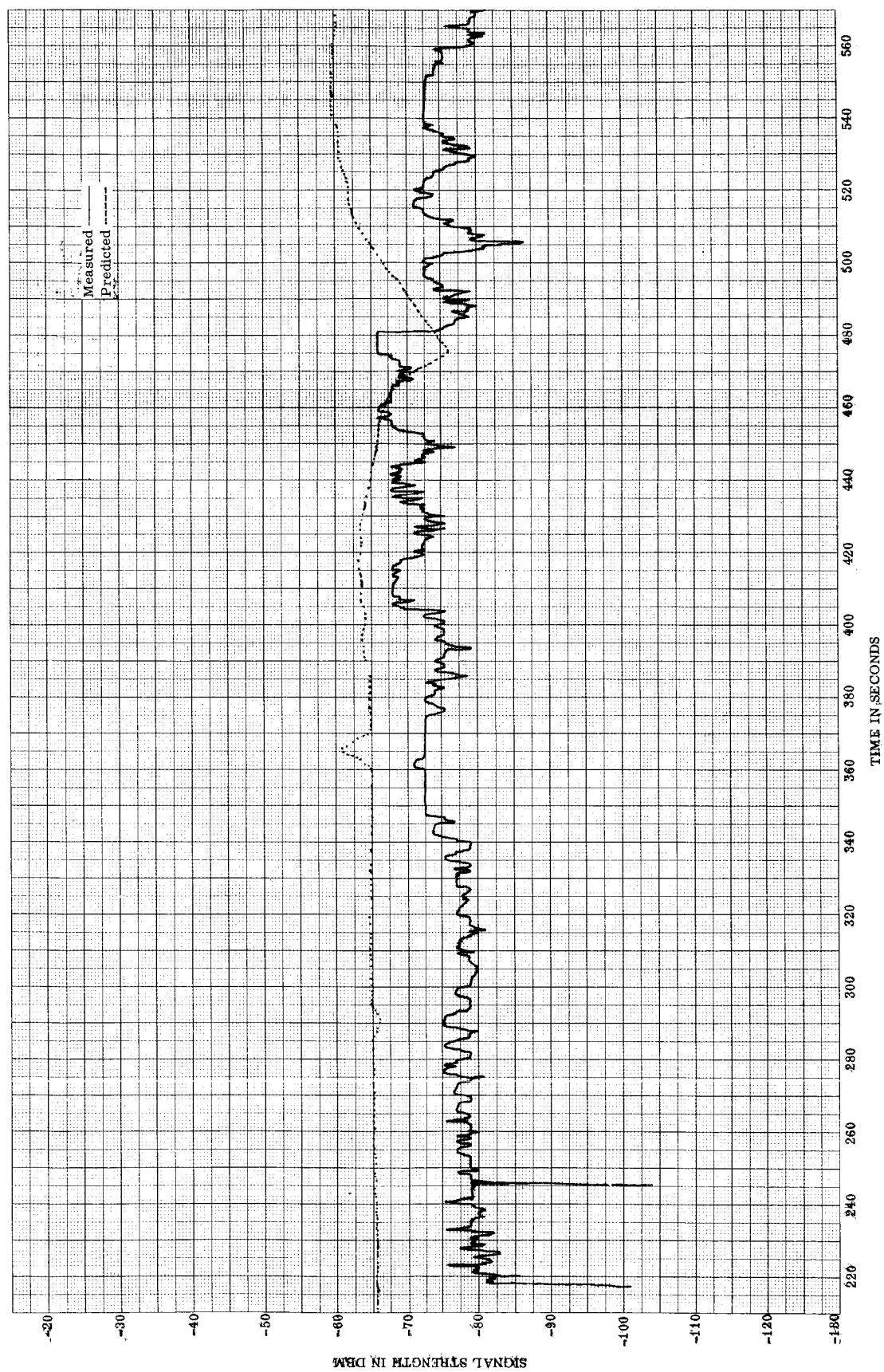
FIGURE 25.   C-BAND RADAR, GRAND TURK

47
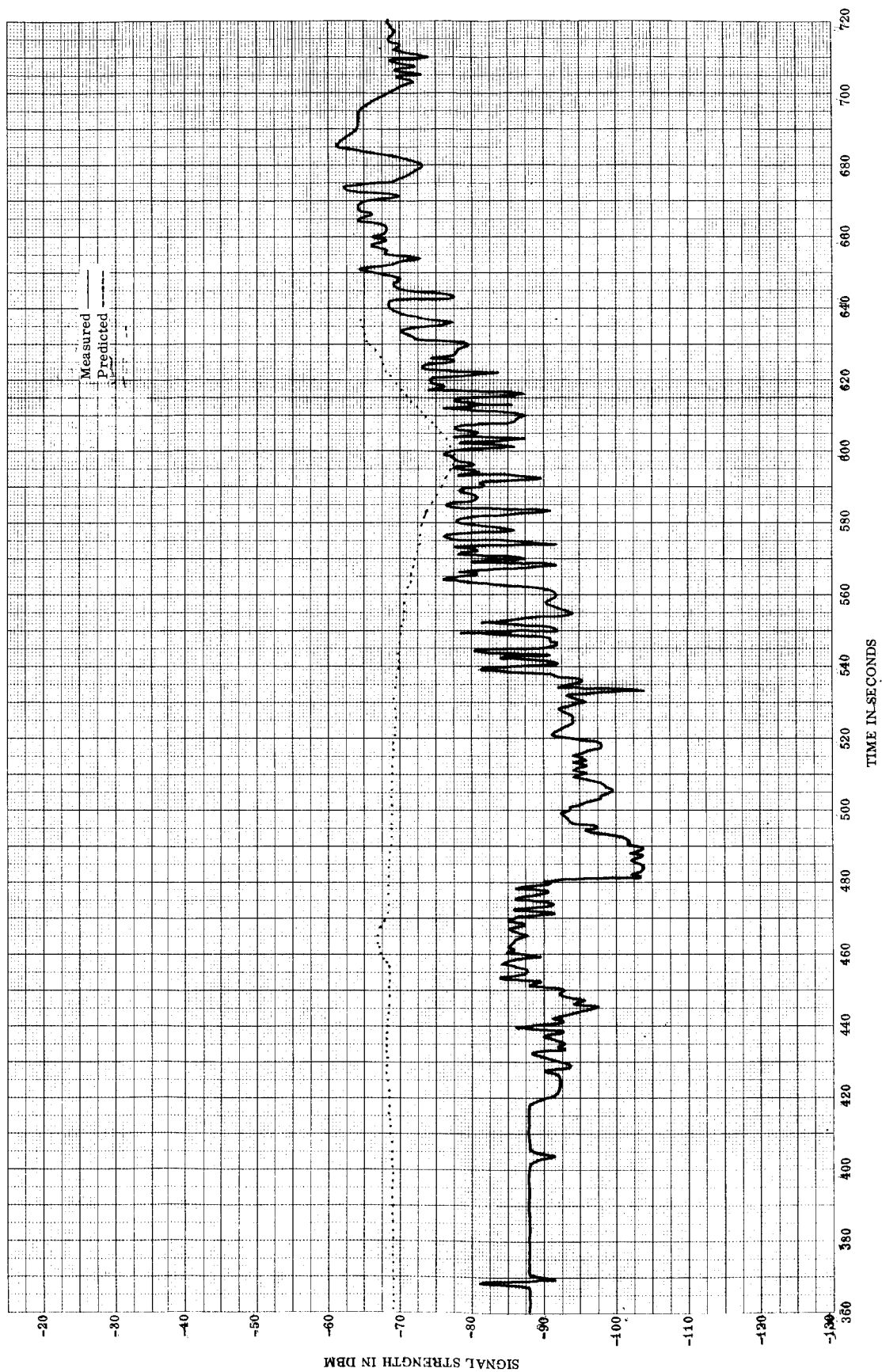
FIGURE 26.   C–BAND RADAR, ANTIGUA

48
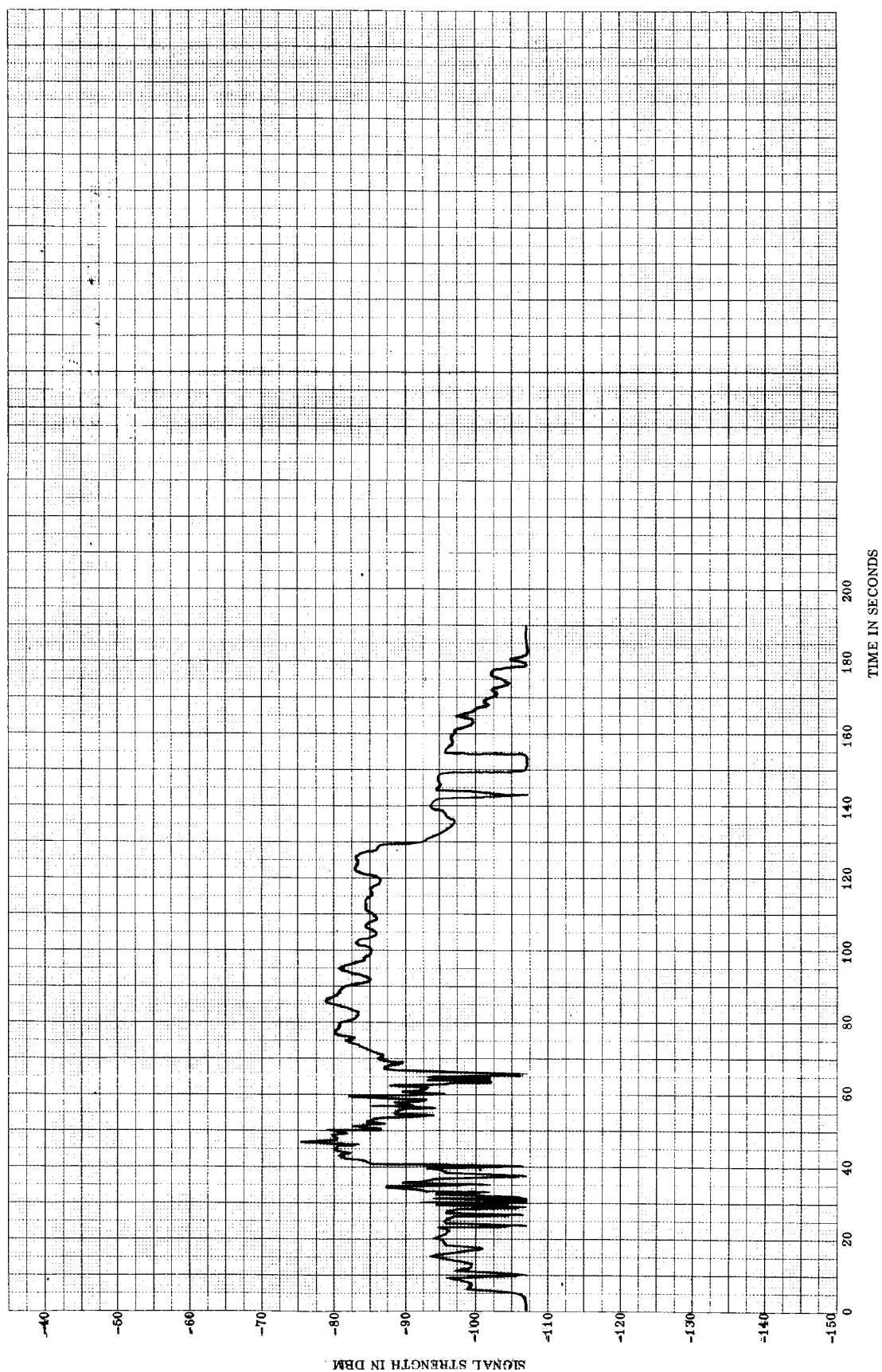
FIGURE 27. ODOP SIGNAL STRENGTH, RIGHT CIRCULAR POLARIZATION, JADE

49
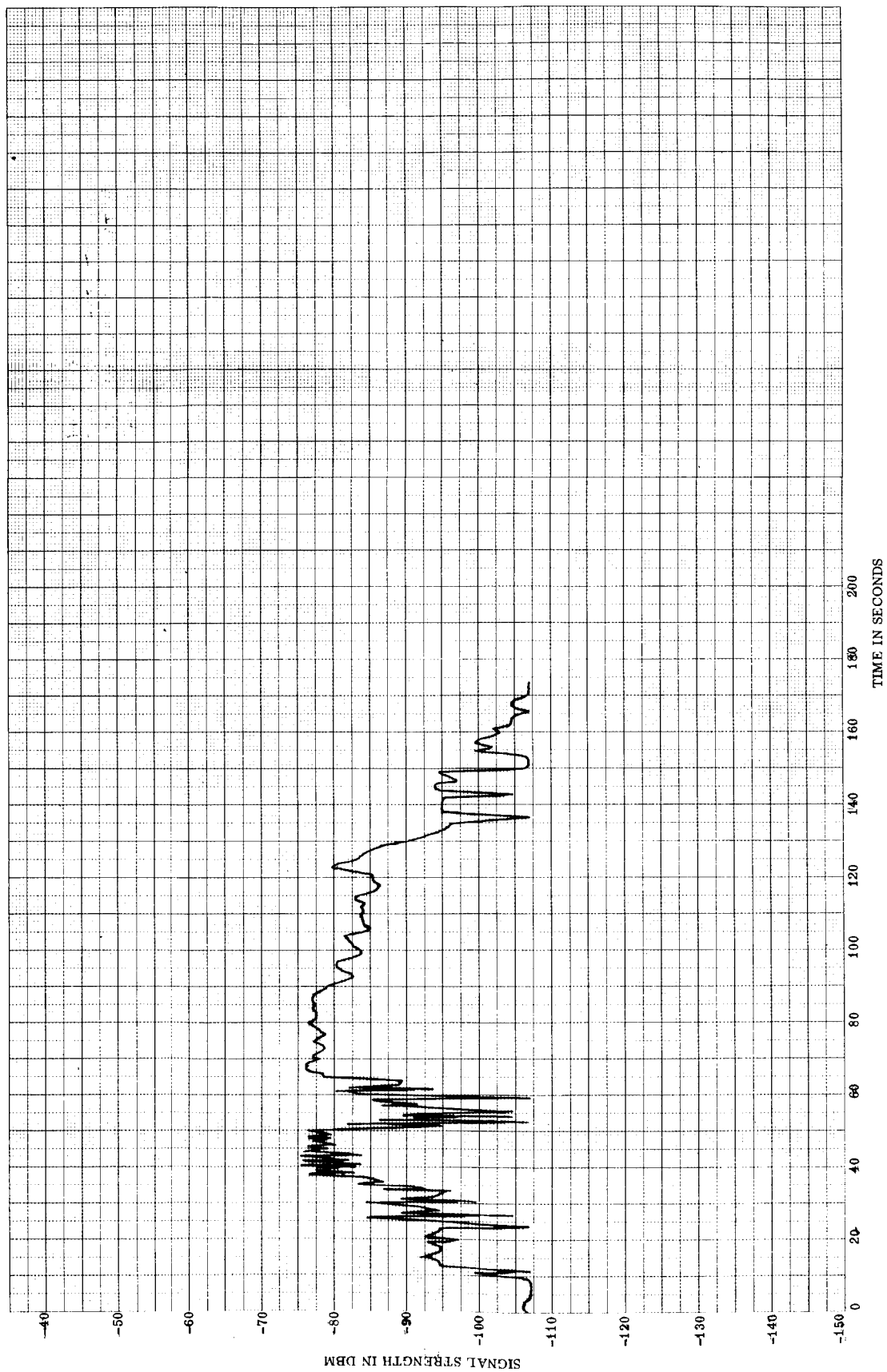
FIGURE 28.   ODOP SIGNAL STRENGTH, LEFT CIRCULAR POLARIZATION, JADE
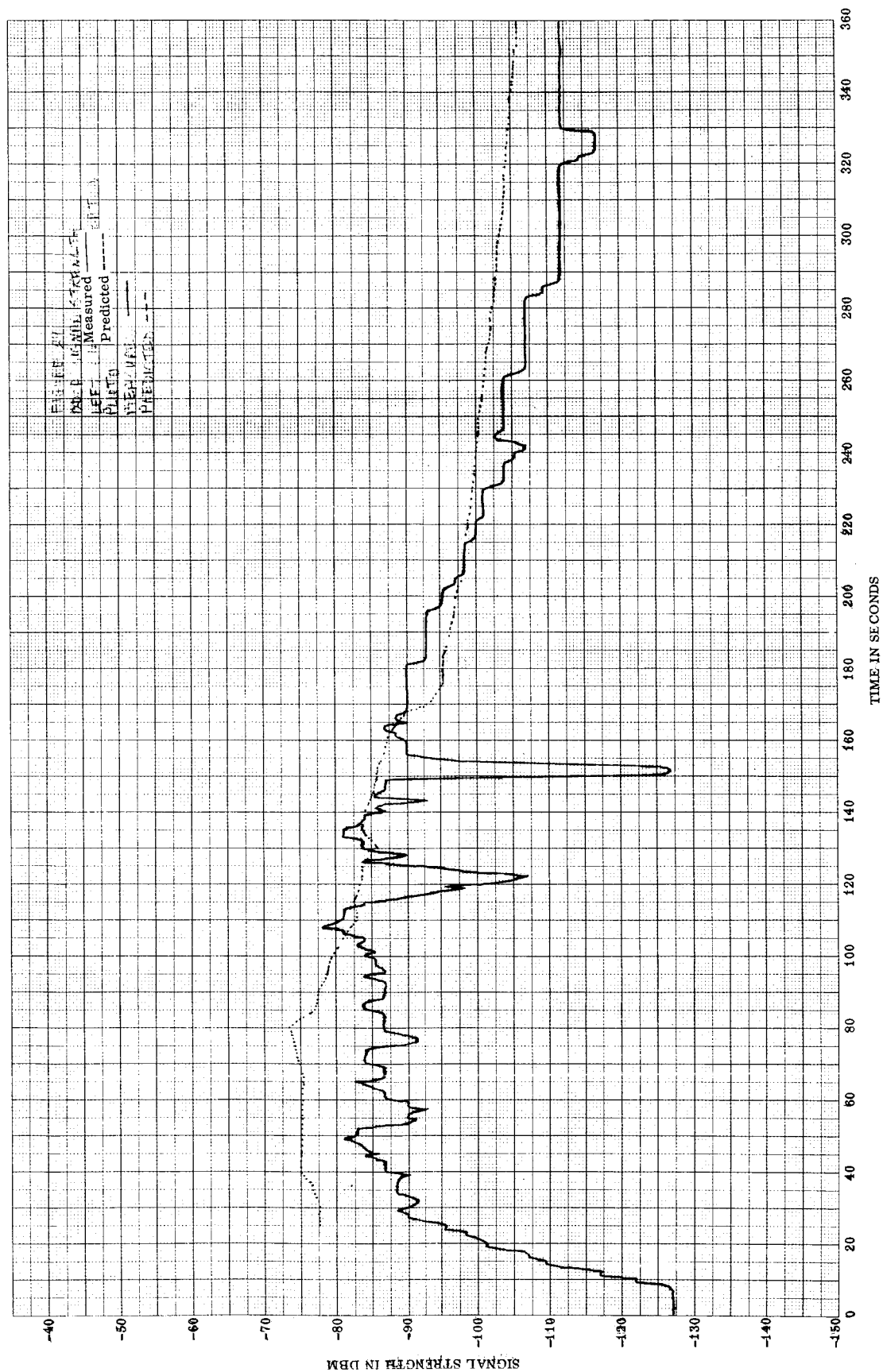
FIGURE 29. ODOP SIGNAL STRENGTH, LEFT CIRCULAR POLARIZATION, PLUTO

51
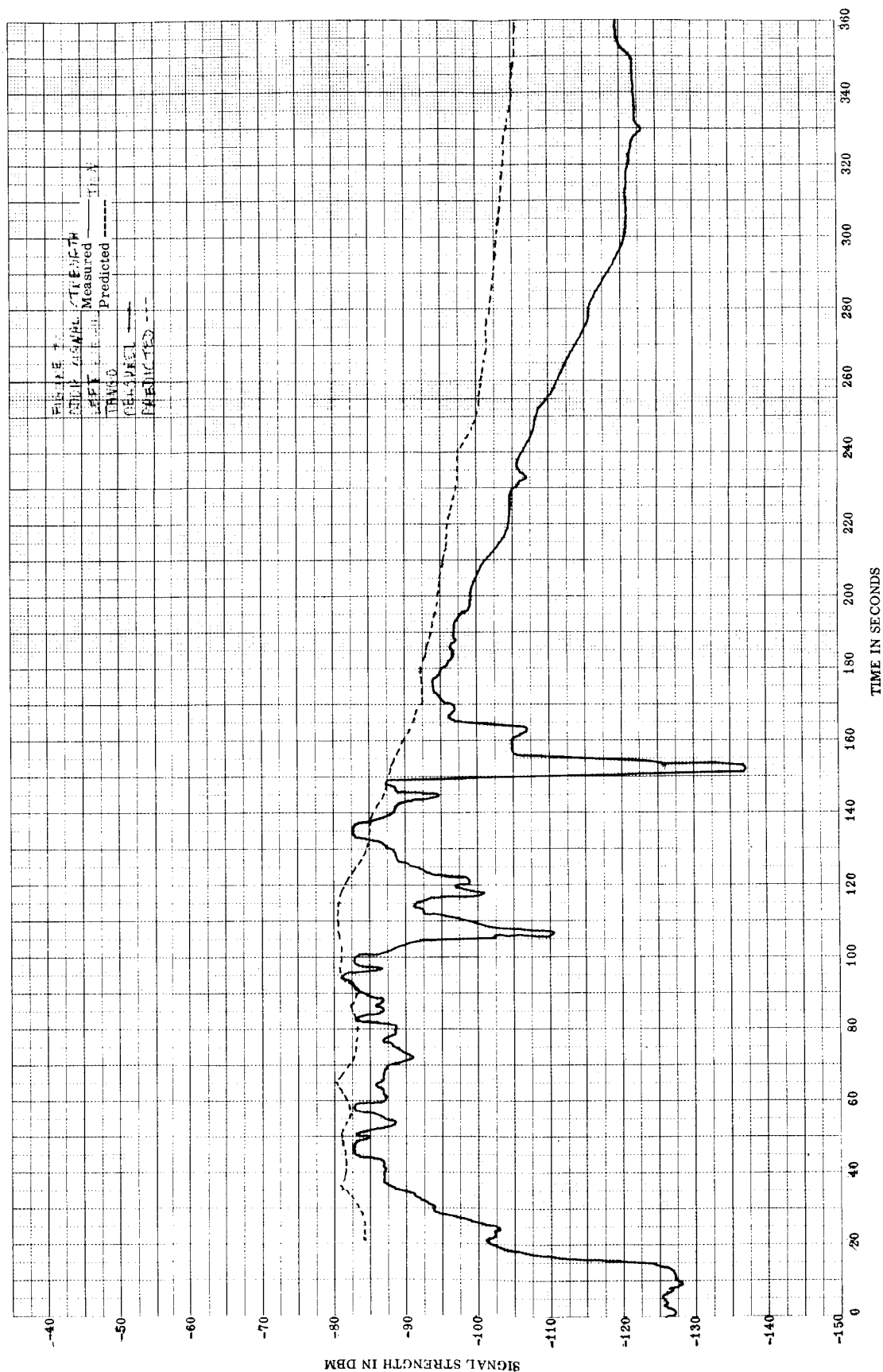
FIGURE 30.   ODOP SIGNAL STRENGTH, LEFT CIRCULAR POLARIZATION, TANGO
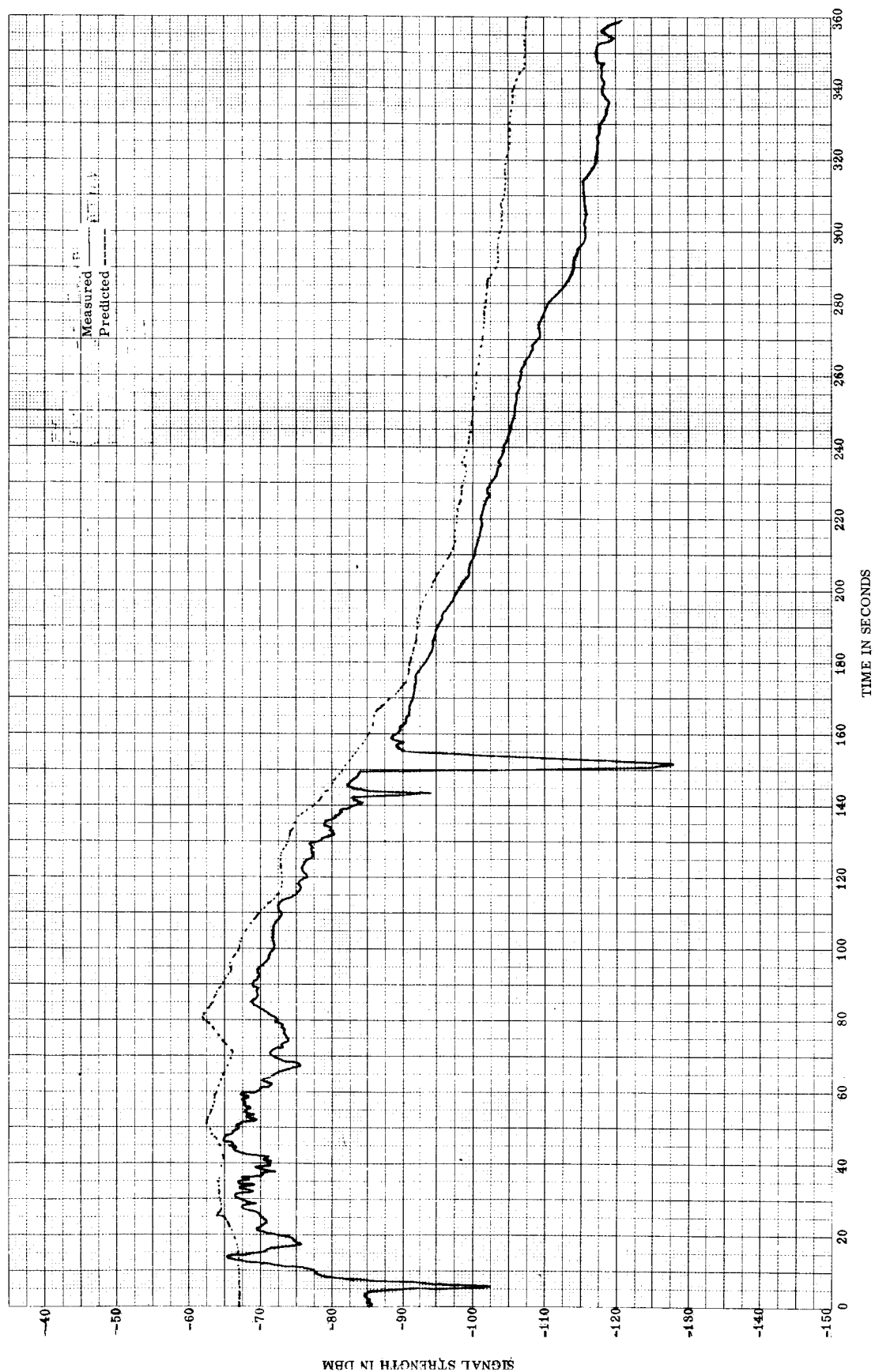
FIGURE 31. ODOP SIGNAL STRENGTH, LEFT CIRCULAR POLARIZATION, MANDY

53
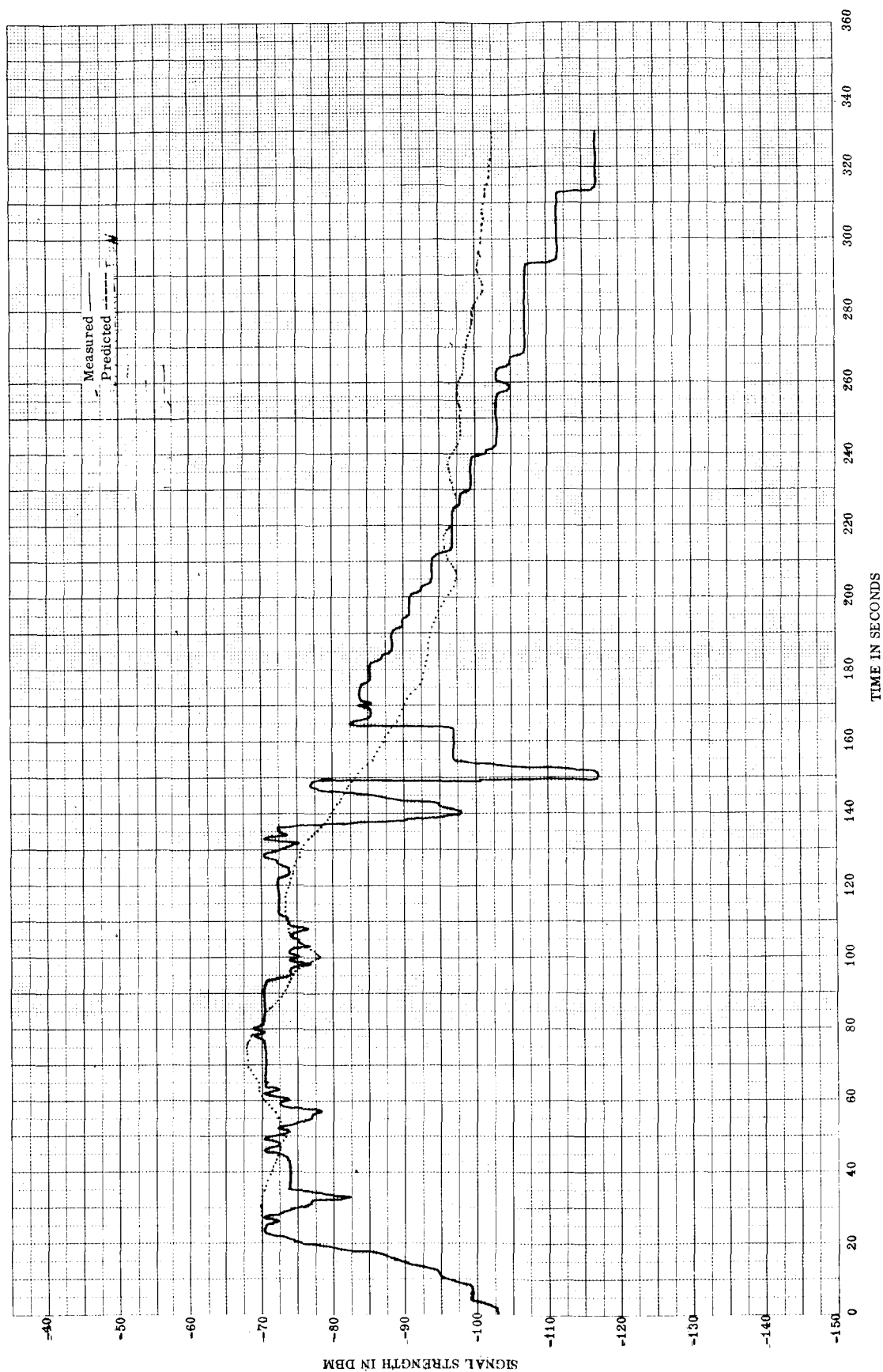
FIGURE 32.   ODOP SIGNAL STRENGTH, LEFT CIRCULAR POLARIZATION, METRO
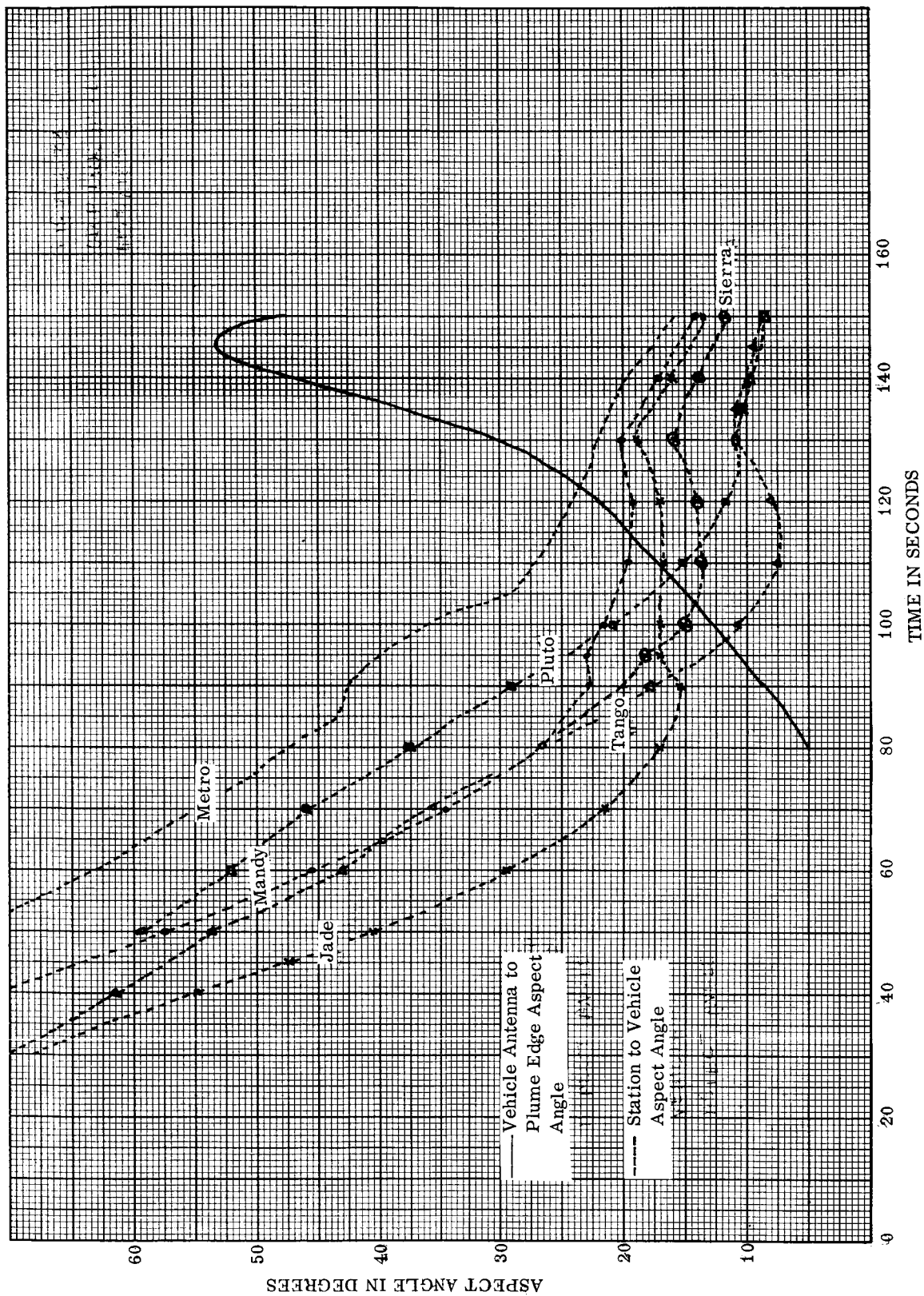
FIGURE 33. ODOP ASPECT ANGLE HISTORIES
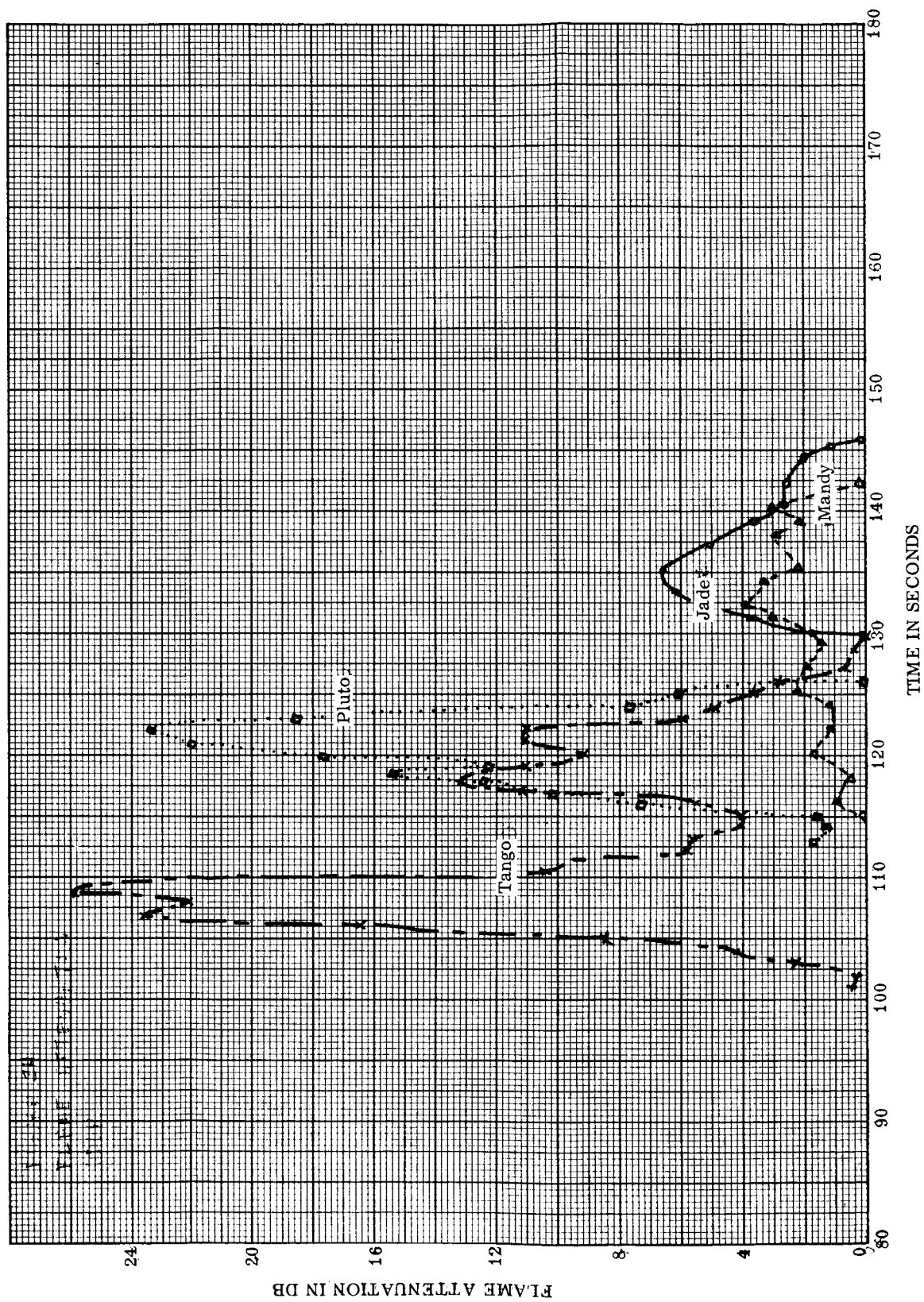
FIGURE 34. FLAME ATTENUATION, ODOP
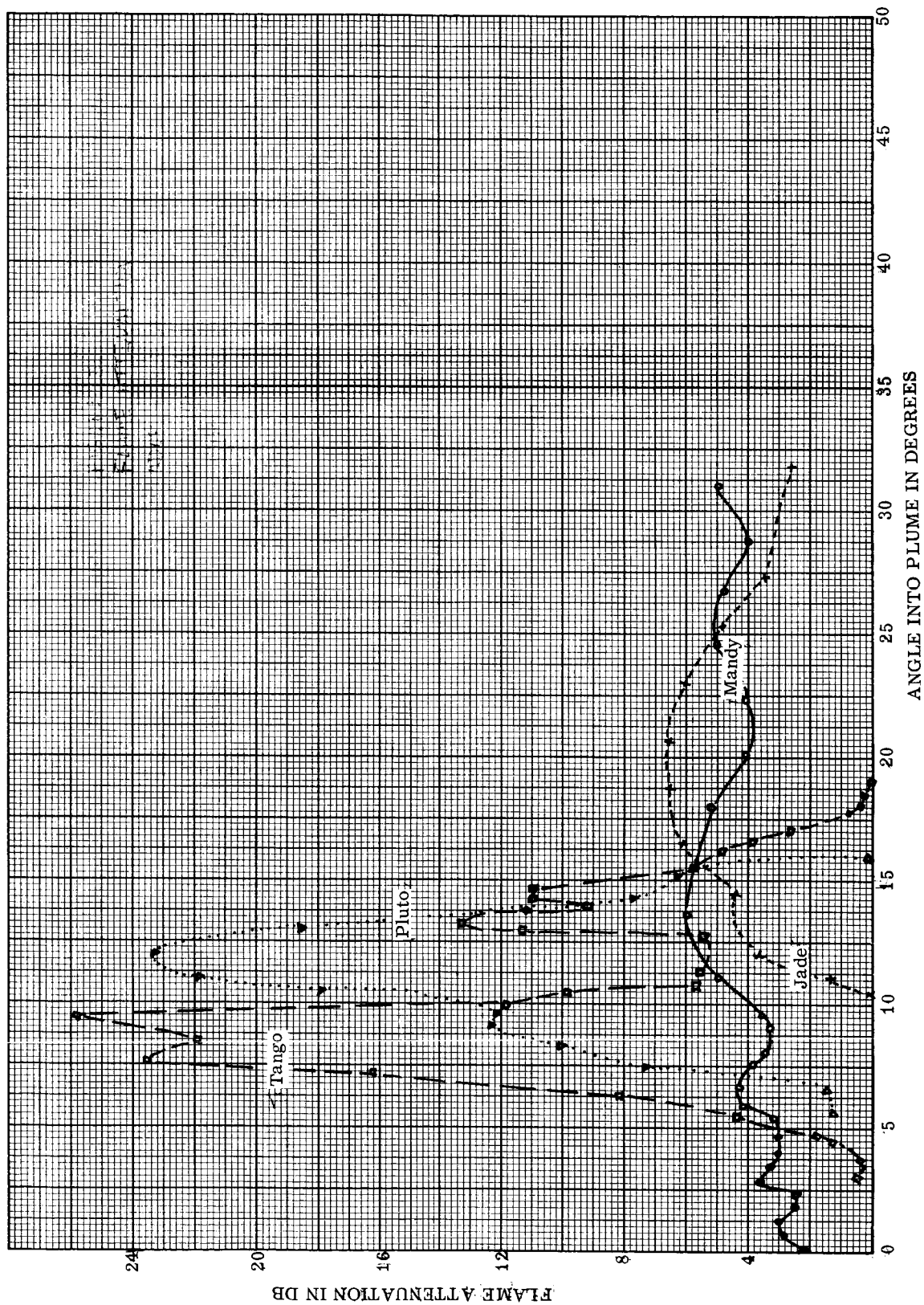
FIGURE 35. FLAME ATTENUATION, ODOP
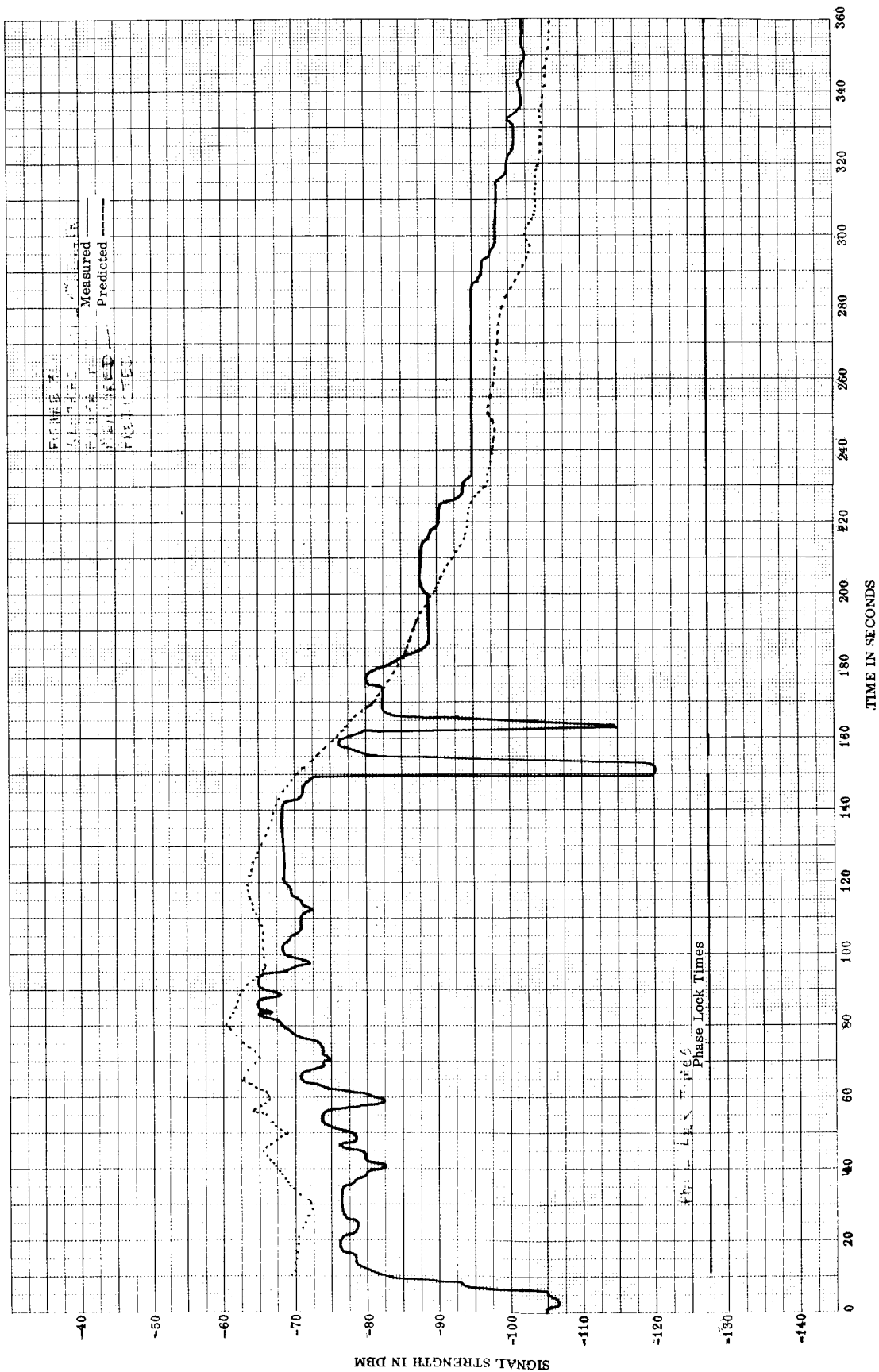
FIGURE 36A. AZUSA MK II SIGNAL STRENGTH

58
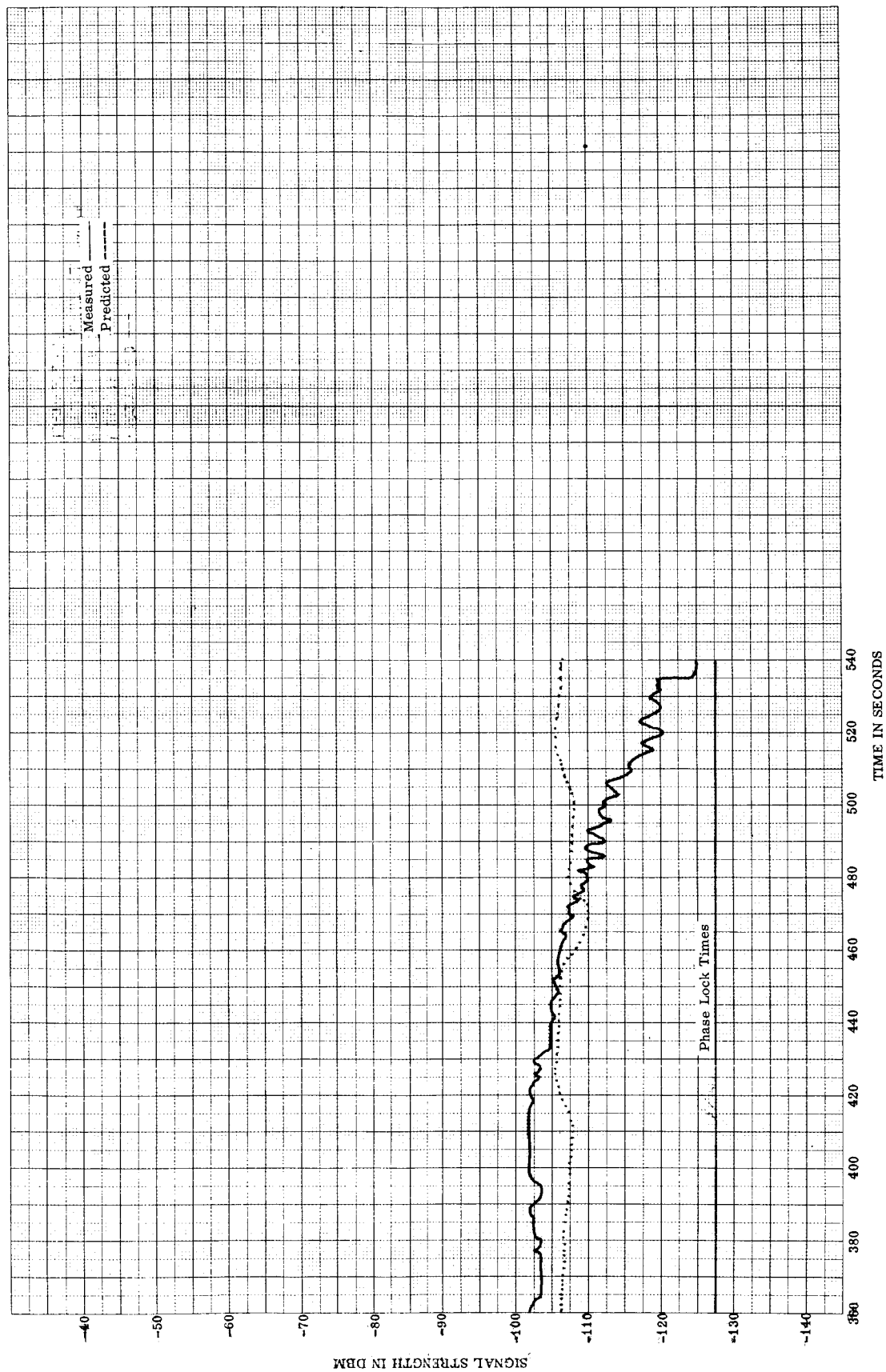
FIGURE 36B.   AZUSA MK II SIGNAL STRENGTH
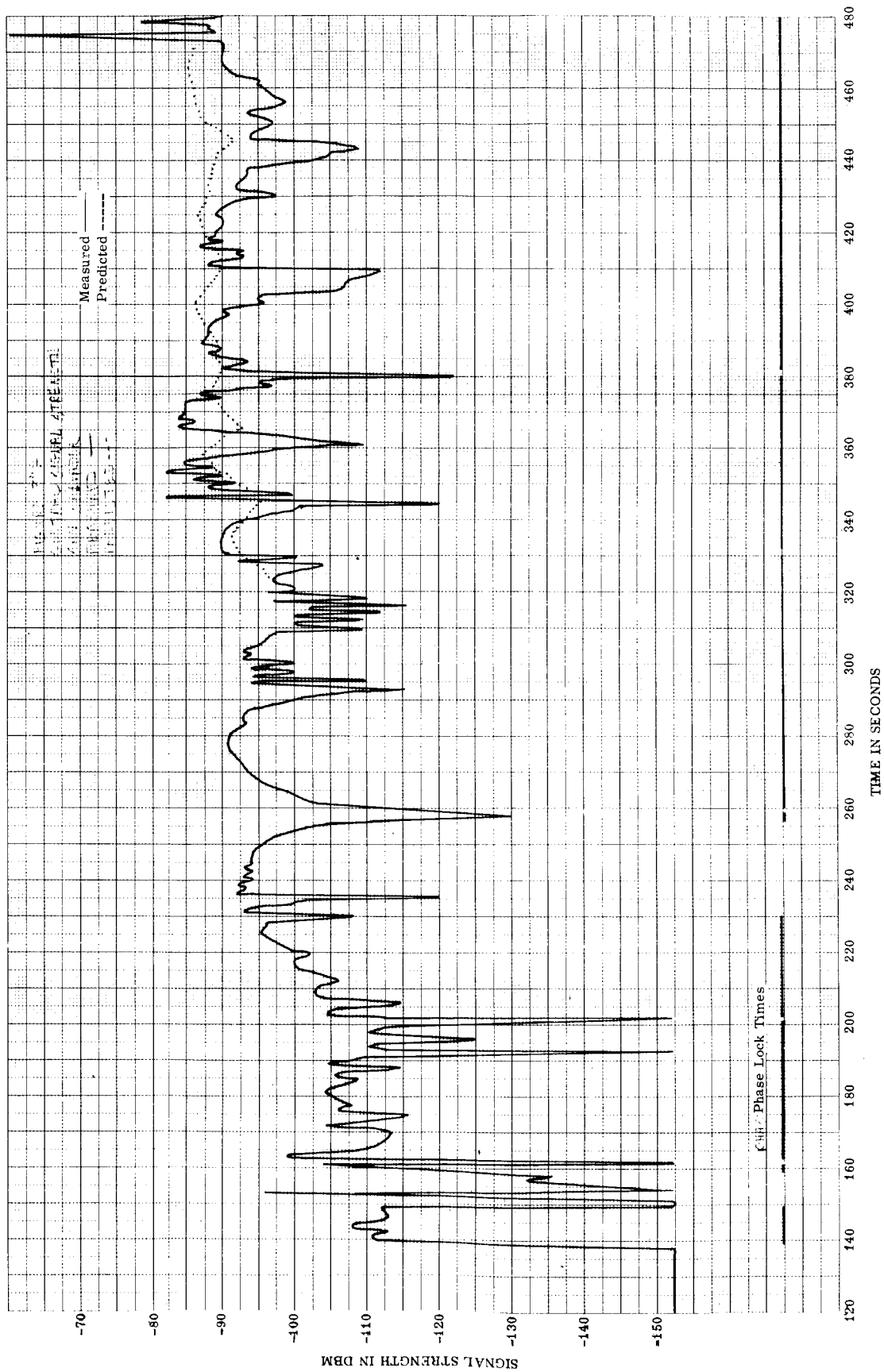
FIGURE 37A. GLOTRAC SIGNAL STRENGTH, SAN SALVADOR
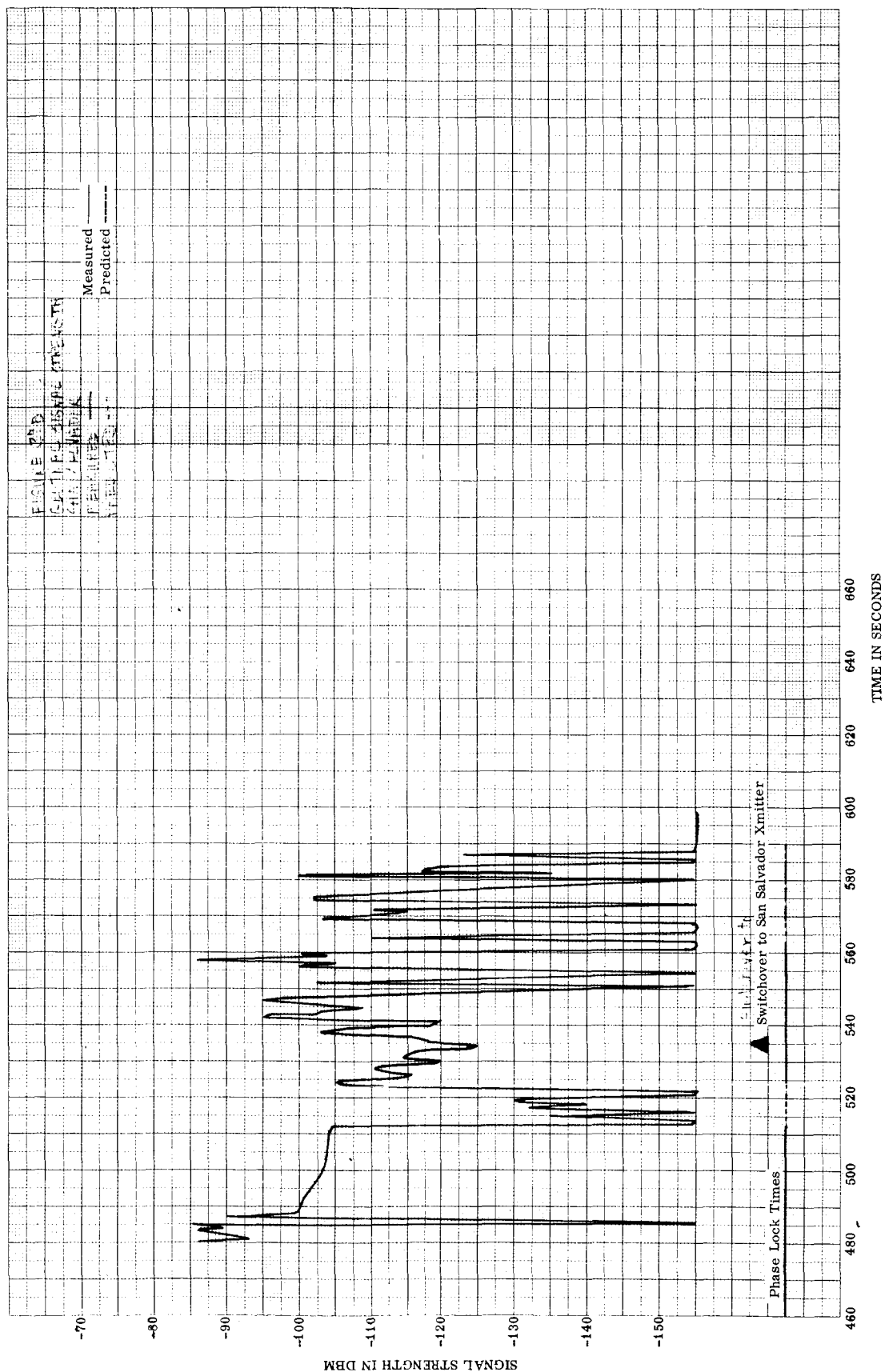
FIGURE 37B. GLOTRAC SIGNAL STRENGTH, SAN SALVADOR
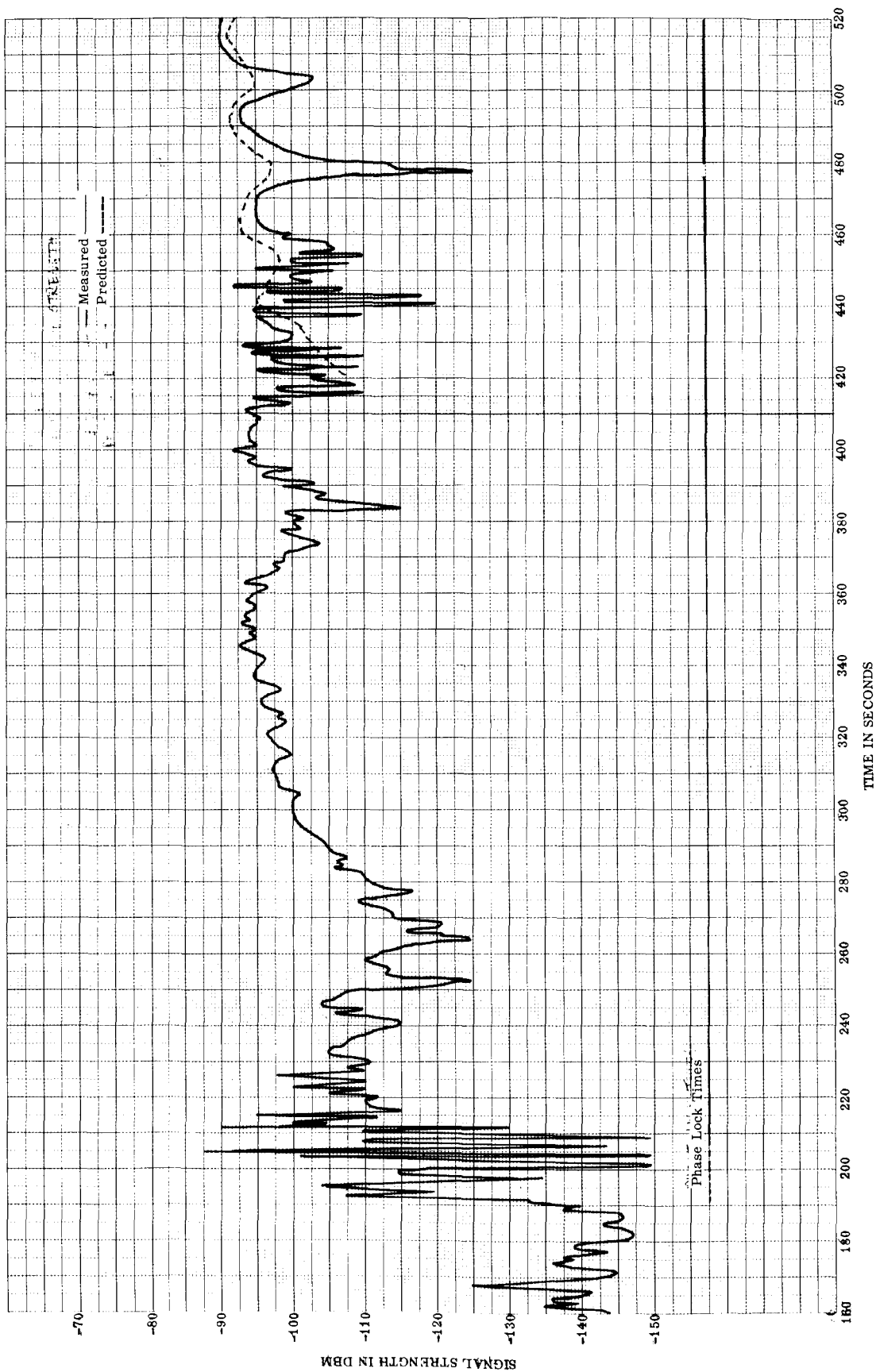
FIGURE 38A. GLOTRAC SIGNAL STRENGTH, GRAND TURK

62
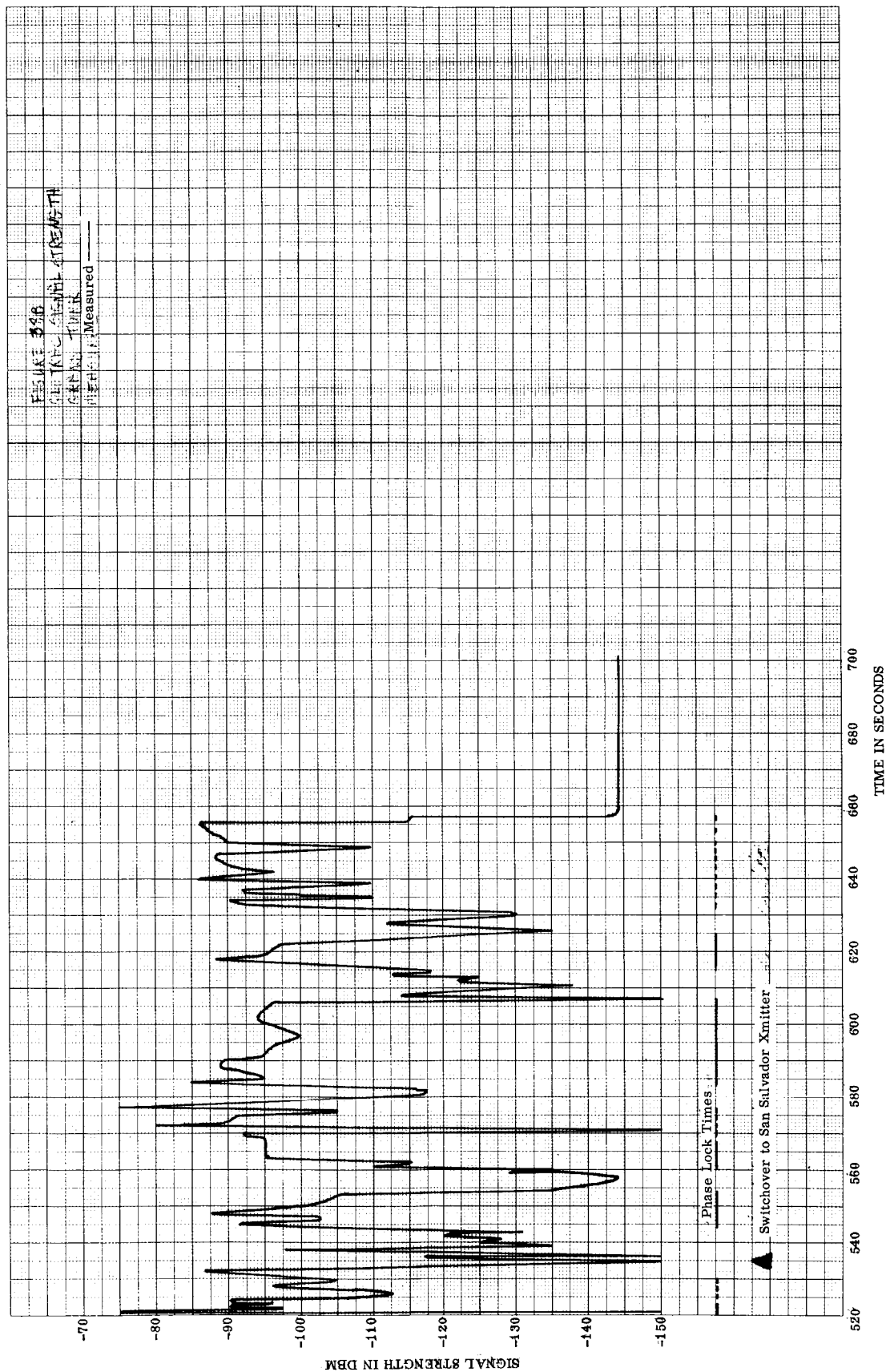
FIGURE 38B.   GLOTRAC SIGNAL STRENGTH, GRAND TURK

63
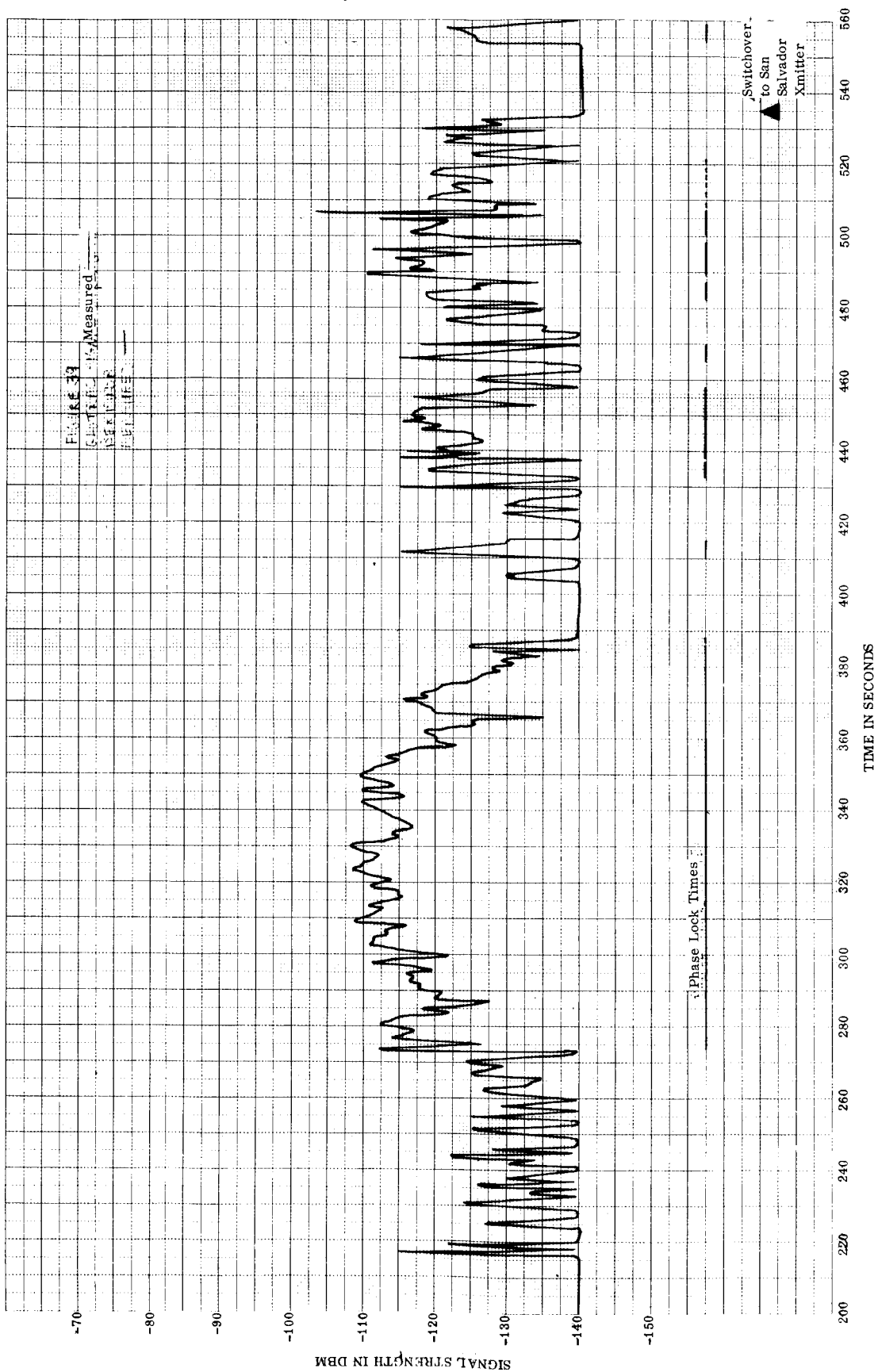
FIGURE 39. GLOTRAC SIGNAL STRENGTH, BERMUDA

64
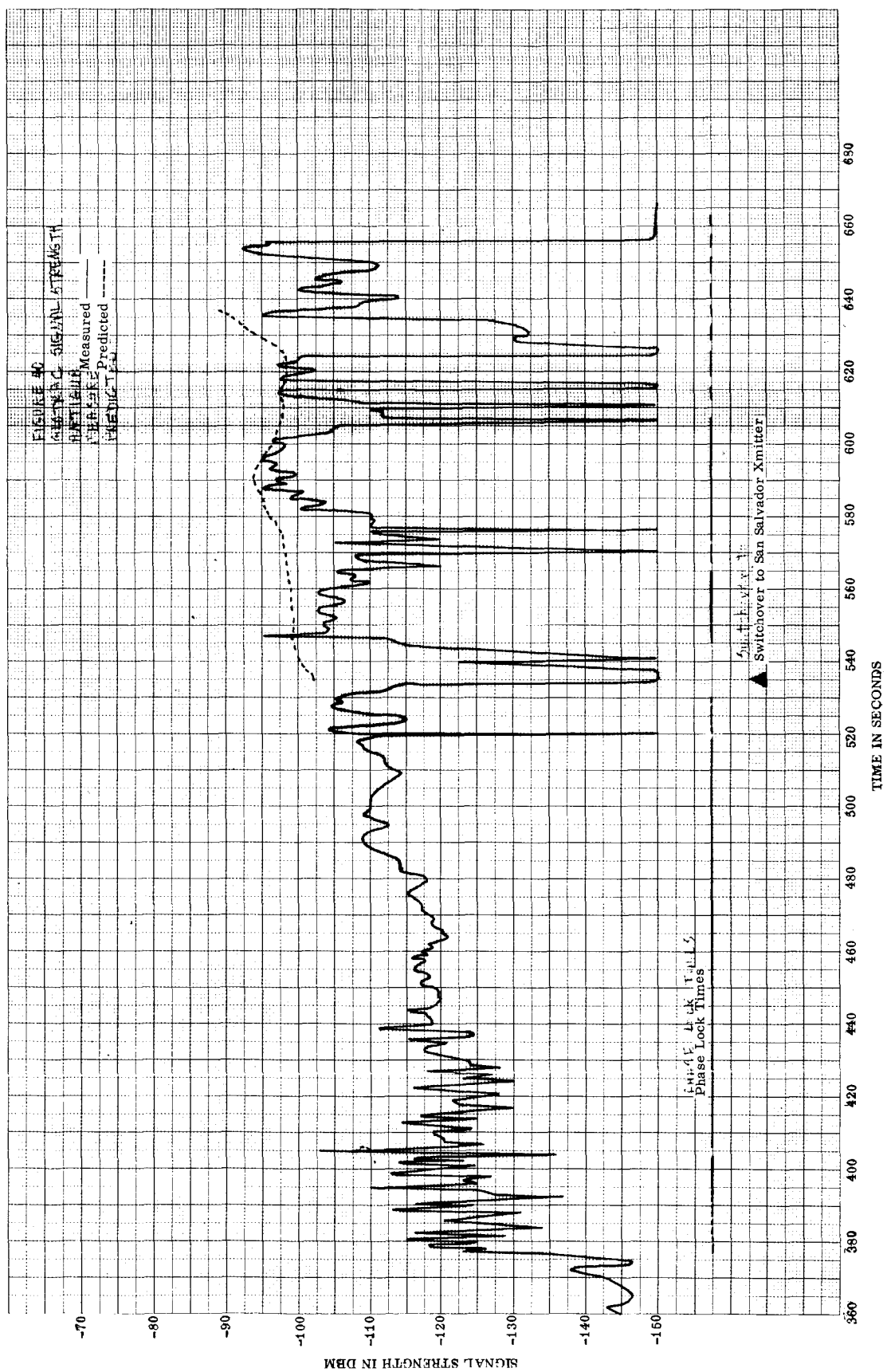
FIGURE 40. GLOTRAC SIGNAL STRENGTH, ANTIGUA

FIGURE 41A. ANTENNA GAIN PATTERNS, AZUSA/GLOTRAC
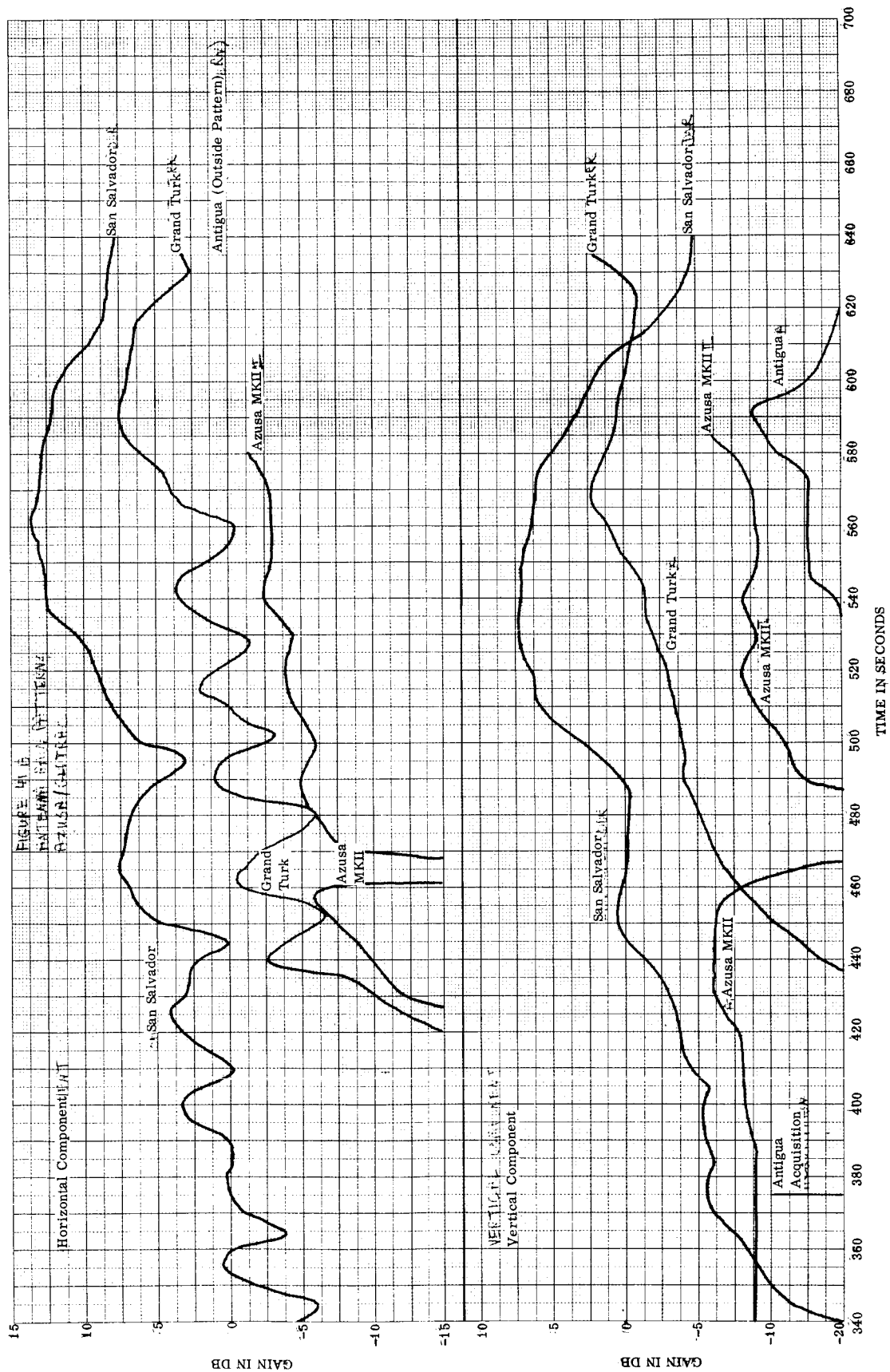
FIGURE 41B. ANTENNA GAIN PATTERNS, AZUSA/GLOTRAC

67
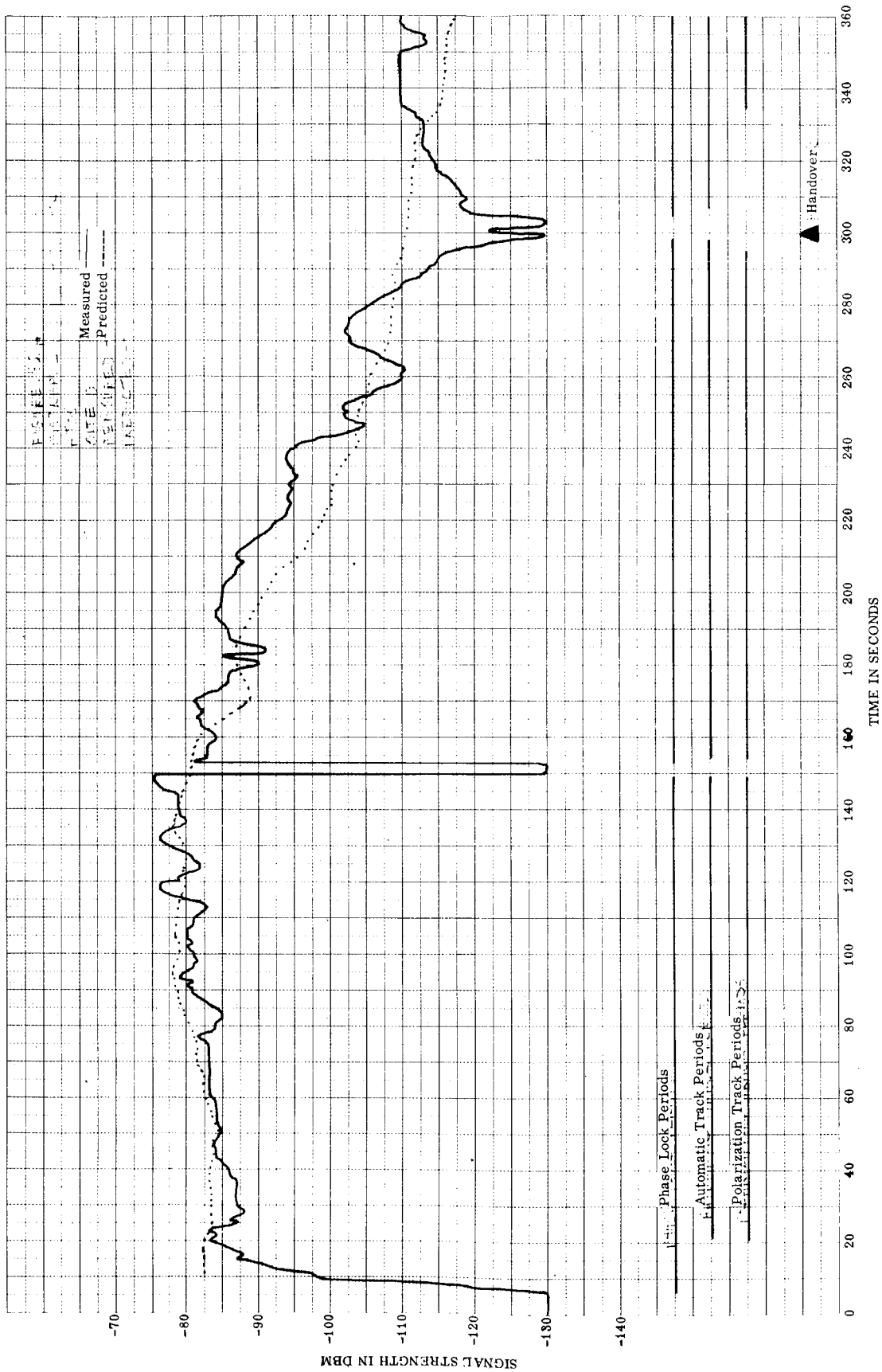
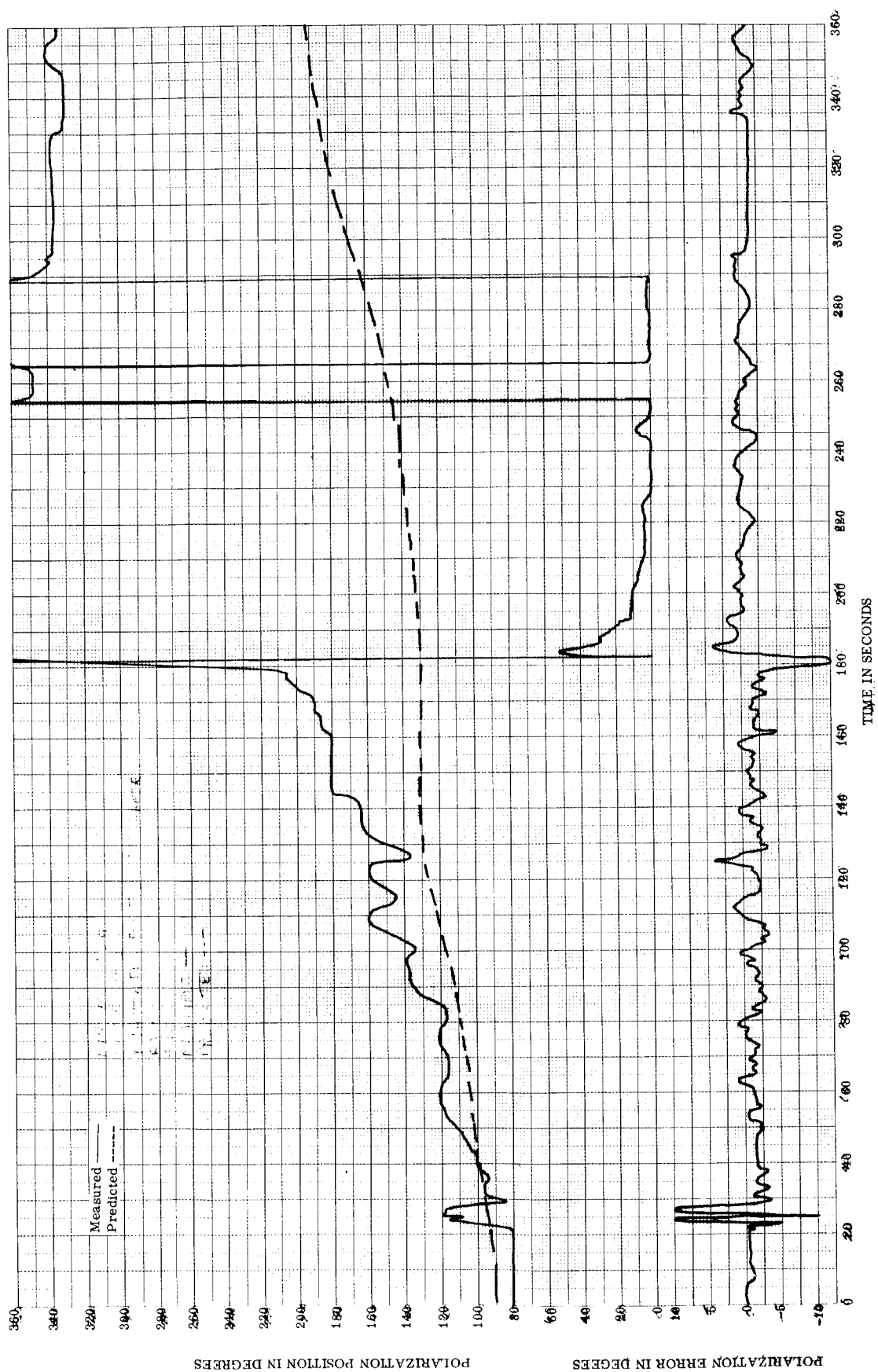FIGURE 42A. MISTRAM I SIGNAL STRENGTH, ATSS SITE O
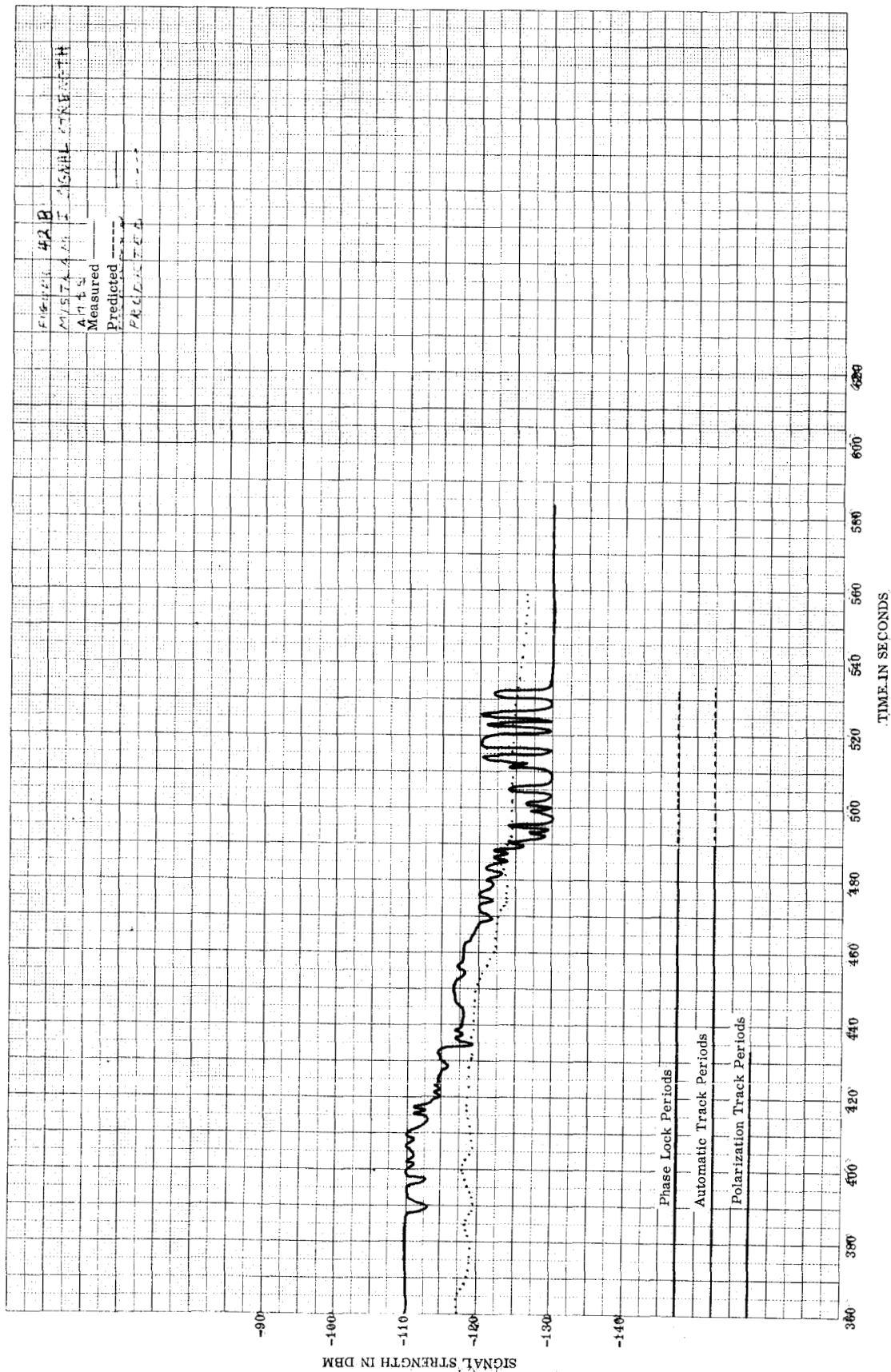
FIGURE 42B. MISTRAM I SIGNAL STRENGTH, ATSS SITE O

69

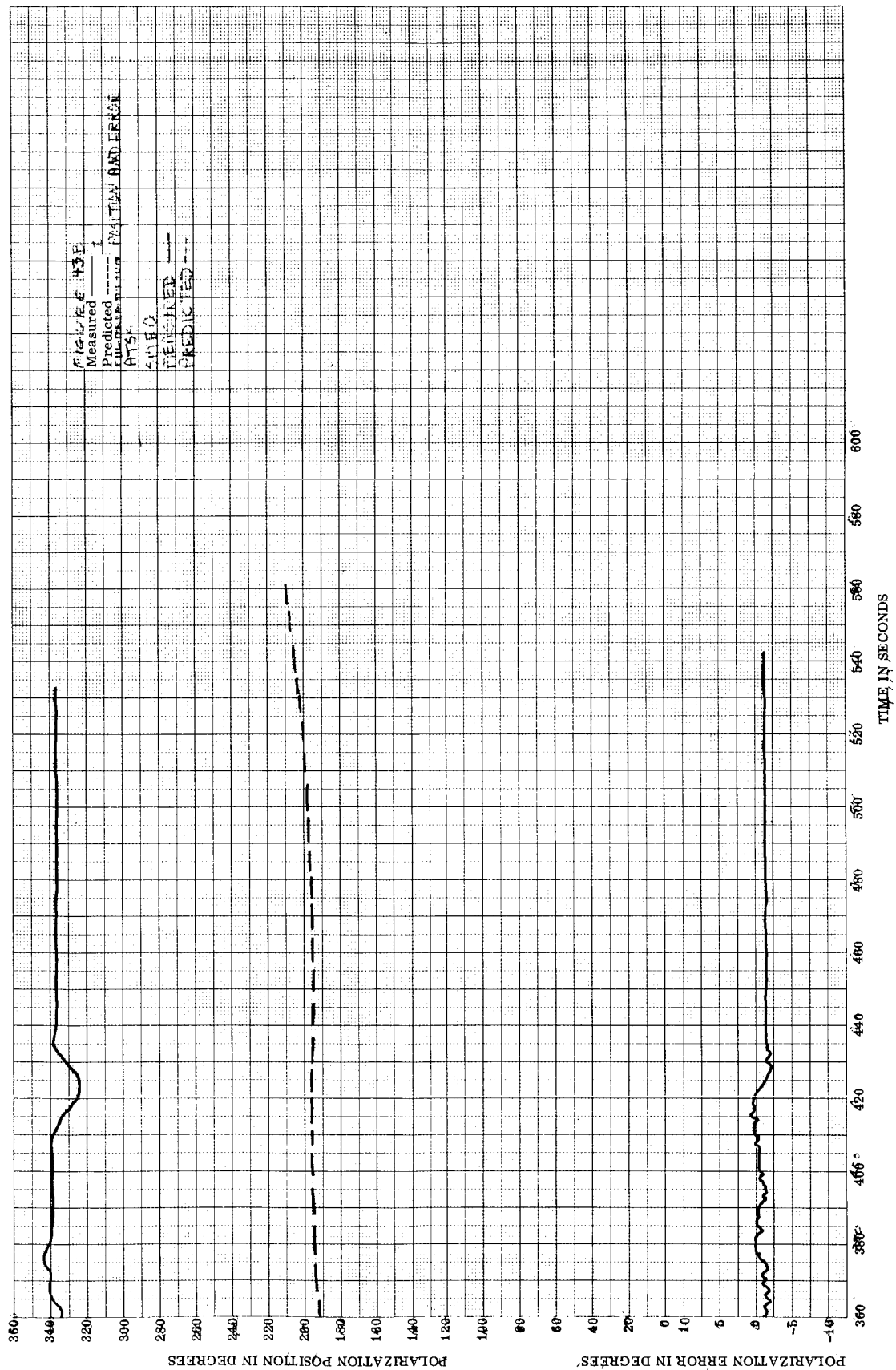FIGURE 43A. MISTRAM I POLARIZATION POSITION AND ERROR,ATSS SITE O

TIME IN SECONDS

POLARIZATION POSITION IN DEGREES

POLARIZATION ERROR IN DEGEES

Measured
Predicted

70

FIGURE 43B.   MISTRAM I POLARIZATION POSITION AND ERROR, ATSS SITE O

71
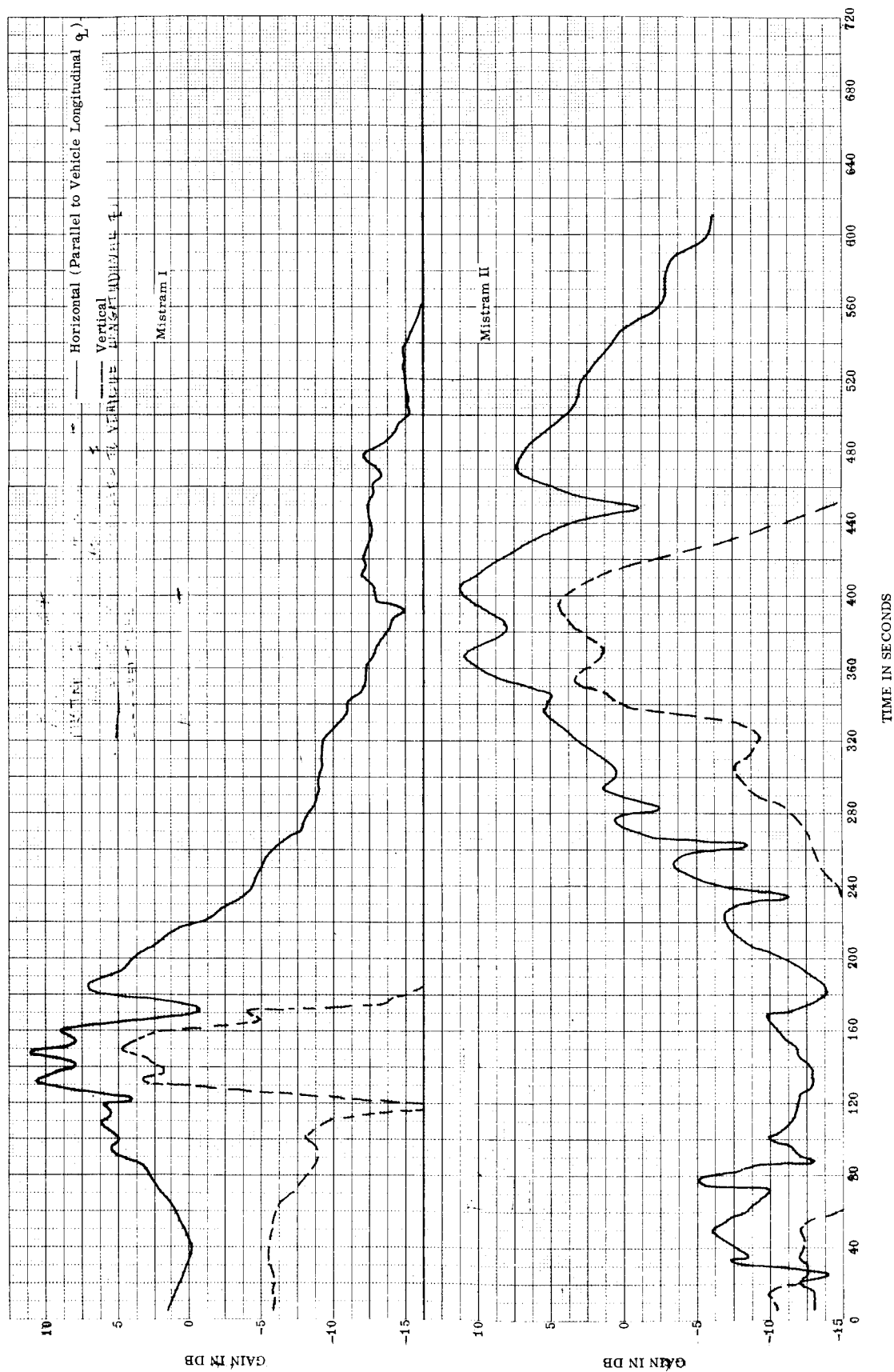
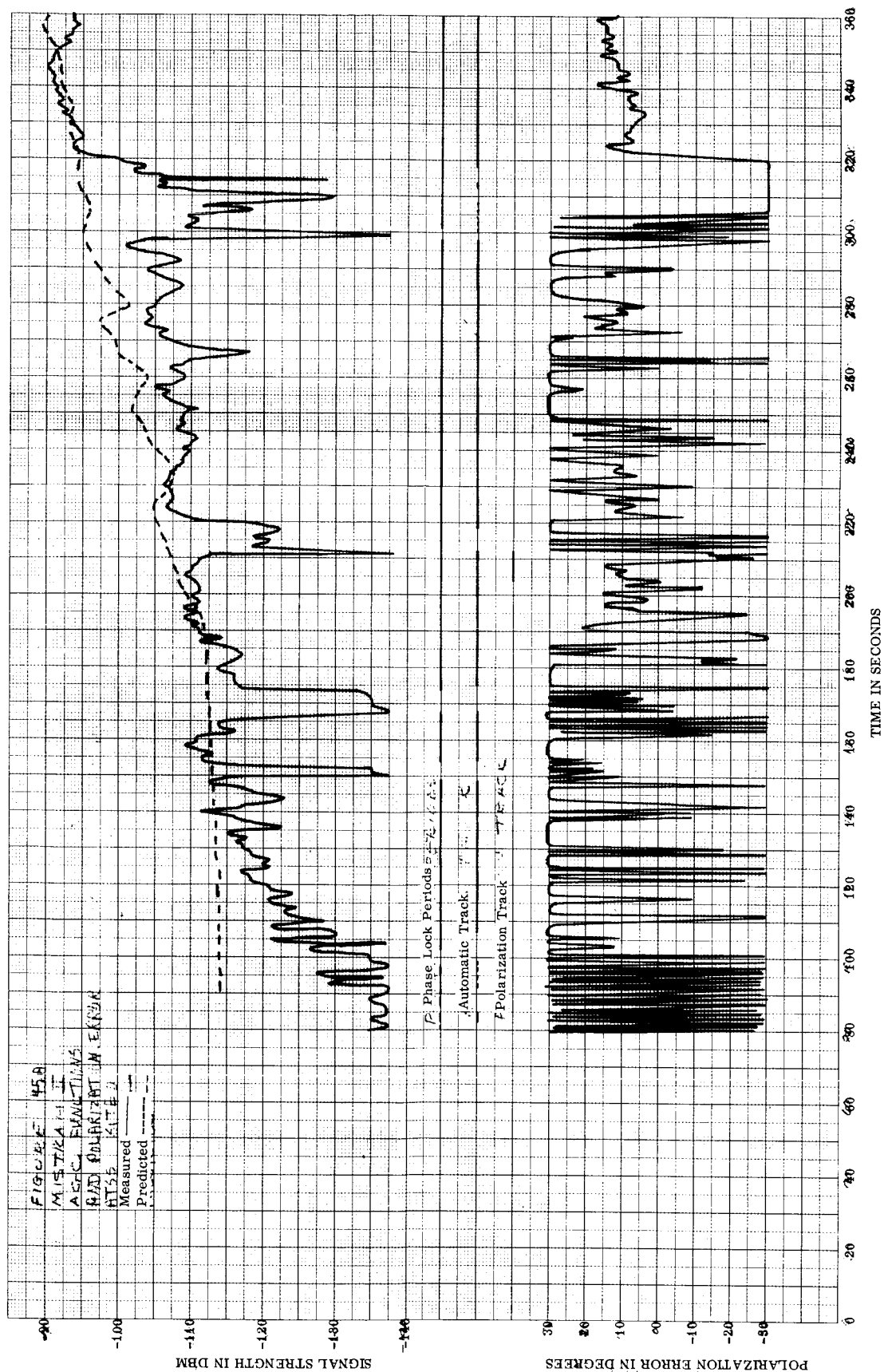FIGURE 44. MISTRAM I AND II ANTENNA GAIN PATTERNS

72

FIGURE 45A. MISTRAM II AGC,FUNCTIONS,AND POLARIZATION ERROR,ATSS SITE O
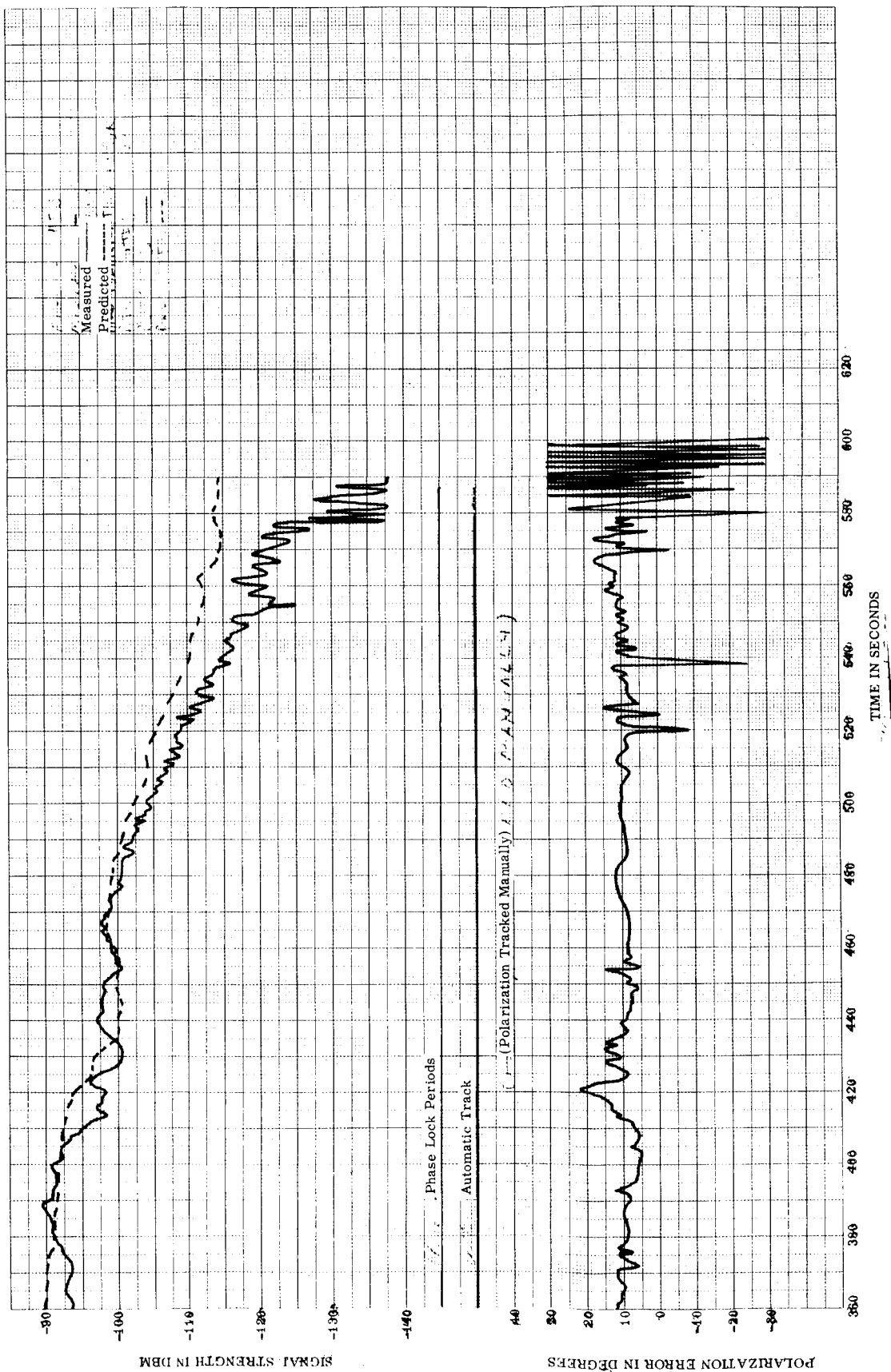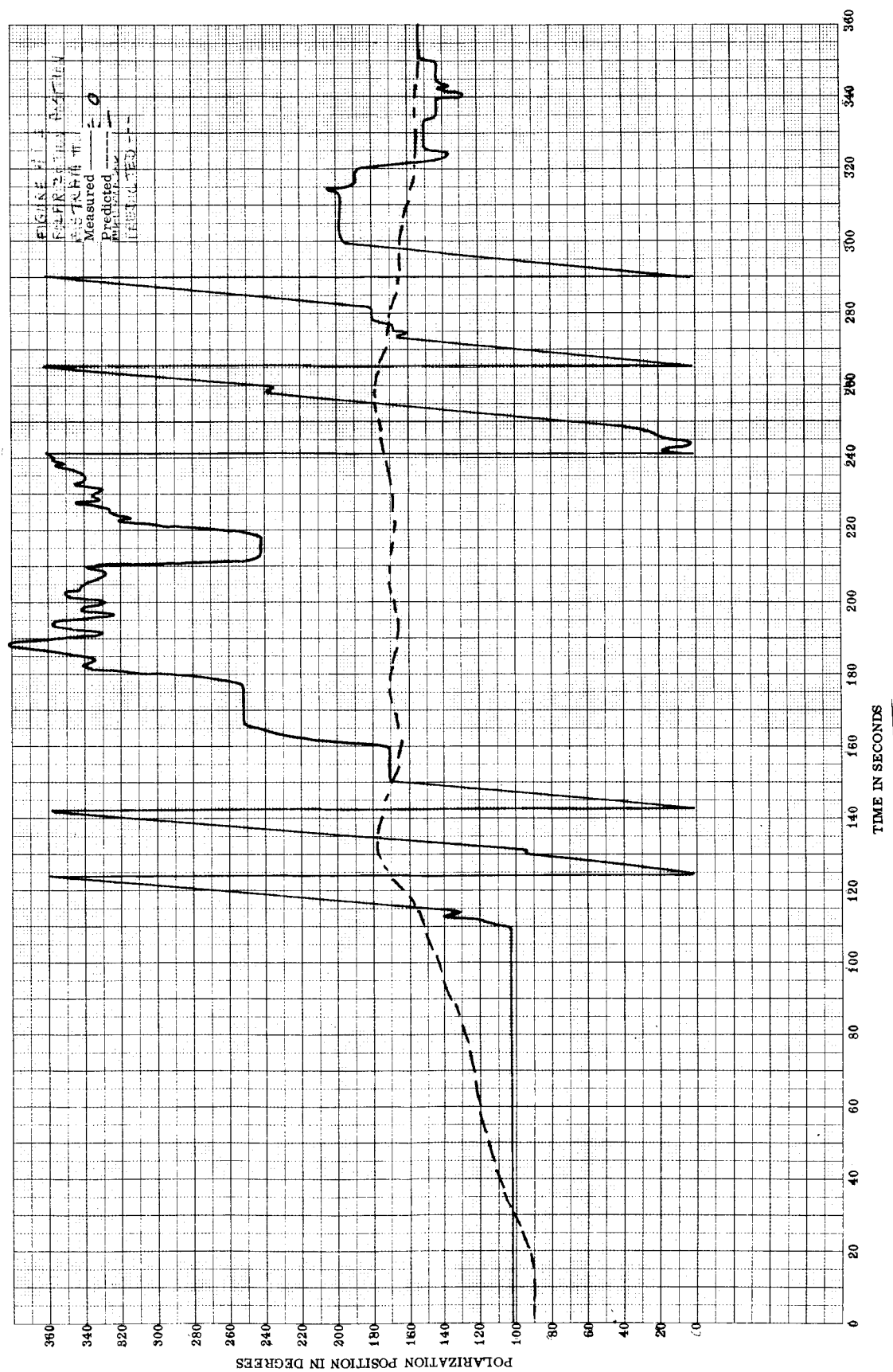
73

FIGURE 45B. MISTRAM II AGC, FUNCTIONS, AND POLARIZATION ERROR, ATSS SITE O

74

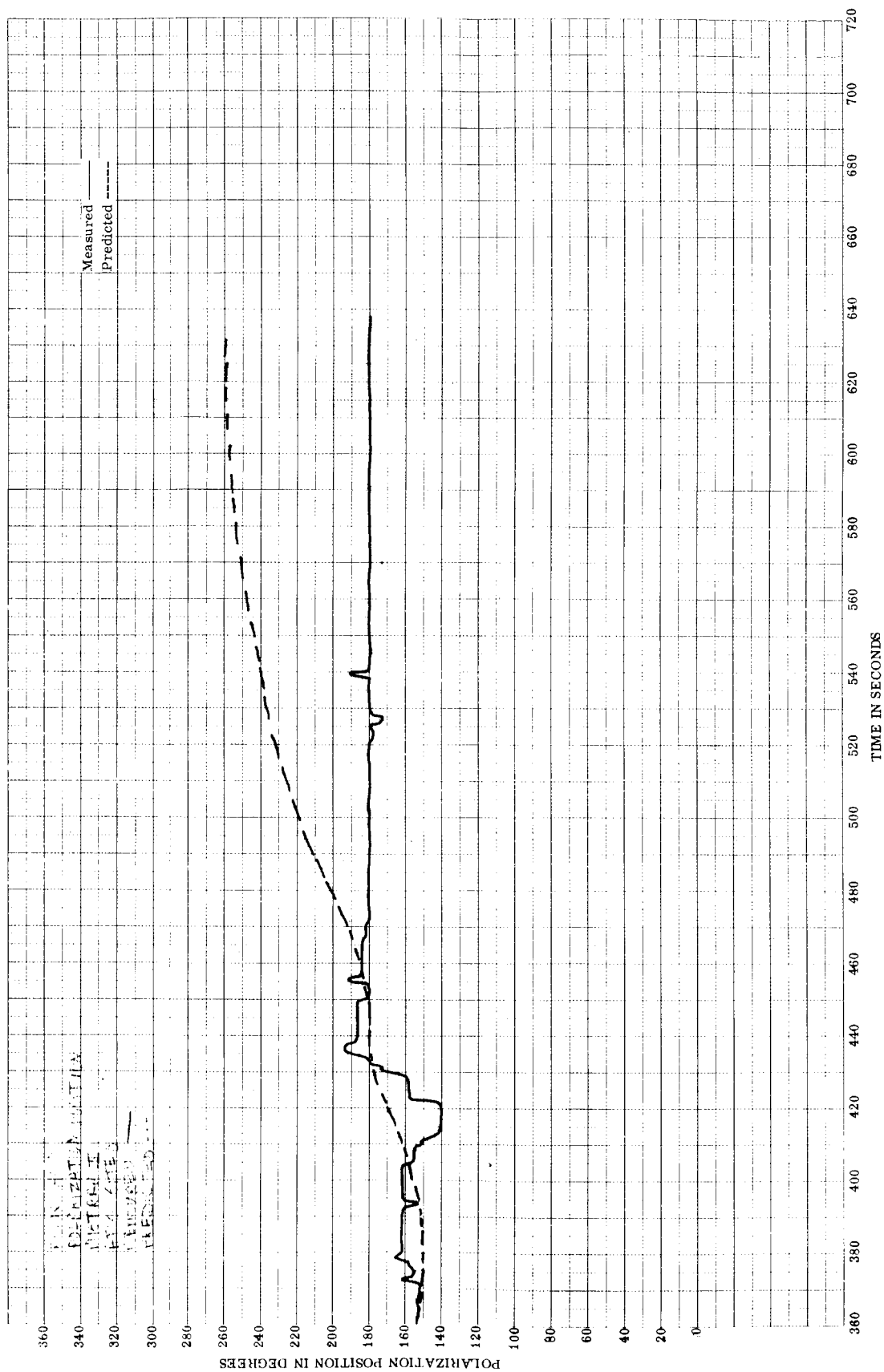FIGURE 46A.   POLARIZATION POSITION, MISTRAM II, ATSS SITE O

75

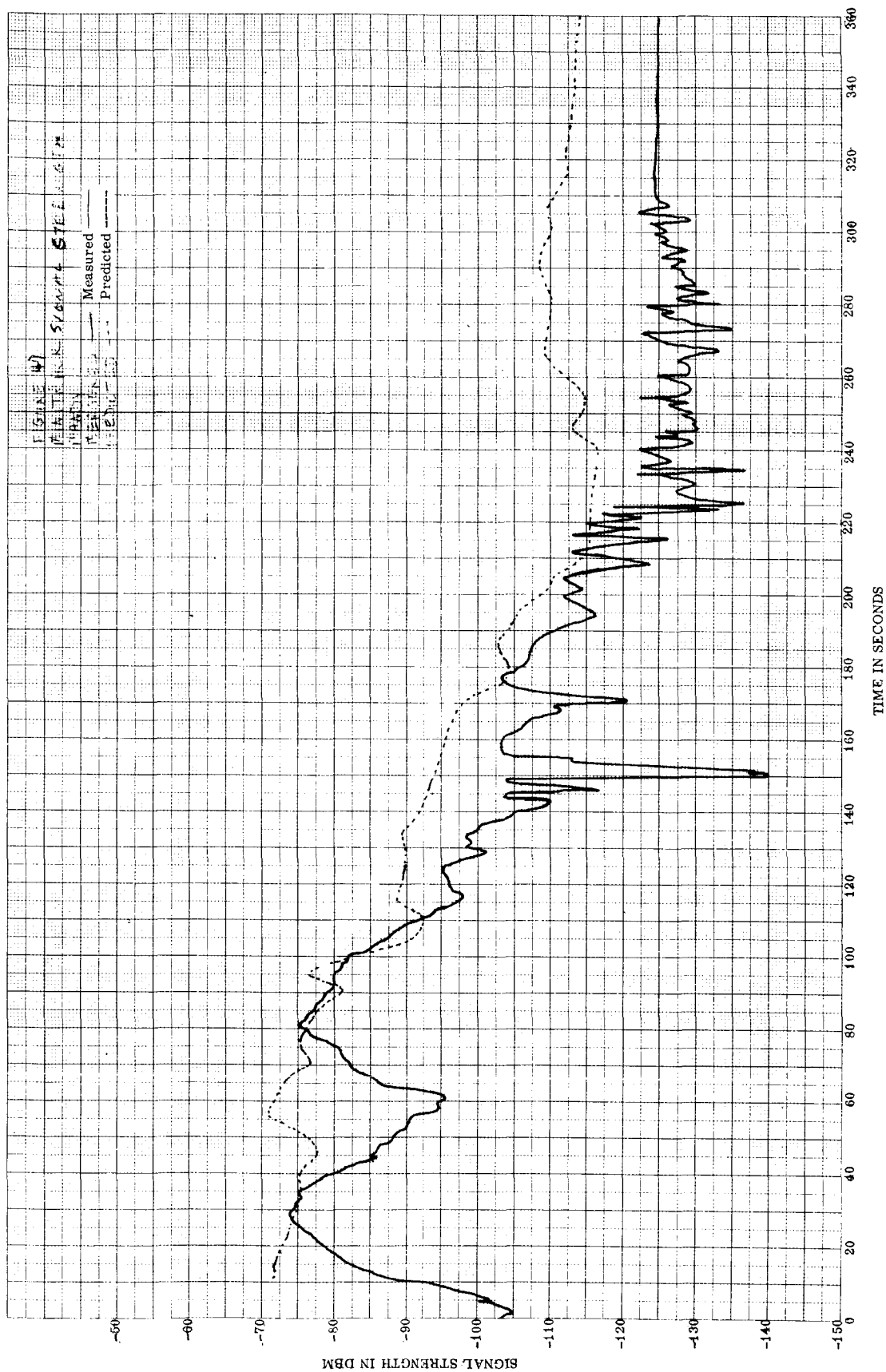FIGURE 46B.   POLARIZATION POSITION, MISTRAM II, ATSS SITE O
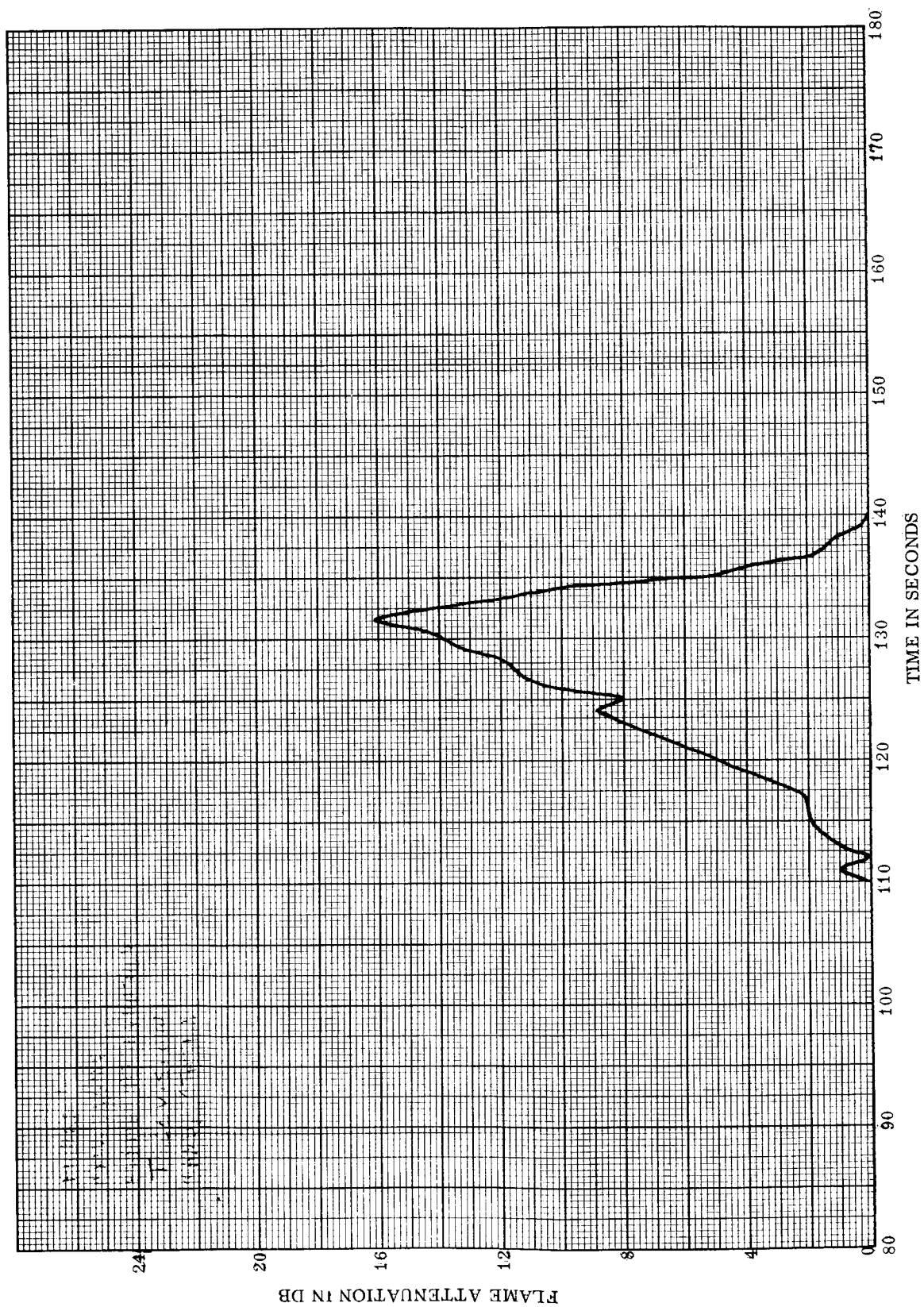
FIGURE 47. MINITRACK SIGNAL STRENGTH, MANDY

77

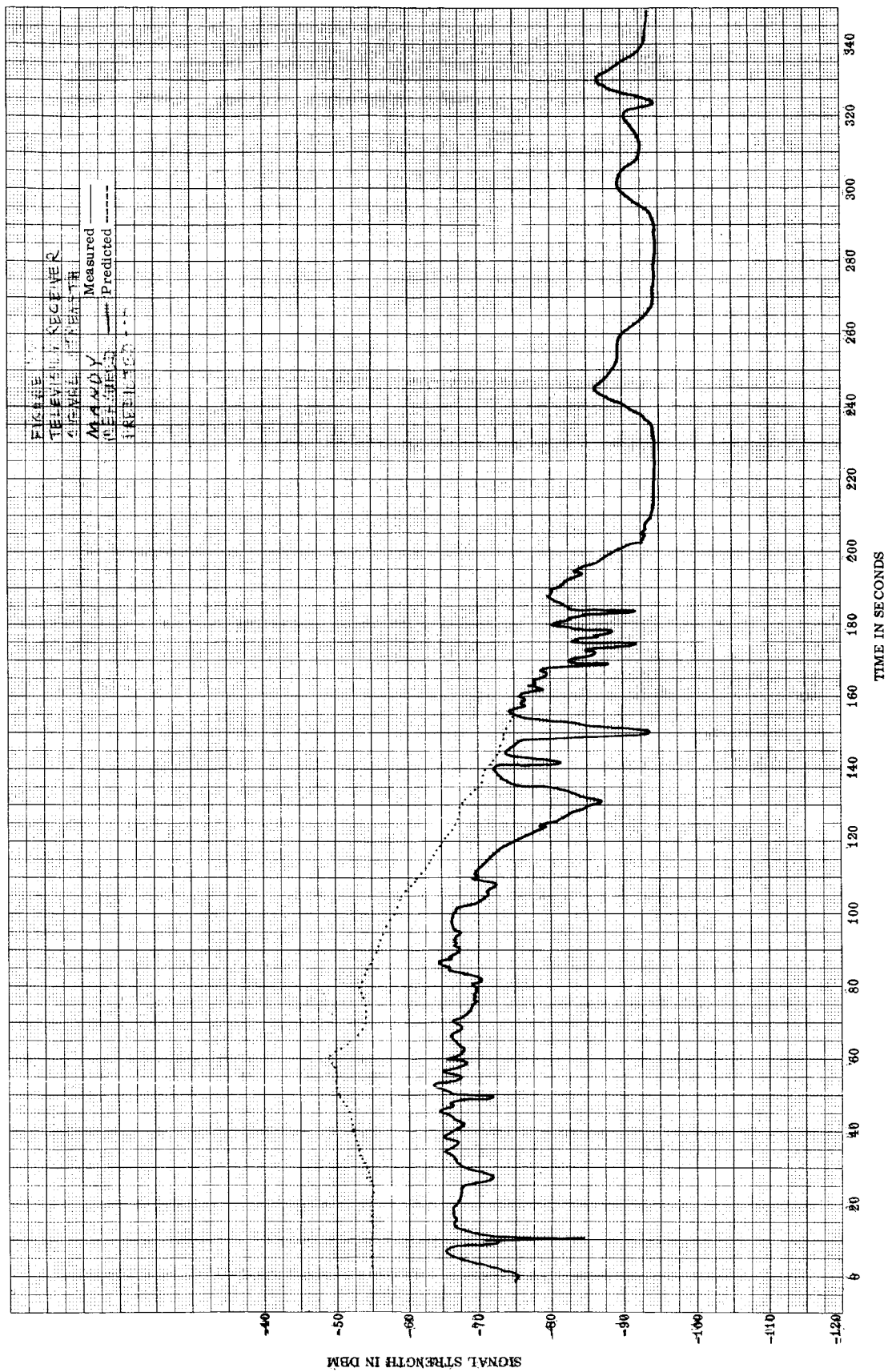FIGURE 48. MAIN ENGINE FLAME ATTENUATION, TELEVISION, MANDY

FIGURE 49. TELEVISION RECEIVER SIGNAL STRENGTH, MANDY

APPROVAL

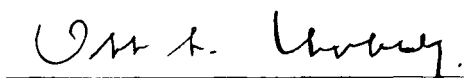## RADIO FREQUENCY EVALUATION OF SA-6 VEHICLE

By

Olen Ely, R. W. Hockenberger,
Parley Howell, and Geddes Boone

The information in this report has been reviewed for security classification. Review of any information concerning Department of Defense or Atomic Energy Commission programs has been made by the MSFC Security Classification Officer. This report, in its entirely, has been determined to be unclassified.

This document has also been reviewed and approved for technical accuracy.

T. A. BARR
Chief, RF Systems Branch

O. A. HOBERG
Chief, Instrumentation and Communication
Division

W. HAEUSSERMANN
Director, Astrionics Laboratory

DISTRIBUTION

Chrysler Corporation
Instrumentation Section
P. O. Box 26018
New Orleans, Louisiana
ATTN: Mr. Ed Lukowski

Douglas Aircraft Company
Missiles and Space System Division
3000 Ocean Park Blvd.
Santa Monica, California
ATTN: Mr. Tom Lundigan
      Mr. Dick Kirk

North American Aviation
12214 Lakewood Blvd.
Downey, California
ATTN: Mr. Mike Zelon

Scientific and Information Facility (25)
P. O. Box 5700
Bethesda, Maryland
ATTN: NASA Rep (S-AK/RKT)

Bellcomm
1100 17th Street, N. W.
Washington 6, D. C.
ATTN: Mr. Bob Chenn

IBM Corporation
P. O. Box 1250
Department 201
Huntsville, Alabama
ATTN: Mr. L. Overhultz

Dr. Fred S. Hanson
ORDBS-IRM-T
White Sands Missile Range, N. M.

RCA Performance Analysis
Cocoa Beach Office
Mail Unit 645
P. O. Box 4036
Patrick AFB, Florida
ATTN: Mr. John Greene
      Mr. Rowland Davis
      Mr. C. Clements
      Mr. E. A. Hoffman-Heyden

The Boeing Corporation
Huntsville, Alabama
ATTN: Mr. Haskell
      Mr. T. Cubbins
      Mr. Ruffner

Dr. Warren A. Dryden
Chairman, EPWG
Mu-511
RCA Missile Test Project
Patrick Air Force Base, Florida

Mr. John T. Downing
AFCRL-CRTP
Hanscom Field
Boston, Massachusetts

Mr. Colin Gardner
Code 3253
PMR
Point Mugu, California

Mr. John Schauble
APGC, PGVEP
Eglin AFB, Florida

CC-P

HME-P

MS-H

MS-IP

MS-IPL (8)

MS-IS
Dr. W. Wolf

I-SE
Mr. L. Bell

R-DIR
Mr. H. K. Weidner

R-AERO-DIR
Dr. E. D. Geissler

R-AERO-F
Dr. F. A. Speer

R-AERO-FO
Mr. H. F. Kurtz, Jr.

R-AERO-FOM
Mrs. A. McNair

R-AERO-FFT
Mr. M. A. Horst

R-RP
Dr. Dozier
Dr. W. Johnson

R-P&VE
Mr. Cline

R-COMP-RRT
Mr. R. Cochran
Mr. R. H. Craft

R-ASTR-DIR
Dr. Haeussermann
Miss Flowers

R-ASTR-A
Mr. F.E. Digesu

R-ASTR-E
Mr. H. J. Fichtner

R-ASTR-M
Mr. J. Boehm

R-ASTR-F
Mr. H. H. Hosenthien

R-ASTR-G
Mr. C. H. Mandel

R-ASTR-N
Mr. F. B. Moore

R-ASTR-P
Mr. W. Angele

R-ASTR-I
Mr. O. A. Hoberg
Mr. J. T. Powell
Mr. G. Saunders

R-ASTR-IE
Mr. J. Cox
Mr. J. Price
Mr. Bratcher
Mr. L. Ginn

R-ASTR-IP
Mr. H. Kampmeier
Mr. C. Chambers
Mr. H. Golden

R-ASTR-IM
Mr. C. T. Paludan

R-ASTR-IR
Mr. T. A. Barr
Mr. O. Duggan
Mr. C. T. Huggins

R-ASTR-IRA
Mr. J. Harper (3)

R-ASTR-IRC
Mr. L. B. Malone (8)
Mr. E. Pitts

R-ASTR-IRT
Mr. J. Gregory
Mr. E. Perry
Mr. B. Reed

R-ASTR-IRD
Mr. O. Ely (40)

R-ASTR-IT
Mr. J. Rorex (2)

R-ASTR-ITP
Mr. W. Threlkeld

R-ASTR-X
Central File

K-ED
Dr. Bruns
Mr. Jelen

K-EF3
Mr. F. Byrne

K-E
Mr. J. White

K-VE
Mr. G. Williams

K-VE2
Dr. D. C. McMath

K-VE23
Mr. Dietz

K-ET
Mr. Collins

MSC-ASPO
Mr. R. E. McKann

Mr. Eugene Fettner
RCA, Tech. Lab.
PAFB, Fla.

Dr. H. A. Poehler, PAA
Bldg. 425, Mail Code 511
PAFB, Fla.

Mr. Olson, Manager
Mistram Tracking Station
Valkaria, Fla.

Manager
Cape Telemetry 2 Station
Cape Kennedy, Fla.

Mr. M. Stinson
Azusa MK II Station
Cape Kennedy, Fla.